CANADIAN THESES
THÈSES CANADIENNES

REDMOND, Erin Kathleen

THE ROLE OF TOB37 AND TOB38 IN MITOCHONDRIAL BETA-BARREL PROTEIN ASSEMBLY

ISBN 978-0-494-45876-1
MR-45876

University of Alberta

The Role of Tob37 and Tob38 in Mitochondrial beta-Barrel Protein Assembly

by

Erin Kathleen Redmond ©

A thesis submitted to the Faculty of Graduate Studies and Research
in partial fulfillment of the requirements for the degree of

Master of Science

in

Molecular Biology and Genetics

Department of Biological Sciences

Edmonton, Alberta

Spring 2008

Library and Archives Canada

Published Heritage Branch

395 Wellington Street
Ottawa ON K1A 0N4
Canada

Bibliothèque et Archives Canada

Direction du Patrimoine de l'édition

395, rue Wellington
Ottawa ON K1A 0N4
Canada

Your file Votre référence
ISBN: 978-0-494-45876-1
Our file Notre référence
ISBN: 978-0-494-45876-1

NOTICE:
The author has granted a non-exclusive license allowing Library and Archives Canada to reproduce, publish, archive, preserve, conserve, communicate to the public by telecommunication or on the Internet, loan, distribute and sell theses worldwide, for commercial or non-commercial purposes, in microform, paper, electronic and/or any other formats.

The author retains copyright ownership and moral rights in this thesis. Neither the thesis nor substantial extracts from it may be printed or otherwise reproduced without the author's permission.

AVIS:
L'auteur a accordé une licence non exclusive permettant à la Bibliothèque et Archives Canada de reproduire, publier, archiver, sauvegarder, conserver, transmettre au public par télécommunication ou par l'Internet, prêter, distribuer et vendre des thèses partout dans le monde, à des fins commerciales ou autres, sur support microforme, papier, électronique et/ou autres formats.

L'auteur conserve la propriété du droit d'auteur et des droits moraux qui protège cette thèse. Ni la thèse ni des extraits substantiels de celle-ci ne doivent être imprimés ou autrement reproduits sans son autorisation.

In compliance with the Canadian Privacy Act some supporting forms may have been removed from this thesis.

While these forms may be included in the document page count, their removal does not represent any loss of content from the thesis.

Conformément à la loi canadienne sur la protection de la vie privée, quelques formulaires secondaires ont été enlevés de cette thèse.

Bien que ces formulaires aient inclus dans la pagination, il n'y aura aucun contenu manquant.

Canada

Abstract

The TOB (Topogenesis of Outer membrane beta-Barrel proteins) complex is required for the assembly of beta-barrel proteins into the mitochondrial outer membrane. Tob37, Tob38, and Tob55 are the core components of the complex. Characterization of *Neurospora crassa* Tob37 and Tob38 revealed that: 1) both proteins are essential for viability, 2) Tob37 is an integral membrane protein whereas Tob38 is a peripheral membrane protein, and 3) both proteins are exposed on the cytosolic side of the mitochondria outer membrane. In cells where the levels of Tob37 and Tob38 have been reduced by genetic manipulation the steady state levels of beta-barrel proteins are reduced in mitochondria. Tob37, Tob38, and Tob55 were shown to interact, although Tob37 appeared to be less tightly associated with the TOB complex than the other two subunits. Tob38 was found to contain a conserved N-terminal region that is required for efficient assembly of the protein into the TOB complex.

Acknowledgements

I would like to thank my supervisor, Frank Nargang, for the opportunity to work in his laboratory and technical guidance throughout this research.

I would also like to thank the members of the Nargang laboratory, Mike Chae, Nancy Go, Cheryl Nargang, Ian Cleary, and Jeremy Wideman for their friendships and technical support provided over the years. In addition, I would also like to thank the Molecular Biology Services Unit for technical support, and the Advanced Microscopy Facility and Shelagh Campbell's laboratory for microscopy support.

I am also grateful to the professors on my committee, Dr. Shelagh Campbell, Dr. Tracy Raivio, and Dr. Moira Glerum for their guidance and comments on my thesis.

I must also acknowledge the support of the Department of Biological Sciences and the Faculty of Graduate Studies and Research at the University of Alberta for funding and scholarships during my degree.

Finally, I would like to thank Peter Kennedy, my parents Patricia and Brian Redmond, and my siblings Eileen and Peter Redmond, all of whom provided exceptional support through all the years of this research.

Section	Page
1. Introduction	1
1.1 Mitochondrial Functions	1
1.2 Evolution of Mitochondria	2
1.3 Mitochondrial Morphology	4
1.4 Mitochondrial Import	5
1.4.1 The TOM Complex	7
1.4.1.1 Tom40	7
1.4.1.2 Tom20 and Tom22	8
1.4.1.3 Tom70	10
1.4.1.4 The Small Toms	12
1.4.2 Assembly of the TOM Complex	13
1.4.3 Import Components of the IMS	16
1.4.4 The TIM23 and PAM Complexes	17
1.4.5 The TIM22 Complex	19
1.4.6 The TOB Complex	19
1.4.6.1 Tob55	20
1.4.6.2 Tob38	21
1.4.6.3 Tob37	23
1.4.7 Defining the TOB Complex and its Components	23
1.4.8 Interaction of Incoming Tom40 Precursor Molecules with the TOB Complex to give a Tom40 Assembly Intermediate	25
1.4.9 Tob38 and Tob37 Co-dependent Relationship	27
1.4.10 Mammalian Metaxin1 and Metaxin2	28
1.4.11 Additional Proteins Interacting with the TOB Complex	29
1.4.11.1 Mim1	30
1.4.11.2 Mdm10	31
1.4.12 The TOB Complex and Alpha Helical Proteins	32
1.4.13 The Tob37 and Tom70 Interaction	33
1.5 Objectives of this Analysis	34

Section	Page
2. Materials and Methods	35
2.1 Growth of *N. crassa*	35
2.2 Sequence Alignment and Phylogeny Construction	35
2.3 Oligonucleotides and Plasmids	39
2.4 Transformation of *N. crassa*	39
2.5 Knockout of Tob38 and Tob37 Using the Split Marker Approach	45
2.6 Creation of Tob38 and Tob37 Mutant Alleles	46
2.7 Tob38 Antibody Production	47
2.8 Preparation of *N. crassa* for Transmission Electron Microscopy	48
2.9 Preparation of *N. crassa* for Fluorescence Microscopy	49
2.10 Isolation of Mitochondrial and Whole Cell Protein	50
2.11 Alkaline Extraction of Membranes and Proteinase K Treatment	50
2.12 Outer Membrane Vesicle (OMV) Isolation	51
2.13 Pulldown Analysis	52
2.14 Blue Native Gel Electrophoresis (BNGE)	53
2.15 *In vitro* Import of Radioactive Tom40, porin, Tob55, Tob38 and Tob37 into Isolated Mitochondria	54
2.16 Pulse Import of Tom40, Tob38, and Tob55 Wildtype Precursors	54
2.17 Other techniques	55
3. Results	56
3.1 Sheltered Heterokaryon Knockout Strains in *N. crassa*	56
3.2 Antibody Production and Testing	66
3.3 Analysis of Knockout Mitochondria	72
3.4 Sequence and Phylogeny Construction	75
3.5 Location and Topology of *N. crassa* Tob37 and Tob38	81
3.6 Microscopy of Tob38↓, Tob37↓ and *tom70*^{RIP} Mitochondria	82
3.7 TOB Complex Interactions	84
3.8 *In vitro* Import	92
3.9 Conserved Regions of Tob38	97

Section	Page
3.10 *In vitro* Import of Tob38 Mutant Proteins into Control (HP1) Mitochondria	104
3.11 Conserved Regions of Tob37	104
3.12 Tob37-20-1 Mutant	118
3.13 Tom70	120
4. Discussion	127
4.1 The *tob38* and *tob37* sheltered heterokaryon knockout strains	127
4.2 The TOB Complexes	129
4.3 Tob38 Location, Topology, and Conserved Regions	129
4.4 Tob37 Location, Topology, and Conserved Regions	130
4.5 The TOM Complex and Assembly Intermediates	132
4.6 The Involvement of Tom70	132
4.7 Future Work	133
References	135

List of Tables **Page**

Table 1	Strains used in this analysis	36
Table 2	Oligonucleotides used in this analysis	40
Table 3	Plasmids used in this analysis	43
Table 4	Comparison of five similar sequences in *N. crassa*	65

List of Figures **Page**

Figure 1	*Neurospora crassa* mitochondrial import machinery	6
Figure 2	The Tom40 assembly pathway	14
Figure 3	Sheltered heterokaryon *tob38*KO strain	57
Figure 4	Tob38 is essential for viability	60
Figure 5	Southern blot analysis of the *tob38*KO strain	62
Figure 6	Western blot analysis using Tob38 antibodies	67
Figure 7	Western blot analysis using Tob37 antibodies	69
Figure 8	Mitochondrial proteins in knockout strains	73
Figure 9	Analysis of protein in whole cell extracts and OMVs	74
Figure 10	Multiple sequence alignment of Tob37	76
Figure 11	Multiple sequence alignment of Tob38	78
Figure 12	An unrooted maximum likelihood tree of Tob37 and Tob38 protein homologs using the JTT matrix	79
Figure 13	Behaviour of Tob38 and Tob37 following proteinase K treatment and carbonate extraction of mitochondria	83
Figure 14	Transmission electron microscopy of mitochondria	85
Figure 15	Fluorescence microscopy of mitochondria	88
Figure 16	Binding of his-tagged TOB complex proteins to Ni-NTA resin and identification of interacting proteins	89
Figure 17	Analysis of TOM and TOB complexes by BNGE	91
Figure 18	Broken mitochondria isolated from *tom70*^{RIP}, Tob38↓, and Tob37↓ strains following proteinase K treatment	93
Figure 19	Import and assembly of mitochondrial precursor proteins into Tob deficient mitochondria	94
Figure 20	Pulse import and assembly of mitochondria precursor proteins into control (HP1) mitochondria	96
Figure 21	Regions of Tob38 targeted for site-directed mutagenesis	98
Figure 22	Growth rates of Tob38 mutant strains	99
Figure 23	Mitochondria proteins in the Tob38 mutants	101

List of Figures **Page**

Figure 24	Analysis of the TOM and TOB complexes in the Tob38 mutants by BNGE	102
Figure 25	Membrane association of mutant Tob38 proteins	103
Figure 26	Import and assembly of mutant Tob38 proteins	105
Figure 27	Regions of Tob37 targeted for site-directed mutagenesis	108
Figure 28	Growth rates of Tob37 mutants	113
Figure 29	Mitochondrial proteins in the Tob37 mutants	116
Figure 30	Mitochondrial proteins in different isolated of the Tob37-35 mutant	119
Figure 31	Analysis of the TOM and TOB complexes in Tob37-20-1 by BNGE	121
Figure 32	Import and assembly of mitochondria precursor proteins into Tob37-20-1 mitochondria	122
Figure 33	Mitochondrial protein levels in the *tom70*^{RIP} strain	124
Figure 34	Analysis of the TOM, TOB, and porin complexes in mitochondria lacking Tom70	125
Figure 35	Import and assembly of mitochondrial precursor proteins into mitochondria lacking Tom70	126

Abbreviations

↓	depleted amount of a given protein
A	alanine
Å	Angstroms
AAC	ADP/ATP carrier
ADP	adenosine diphosphate
ATP	adenosine triphosphate
BSA	bovine serum albumin
ben	benomyl
BNGE	blue native gel electrophoresis
bp	base pair
°C	degree Celsius
C-terminus	hydroxyl termini
CCHL	cytochrome *c* heme lyase
cDNA	complementary deoxyribonucleic acid
Δ	deletion
DHFR	dehydrofolate reductase
DMSO	dimethylsulfoxide
DNA	deoxyribonucleic acid
dNTP	deoxy nucleotide triphosphate
E. coli	*Escherichia coli*
ECL	enhanced chemiluminescence
EDTA	ethylendinitrilo tetra acetic acid
EM	EDTA, MOPS
ETC	electron transport chain
F1β	F1 beta subunit of the ATP synthase
$FADH_2$	flavin adenine dinucleotide, reduced form
Fe-S	iron sulfur
fpa	p-fluoro-DL-phenyl-alanine
g	gravitational force
GTP	guanine triphosphate
hr	hour
his	histidine
IMS	intermembrane space
IPTG	isopropyl-beta-D-thiogalactopyranoside
JTT	Jones-Taylor-Thornton substitution matrix
kb	kilo basepair
kDa	kilo Dalton
KO	knockout
kV	kilo Volt
L	leucine
LG	linkage group
µg	microgram
µl	microliter
µm	micrometer

M	molar
mg	milligram
MIM	mitochondrial inner membrane
min	minute
MIP	mitochondrial intermediate peptidase
ml	milliliter
mM	millimolar
MOM	mitochondrial outer membrane
MOPS	4-morpholinepropanesulfonic acid
mRNA	messenger ribonucleic acid
MSF	mitochondrial import stimulating factor
mtDNA	mitochondrial deoxyribonucleic acid
N. crassa	*Neurospora crassa*
N-terminus	amino terminus
NAD^+	nicotinamide adenine dinucleotide, oxidized form
NADH	nicotinamide adenine dinucleotide, reduced form
NiNTA	nickel-nitrilotriacetic acid
nm	nanometer
OMV	outer membrane vesicle
OXA	oxidase assembly mutant
PAGE	polyacrylamide gel electrophoresis
PAM	presequence translocase associated motor
pan	pantothenate
PCR	polymerase chain reaction
PMSF	phenylmethylsulfonyl fluoride
PVDF	polyvinylidene fluoride
^{R}	resistant
RIP	repeat induced point mutation
RNA	ribonucleic acid
rpm	rotations per minute
rRNA	ribosomal ribonucleic acid
s	second
S. cerevisiae	*Saccharomyces cerevisiae*
S. pombe	*Schizosaccharomyces pombe*
SDS	sodium dodecyl sulfate
sdH_2O	sterile distilled water
SEM	sucrose, EDTA, MOPS
SEMP	sucrose, EDTA, MOPS, PMSF
SEMK	sucrose, EDTA, MOPS, potassium chloride
TCA	trichloroacetic acid
TEM	transmission electron microscopy
TIM	translocase of the inner mitochondrial membrane
TMD	transmembrane domain
Tris	tris (hydroxymethyl) aminomethane
TOB	topogenesis of mitochondrial outer membrane beta-barrels
TOM	translocase of the outer mitochondrial membrane

tRNA	transfer ribonucleic acid
TPR	tetratricopeptide repeat
UTR	untranslated region
V	Volt
VDAC	voltage dependent anion channel
vol	volume
w/vol	weight per volume

1. Introduction

1.1 Mitochondrial Functions and mtDNA

Mitochondria are eukaryotic organelles 0.25 to 1.5 μm in diameter that consist of four compartments: the mitochondrial outer membrane (MOM), the intermembrane space (IMS), the mitochondrial inner membrane (MIM), and the matrix (Nicastro *et al.*, 2000; Griparic and van der Bliek, 2001; Mannella, 2006). Mitochondria are involved in multiple pathways in the eukaryotic cell, including the function of generating adenosine triphosphate (ATP) via oxidative phosphorylation, iron sulfur (Fe-S) cluster metabolism, beta-oxidation of fatty acids, calcium regulation, and the biosynthesis of cellular metabolites (Attardi and Schatz, 1988; Saraste, 1999; Lill and Kispal, 2000; Gunter *et al.*, 2004; Bartlett and Eaton, 2004; Joseph-Horne *et al.*, 2001; Lill and Muhlenhoff, 2005; Graier *et al.*, 2007).

ATP synthesis occurs through the oxidation of electron carriers and the reduction of molecular oxygen (Attardi and Schatz, 1988; Saraste, 1999; Joseph-Horne *et al.*, 2001). Electrons are transported from various metabolic processes, such as glycolysis, the Krebs cycle, and beta-oxidation, by the electron carriers $NADH+H^+$ and $FADH_2$ to the electron transport chain (ETC). The ETC is a series of four large redox complexes (named Complex I, II, III, and IV) and smaller carrier molecules located in the MIM. By passing the electrons through the chain a hydrogen ion gradient is generated across the MIM which is used to power complex V, an ATP synthase, for the production of ATP. The reduced electron carriers are then available for the continuation of glycolysis and the Kreb cycle (Joseph-Horne *et al.*, 2001). Alternative oxidases are found in higher plants, some protists, some animals (not mammals), and some fungi. This enzyme shuttles electrons directly from ubiquinol to molecular oxygen allowing bypass of Complexes III and IV. At times when the latter complexes are not functional, this allows continued electron flow and ATP production (Lambowitz *et al.*, 1972; Vanlerberghe and McIntosh, 1997; Joseph-Horne *et al.*, 2001; McDonald and Vanlerberghe, 2004; Chaudhuri *et al.*, 2006; Chae *et al.*, 2007).

Mitochondrial genomes vary in size in different classes of organisms, but even the largest encode only a small fraction of the proteins required for complete mitochondrial

function (Attardi and Schatz, 1988; Gray *et al.*, 2004). The mitochondrial genome in *Neurospora crassa* is 65 kbp in size, encoding for 14 protein components of the oxidative phosphorylation system as well as mitochondrial tRNAs and rRNAs, the 5S ribosome subunit, and maturases (Kennell *et al.*, 2004). However, the vast majority of proteins in mitochondria are encoded in the nucleus, translated on cytosolic ribosomes, and imported into mitochondria (Wiedmann *et al.*, 2003; Pfanner *et al.*, 2004; Paschen *et al.*, 2005). Mitochondria have become increasingly important from a medical standpoint as aging and a growing number of human diseases are being related to this organelle (Schapira, 1999; Singh, 2004; Detmer and Chan, 2007; MacKenzie and Payne, 2007; Petrozzi *et al.*, 2007).

1.2 Evolution of Mitochondria

Mitochondria are the result of an endosymbiotic event involving a bacterial endosymbiont and a host. Alpha-proteobacteria are accepted as the ancestors to mitochondria based on phylogenetic analysis using rRNA and protein coding genes, and homologous gene arrangements (Lang *et al.*, 1997, Lang *et al.*, 1999b; Andersson *et al.*, 1998; Gray *et al.*, 1999). The nature of the host is a matter of debate, but was most likely either a primitive nucleus-containing-eukaryote or archaea-related prokaryote (Gray *et al.*, 1999; Lang *et al.*, 1999a; Poole and Penny, 2007). Subsequent gene loss from the endosymbiont to the host genome led to the small size of the present day mitochondrial genome (Margulis, 1975; Gray *et al.*, 1999; Lang *et al.*, 1999a).

There are various models to explain the driving force for the endosymbiotic event that resulted in mitochondria. The hydrogen hypothesis is a relatively recent model that proposes a symbiotic metabolic association between an anaerobic autotrophic host and a fermentative (alpha-proteobacterial) symbiont in an anaerobic environment (Martin and Muller, 1998). The symbiont provided hydrogen to the host in return for metabolites. As dependence increased, so did cell-to-cell contact and eventually the host engulfed the symbiont. Although mitochondria now provide ATP to the cell, it was unlikely that this was the initial driving force for the endosymbiotic event because it is doubtful that the host was unable to produce enough ATP for its own survival or that the symbiont would excrete excess ATP (Martin and Muller, 1998).

Some extant eukaryotic lineages lack true mitochondria, but contain related organelles. These are proposed to be post-endosymbiotic eukaryotes but due to differences in metabolic requirements their mitochondria subsequently lost various functions (Andersson and Kurland, 1999; Gray *et al.*, 1999; Lang *et al.*, 1999a). Hydrogenosomes are remnant mitochondria which typically lack a genome but do possess a double membrane, enzymes involved in Fe-S cluster synthesis and produce ATP anaerobically with hydrogen as the end product (Muller, 1993; Anderson and Kurland, 1999; Embley *et al.*, 2003; Sutak *et al.*, 2004; Lill and Muhlenhoff, 2005; Hackstein *et al.*, 2006). Mitosomes are small organelles that do not produce ATP (Tovar *et al.*, 1999; Hackstein *et al.*, 2006). Nevertheless, they are thought to represent the remnants of mitochondria since they have a double membrane and contain enzymes required for Fe-S cluster synthesis (Tovar *et al.*, 1999; Hackstein *et al.*, 2006). Other characteristics that suggest a relationship of both hydrogenosomes and mitosomes to mitochondria are the presence of α-proteobacterial genes in the nuclear genome of the host and the similarity of the protein import pathways into these organelles (Plumper *et al.*, 2000; Dyall *et al.*, 2000; Embley *et al.*, 2003; Hackstein *et al.*, 2006). For example, Dyall *et al.* (2000) isolated a hydrogenosomal ADP/ATP carrier (AAC) which could be imported into the MIM of *Saccharomyces cerevisiae* through the Tim9-10 and TIM22 (Translocase of the Inner mitochondrial Membrane) pathway. In addition, the hydrogenosomal AAC import required ATP for receptor-chaperone interactions, membrane potential, the presence of cytosolic proteins, and was protease sensitive; all characteristics of known mitochondrial protein import pathways (Plumper *et al.*, 2000). Furthermore, research in *Trichomonas vaginalis* revealed Hmp35, a predicted beta-barrel protein located in the hydrogenosomal outer membrane in a 300 kDa complex that may be homologous in function to Tom40 (Dyall *et al.*, 2006). Mitosomes were also shown to use mitochondrial targeting signals for the localization of the eubacterial-derived Cpn60, a protein found in mitochondria of other eukaryotes (Tovar *et al.*, 1999). Finally, a rudimentary genome found in the hydrogenosome of *Nyctotherus ovalis* that encodes mitochondria-type electron transport chain components provides additional compelling evidence for the relationship between hydrogenosomes and mitochondria (Boxma *et al.*, 2005).

1.3 Mitochondrial Morphology

Mitochondria are dynamic organelles that undergo constant fission and fusion, form tubular networks, and move along cytoskeletal elements (Okamoto and Shaw, 2005). Fission is a GTP-dependent process by which mitochondria divide. When this pathway is blocked mitochondria form large interconnected tubules (Okamoto and Shaw, 2005; Hoppins *et al.*, 2007a). Fusion is a GTP- and MIM potential-dependent process by which mitochondria combine. Small, fragmented mitochondria result from defects in this pathway (Okamoto and Shaw, 2005; Hoppins *et al.*, 2007a).

Defects in tubulation result in large spherical mitochondria (Okamoto and Shaw, 2005). Mitochondrial tubulation in yeast requires a complex composed of Mmm1, Mdm10, Mdm12, and Mmm2 (Burgess *et al.*, 1994; Sogo and Yaffe, 1994; Berger *et al.*, 1997; Boldogh *et al.*, 2003; Youngman *et al.*, 2004). In addition to its role in maintaining mitochondrial morphology, the complex is also required for mitochondrial attachment to actin, control of movement, and inheritance of mtDNA (Boldogh *et al.*, 1998; Boldogh *et al.*, 2003). In *N. crassa*, *Schizosaccharomyces pombe*, and mammals mitochondrial movement is microtubule based (Heggeness *et al.*, 1978; Yaffe *et al.*, 1996; Steinberg and Schliwa, 1993; Fuchs *et al.*, 2002). Lack of Mmm1 in *N. crassa* alters only mitochondrial morphology and mitochondria are still able to bind microtubules *in vitro* (Prokisch *et al.*, 2000; Fuchs *et al.*, 2002). Interestingly, *N. crassa* Mmm1 restores mitochondrial morphology and mtDNA inheritance in yeast *mmm1* deletion (Δ) strains, indicating a conservation of function (Kondo-Okamoto *et al.*, 2003).

Recently, additional roles for Mdm10, Mdm12, and Mmm1 in the import and assembly of beta-barrel proteins have been suggested in yeast (see section 1.4.11.2) (Meisinger *et al.*, 2006; Stojanovski *et al.*, 2006; Meisinger *et al.*, 2007). Furthermore, a yeast screen identified the TOM (Translocase of the Outer mitochondrial Membrane), TOB (Topogenesis of mitochondrial Outer membrane beta-Barrels) and TIM23 (Translocase of the Inner mitochondrial Membrane) complexes as involved in mitochondrial morphology due to aberrant morphology phenotypes resulting from the depletion of certain subunits (Altmann and Westermann, 2005). These data indicate an interesting connection between the import and assembly of beta-barrel proteins and mitochondrial morphology.

1.4 Mitochondrial Import

Most mitochondrial proteins are nuclear-encoded and translated on cytosolic ribosomes. These proteins are synthesized as precursors that contain targeting signals to ensure their import into mitochondria. The process of importing proteins into mitochondria requires the action of several complexes in the MOM, IMS, and MIM.

The MOM contains two main complexes required for protein import. The TOM complex mediates the recognition and translocation of most nuclear-encoded mitochondrial precursor proteins into or across the MOM (Fig. 1) (Prokisch *et al.*, 2002; Koehler, 2004; Neupert and Herrmann, 2007). From the TOM complex, proteins are sorted to additional complexes to reach their final mitochondrial destination. One of these is the second import complex of the MOM, the TOB complex (Wiedmann *et al.*, 2003; Pfanner *et al.*, 2004; Paschen *et al.*, 2005; Habib *et al.*, 2005). The TOB complex is required for the proper assembly and insertion of beta-barrel proteins into the MOM (Kozjak *et al.*, 2003; Wiedemann *et al.*, 2003; Paschen *et al.*, 2003). Mitochondrial beta-barrel proteins include Tom40, porin, Tob55, Mmm2, and Mdm10.

The IMS contains the Tim8-Tim13 and Tim9-Tim10 complexes which are chaperone-like complexes involved in mediating the transfer of protein intermediates from the TOM complex to the TOB complex or to the TIM22 complex (Koehler *et al.*, 1998; Bauer *et al.*, 2000; Davis *et al.*, 2000; Paschen *et al.*, 2000; Wiedemann *et al.*, 2003; Hoppins and Nargang, 2004). In addition to these well known pathways of translocation, recent research has indicated an import and assembly pathway for MOM proteins anchored by multiple alpha-helical transmembrane segments which requires Tom70 and IMS components but not the TOM complex (Otera *et al.*, 2007). This pathway is ATP-dependent for membrane integration following targeting by Tom70, but the exact mechanisms of integration are unknown (Otera *et al.*, 2007).

The MIM contains three main complexes involved in protein import and export: the TIM23, TIM22, and OXA (Oxidase Assembly) complexes. The TIM23 complex imports precursor proteins with N-terminal presequences through the MIM to the matrix with the assistance of the PAM

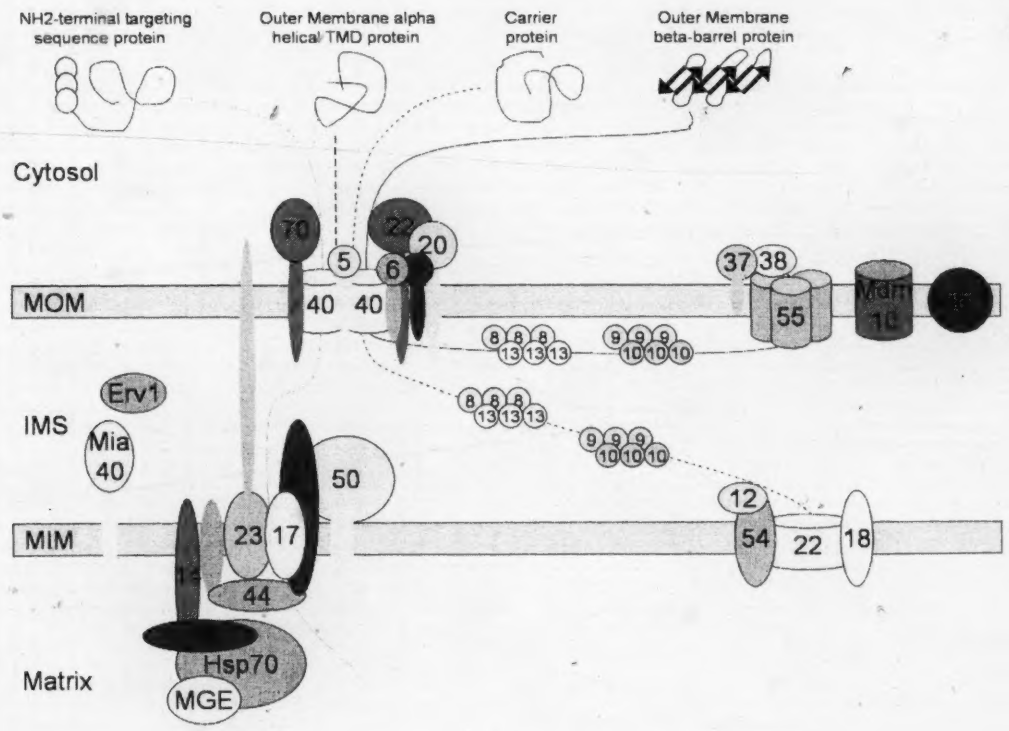

Figure 1: *Neurospora crassa* mitochondrial import machinery. The TOM core complex consists of Tom40, Tom22, Tom7, Tom6, and Tom5. Tom70 and Tom20 serve as cytosolic receptors and are part of the TOM holo-complex. The core TOB complex consists of Tob55, Tob37 and Tob38, while Mim1 and Mdm10 may also have more transient associations with the complex. Proteins are transferred from the TOM complex to the TOB complex via the intermembrane space complexes Tim8-Tim13 or Tim9-Tim10. The TIM22 complex is responsible for importing certain classes of inner membrane proteins. The TIM23 complex is responsible for importing matrix proteins and also imports some inner membrane proteins with single transmembrane domains by the stop transfer pathway. Mia40 and Erv1 are involved in import and assembly of IMS proteins.

(Presequence Translocase associated Motor) complex which provides energy required for translocation across the MIM via ATP hydrolysis (Bauer *et al.*, 2000; Prokisch *et al.*, 2002; Neupert and Herrmann, 2007). The TIM22 complex imports hydrophobic precursor proteins with multiple transmembrane domains (TMD) and internal targeting sequences into the MIM. This requires a membrane potential but not ATP (Bauer *et al.*, 2000; Prokisch *et al.*, 2002; Neupert and Herrmann, 2007). The OXA complex is involved in mitochondrial-encoded or nuclear-encoded protein insertion from the matrix into the MIM, also referred to as mitochondrial protein export (Nargang *et al.*, 2002; Stuart, 2002; Hermann and Bonnefoy, 2004; Koehler, 2004; Fiumera *et al.*, 2007).

1.4.1 The TOM Complex

The TOM complex is responsible for the recognition and import through the MOM of most mitochondrial precursor proteins from the cytosol. The core TOM complex consists of Tom40, Tom22, Tom7, Tom6, and Tom5 (Dekker *et al.*, 1998). The holo-complex also contains the receptor proteins Tom70 and Tom20 which are less tightly associated (Dekker *et al.*, 1998).

1.4.1.1 Tom 40

Tom40 is a MOM beta-barrel protein which forms the translocation pore of the TOM complex and is essential in yeast and *N. crassa* (Baker *et al.*, 1990; Hill *et al.*, 1998; Ahting *et al.*, 2001; Taylor *et al.*, 2003). Yeast Tom40 was predicted to contain 33 to 43% beta-sheets and *N. crassa* Tom40 to contain 30 to 46% beta-sheets based on circular dichroism spectroscopy and computer predictions (Court *et al.*, 1995; Hill *et al.*, 1998; Ahting *et al.*, 2001; Becker *et al.*, 2005). However, it should be noted that the number and position of beta-sheets predicted varies using different computer programs. Both the N- and C-termini of Tom40 are predicted to be located in the IMS (Kunkele *et al.*, 1998; Becker *et al.*, 2005). The other TOM complex members are anchored to the MOM by membrane-spanning alpha helices and are involved in complex stability, precursor protein binding sites, and receptor functions (Dekker *et al.*, 1998; Rapaport *et al.*, 1998a; Rapaport, 2002). Dimers of Tom40 are thought to form channel units roughly 22 Å wide (Hill *et al.*, 1998; Ahting *et* al., 1999). Each TOM complex is proposed to

contain two channels which are cation-selective, voltage-gated and present in multiple conductance states (Hill *et al.*, 1998; Künkele *et al.*, 1998; Rapaport *et al.*, 1998a; Ahting *et* al., 1999). The channels can be visualized by electron microscopy (Ahting *et al.*, 1999). A third channel seen in a fraction of the purified holo-complex molecules disappears upon removal of Tom70 and Tom20 (Ahting *et al.*, 1999).

Tom40 is also involved in the formation of the so-called *cis* (cytosolic side) and *trans* (IMS side) binding sites which, in association with other TOM complex members, bind precursor proteins in transit to move them sequentially through the MOM (Rapaport *et al.*, 1998b). During precursor protein translocation, Tom40 undergoes various structural rearrangements and alterations in pore gating which are probably involved in the movement of precursor protein across the MOM and are triggered by the binding of the precursor protein presequences (Hill *et al.*, 1998; Rapaport *et al.*, 1998a; Rapaport *et al.*, 1998b).

Depletion of Tom40 in *N. crassa* resulted in reduced steady state levels of Tom22 and Tom6 and deficient import of mitochondrial precursor proteins including the matrix protein MPP (mitochondrial processing peptidase) and the MIM protein AAC (Taylor *et al.*, 2003). Mitochondria depleted of Tom40 (Tom40↓)[1] were smaller than wildtype and contained virtually no cristae as determined by transmission electron microscopy (TEM) (Taylor *et al.*, 2003).

1.4.1.2 Tom20 and Tom22

The majority of mitochondrial proteins are post-translationally imported, although some examples of co-translational import have been shown for proteins with rapid folding kinetics (Fujiki and Verner, 1993; Sylvestre *et al.*, 2003; Ahmed *et al.*, 2006). Translated precursor proteins are maintained in an unfolded or loosely folded import-competent state by cytosolic chaperones such as Hsp70 and mitochondrial import stimulating factor (MSF) (Komiya *et al.*, 1997; Beddoe and Lithgow, 2002). Precursor proteins are recognized by receptors that are part of the TOM holo complex which have large domains that extend into the cytosol for protein-protein interactions. The TOM

[1] Throughout this thesis, a protein name followed by a downward pointing arrow will indicate that the protein is depleted in amount.

complex contains two receptor proteins: Tom20, and Tom70 (Hines *et al.*, 1990; Harkness *et al.*, 1994b; Endo and Kohda, 2002). The cytosolic domain of Tom22 is also thought to act as a receptor in conjunction with Tom20 (Mayer *et al.*, 1995).

Tom20 contains an N-terminal anchor in the MOM and a large cytosolic C-terminal domain that contains a tetratricopeptide repeat (TPR) motif involved in protein-protein interactions (Harkness *et al.*, 1994b; Blatch and Lassle, 1999). The majority of precursor proteins are targeted to mitochondria by non-homologous, but structurally conserved, presequences usually consisting of 20 to 60 residues. The presequences are enriched for positively charged, hydrophobic, and hydroxylated residues that form an amphipathic alpha-helix when recognized and bound by Tom20 (Endo and Kohda, 2002). Structural studies have revealed that the Tom20 C-terminal domain forms a series of alpha helices, including the TPR domain, which form a groove that binds a variety of presequences via hydrophobic interactions (Abe *et al.*, 2000; Endo and Kohda, 2002). Further studies showed that Tom20 is capable of interactions with the presequences in different structural modes and the presequences have mobility within the groove, suggesting a dynamic recognition mechanism by which a broad range of signal sequences might be recognized (Abe *et al.*, 2000; Saitoh *et al.*, 2007). Tom20 is thought to contribute to the formation of the *cis* binding site of the TOM complex from which precursor proteins are then guided to the TOM complex pore via Tom22 (Kiebler *et al.*, 1993; Mayer *et al.*, 1995).

Tom20 and Tom70 are not independently essential in either yeast or *N. crassa*, but deletion of both receptors in yeast is lethal (Ramage *et al.*, 1993). Cells lacking Tom20 grow slowly, have reduced steady state levels of Tom22 and MIM proteins, increased steady state levels of Hsp70, and have reduced import rates of most mitochondrial proteins (Ramage *et al.*, 1993; Harkness *et al.*, 1994a; Harkness *et al.*, 1994b). *N. crassa* mitochondria lacking Tom20 were decreased in size and lacked cristae (Harkness *et al.*, 1994b). Yeast cells lacking Tom20 were unable to grow on nonfermentable carbon sources, but this phenotype could be overcome by the overexpression of Tom70, indicating a degree of functional redundancy (Ramage *et al.*, 1993). Later research in yeast showed that the defects in the *tom20*Δ mutants were in part due to subsequent decreased levels of Tom22, and that the lethality and import

defects of the *tom20Δ/tom70Δ* double mutant is overcome if Tom22 levels are restored (Ramage *et al.*, 1993; Lithgow *et al.*, 1994). Insertion and assembly of Tom20 and Tom70 into the MOM in yeast require Mim1, a protein proposed interact with the TOB complex (see section 1.4.11.1) (Popov-Celeketic *et al.*, 2007; Becker *et al.*, 2008; Hulett *et al.*, 2008).

Unlike the other TOM complex receptors, Tom22 contains a central TMD resulting in both cytosolic and IMS precursor protein binding domains (Lithgow *et al.*, 1994; Nargang *et al.*, 1995; van Wilpe *et al.*, 1999). Tom22 functions with Tom20 and Tom70 to pass precursor proteins from the receptors to the Tom40 pore (Kiebler *et al.*, 1993; Mayer *et al.*, 1995; Nargang *et al.*, 1995). Tom22 also functions as the binding site of Tom20 and Tom70 to the TOM complex, as mutants lacking Tom22 are also deficient in Tom20 and Tom70 (van Wilpe *et al.*, 1999). In yeast, Tom22 is not essential but deletion of the protein resulted in severely reduced growth, loss of mtDNA, and decreased import of mitochondrial proteins (van Wilpe *et al.*, 1999). Tom22 is essential in *N. crassa* (Nargang *et al.*, 1995). Depletion of Tom22 in *N. crassa* resulted in reduced growth, reduced steady state levels of Tom20 and reduced import of most mitochondrial proteins (Nargang *et al.*, 1995). Tom22 depleted mitochondria were also decreased in size and lacked cristae, although not to the same extent as observed in mitochondria lacking Tom20 (Harkness *et al.*, 1994b; Nargang *et al.*, 1995). Import and assembly of Tom22 has been shown to be dependent on the TOB complex (see section 1.4.12) (Stojanovski *et al.*, 2007).

1.4.1.3 Tom70

Tom70 is a large receptor protein of the TOM complex which contains an N-terminal anchor and a large cytosolic domain containing seven TPR motifs (Hines *et al.*, 1990; Blatch and Lassle, 1999). The protein is not essential in either yeast or *N. crassa* (Hines *et al.*, 1990; Grad *et al.*, 1999). Tom70 is the receptor protein responsible for the recognition of a major class of mitochondrial precursor proteins with internal targeting signals, the carrier family proteins of the MIM (Hines *et al.*, 1990; Komiya *et al.*, 1997). Previous research indicated Tob37 (then called Tom37) and Tom70 functioned as a heterodimer in the import of MSF-bound precursor proteins, but further research

disproved this hypothesis (see section 1.4.13) (Gratzer *et al.*, 1995; Hachiya *et al.*, 1995; Ryan *et al.*, 1999).

Substrates for Tom70 are highly hydrophobic precursor proteins which require chaperones, such as MSF, to be maintained in an unfolded state in the cytosol (Hachiya *et al.*, 1995; Komiya *et al.*, 1997; Endo and Kohda, 2002). Tom70 has been shown to interact with both molecular chaperones and the AAC precursor protein (Hachiya *et al.*, 1995; Komiya *et al.*, 1997). MSF-bound precursor proteins interact initially with Tom70 and, following ATP hydrolysis to release MSF, are transferred to the Tom20-Tom22 receptor for import into mitochondria, although these proteins can be imported more slowly by just the Tom20-Tom22 receptor (Steger *et al.*, 1990; Hachiya *et al.*, 1995; Komiya *et al.*, 1997). *N. crassa* cells lacking Tom70 had a slightly reduced growth rate in contrast to the more severe growth rate reductions observed in cells lacking Tom20 or deficient in Tom22 (Hines *et al.*, 1990; Harkness *et al.*, 1994b; Nargang *et al.*, 1995; Grad *et al.*, 1999). This supports the model that Tom70 increases the efficiency of importing some proteins via the Tom20-Tom22 receptor (Steger *et al.*, 1990; Ramage *et al.*, 1993). *N. crassa* cells lacking Tom70 had enlarged mitochondria with disorganized cristae in contrast to the small cristae and reduced mitochondrial size observed in cells lacking Tom20 or Tom22 (Harkness *et al.*, 1994b; Nargang *et al.*, 1995; Grad *et al.*, 1999).

S. cerevisiae contains Tom71, a protein with 53% sequence identity to Tom70, which can be co-immunoprecipitated with Tom70 and Tom40 (Schlossmann *et al.*, 1996). The protein binds AAC, and contains the seven TPR motifs found in Tom70 (Schlossmann *et al.*, 1996). Tom70 and Tom71 have been shown to function directly in the recruitment of the soluble protein Mfb1 to the mitochondrial surface, (Kondo-Okamoto *et al.*, 2007). Other components do not appear to be necessary, as Mfb1 is properly targeted to mitochondria in *mmm1*Δ, *mmm2*Δ, *mdm10*Δ, *mdm12*Δ, *tob37*Δ, and *tom7*Δ cells, and in Tom40 and Tob55 temperature sensitive mutants generated by error-prone PCR (Kondo-Okamoto *et al.*, 2006). Mfb1 is involved in mitochondrial morphology and is an F-box protein required for the regulation of the length and connectivity of mitochondrial tubules (Durr *et al.*, 2006; Kondo-Okamoto *et al.*, 2006). The mitochondrial morphological phenotypes seen in *tom70/tom71* double knockouts

were likely due to decreased Mfb1 mitochondrial localization (Kondo-Okamoto *et al.*, 2007). *N. crassa* does not have a Tom71 homolog and the functions of both Tom70 and Tom71 are thought to be performed by Tom70 (Schlossmann and Neupert, 1995; Grad *et al.*, 1999).

1.4.1.4 The Small Toms

The small Tom proteins, Tom5, Tom6, and Tom7, are components of the TOM core complex (Dekker *et al.*, 1998; Ahting *et al.*, 1999). They are anchored to the MOM by membrane-spanning alpha helices and are involved in complex assembly, stability, and precursor protein binding sites (Dekker *et al.*, 1998; Ahting *et al.*, 1999; Model *et al.*, 2001; Sherman *et al.*, 2005). In yeast, Tom7 is involved in precursor protein sorting and the formation of the TOM complex *trans* binding site (Honlinger *et al.*, 1996; Esaki *et al.*, 2004). Tom6 is thought to promote the stable association of Tom40 and Tom22, but Tom7 seems to be involved in destabilizing this core complex (Honlinger *et al.*, 1996; Dekker *et al.*, 1998; Model *et al.*, 2001). Deletion of Tom7 resulted in enlarged mitochondrial morphology in yeast (Meisinger *et al.*, 2006). This was not observed in yeast lacking Tom6 or Tom5 (Meisinger *et al.*, 2006). Cells lacking Tom7 also had greatly reduced steady state levels and import rates of porin (Honlinger *et al.*, 1996). Yeast cells lacking Tom5 grew more slowly and had reduced import rates of precursor proteins to all mitochondrial subcompartments (Dietmeier *et al.*, 1997). In addition, *tom5*Δ was synthetically lethal when combined with the absence of Tom6, Tom7, Tob37, Tom20 or Tom70 (Honlinger *et al.*, 1996; Dietmeier *et al.*, 1997).

In *N. crassa*, Tom6 was shown to interact with Tom22 and Tom40 and this interaction was variable depending on precursor binding (Dembowski, *et al.*, 2001). A similar interaction with Tom22 was not observed for Tom7, although Tom7 was shown to interact with Tom40 (Dembowski, *et al.*, 2001). *N. crassa* Tom5 rescued the yeast *tom5*Δ mutant, but *N. crassa* cells lacking Tom5 did not exhibit the growth or protein import defects observed in yeast (Dietmeier *et al.*, 1997; Schmitt *et al.*, 2005). *N. crassa* double knockouts of *tom5*/*tom6* or *tom5*/*tom7* did not exhibit a growth phenotype, but *tom6*/*tom7* had serious growth defects (Sherman *et al.*, 2005). Genetic crosses designed to produce a triple knockout of the small Tom proteins in *N. crassa* were unsuccessful,

suggesting that the loss of all small Toms is lethal (Sherman *et al.*, 2005). The loss of Tom6/Tom7 resulted in decreased steady state levels of Tom5, Tom20 and Tom22, and increased levels of Tob55 (Sherman *et al.*, 2005).

1.4.2 Assembly of the TOM Complex

Tom20 and Tom70 were once thought to interact directly with Tom40 (Schneider *et al.*, 1991; Schlossmann and Neupert, 1995) but now have been shown to require Mim1 for their insertion and assembly (Popov-Celeketic *et al.*, 2007; Becker *et al.*, 2008; Hulett *et al.*, 2008). Tom22 requires an existing Tom20-Tom22 receptor, Tom70, and the TOB complex for efficient import and correct assembly (see section 1.4.12) (Model *et al.*, 2001; Stojanovski *et al.*, 2007). Tom6 and Tom7 require the Tom20-Tom22 receptor whereas Tom5 does not require any of the TOM receptors; though all small Toms have been shown to require Tob37 for assembly into the TOM complex (see section 1.4.12) (Dembowski *et al.*, 2001; Model *et al.*, 2001; Horie *et al.*, 2003; Stojanovski *et al.*, 2007).

The Tom40 assembly pathway has been studied extensively in yeast and *N. crassa*, though not all of the details discussed below have been verified in *N. crassa*. In a few cases the data differ in the two organisms as noted. The Tom40 precursor is recognized on the cytosolic side of the MOM by the Tom20-Tom22 and Tom70 receptors as well as Tom5, though the latter subunit does not appear to be involved in the process in *N. crassa* (Model *et al.*, 2001; Sherman *et al.*, 2005). In *S. cerevisiae*, Tom7 is involved in releasing the Tom40 precursor from the TOM receptors (Honlinger *et al.*, 1996; Model *et al.*, 2001; Esaki *et al.*, 2004). When the Tom40 precursor crosses the MOM it interacts with soluble IMS complexes, Tim8-Tim13 or Tim9-Tim10 (Hoppins and Nargang, 2004; Wiedemann *et al.*, 2004). The small Tim complexes are thought to act as chaperones that guide the incoming Tom40 precursor to the IMS side of the TOB complex, where it forms assembly intermediate I in the Tom40 assembly pathway (Rapaport and Neupert, 1999; Model *et al.*, 2001).

Assembly intermediate I represents the Tom40 precursor bound to the TOB complex (Fig. 2) (Paschen *et al.*, 2003; Wiedemann *et al.*, 2003; Pfanner *et al.*, 2004) (The role of the TOB complex in Tom40 assembly into the TOM complex is discussed

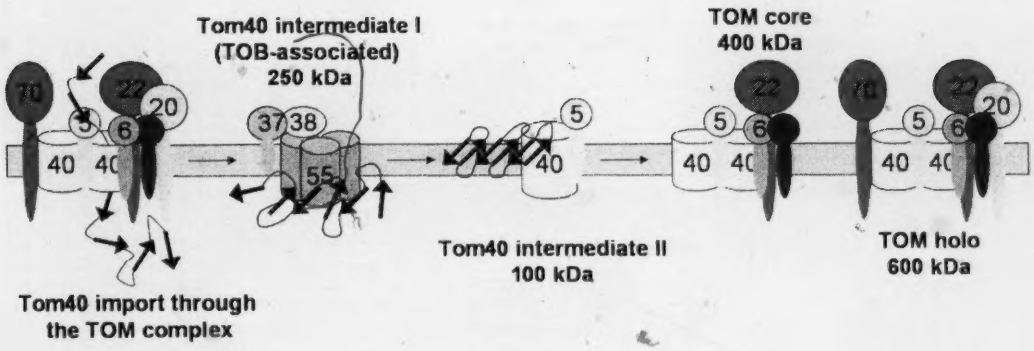

Figure 2: The Tom40 assembly pathway. A Tom40 precursor protein (as indicated by the thin line containing arrows to represent beta-strands) is transferred across the MOM through an existing TOM complex and then transferred to the TOB complex via the small Tim complexes of the IMS. The incoming Tom40 molecule associated with the TOB complex forms assembly intermediate I. Once inserted into the MOM, Tom40 interacts with Tom5 and an existing Tom40 molecule, forming assembly intermediate II. Assembly intermediate II then interacts with Tom6, Tom7, Tom22, and other pre-existing Tom40 dimers to form the TOM holo complex.

more fully in section 1.4.8.). The TOB complex inserts the Tom40 precursor into the MOM and is probably involved in folding Tom40 into its beta-barrel structure (Kozjak *et al.*, 2003; Paschen *et al.*, 2005; Rapaport, 2005). Mutations in the N-terminal region of the Tom40 precursor prevent assembly past assembly intermediate I, indicating that the region may be involved in membrane integration (Rapaport *et al.*, 2001; Taylor *et al.*, 2003). Mim1 is thought to be involved in the transition from assembly intermediate I to II (see section 1.4.11.1) (Waizenegger *et al.*, 2004; Becker *et al.*, 2008).

Tom40 assembly intermediate II (100 kDa) is formed following or during the insertion of the Tom40 precursor into the MOM. Tom5 binds to the Tom40 precursor and associates with a preexisting Tom40 molecule, forming a dimer (Model *et al.*, 2001; Wiedemann *et al.*, 2003; Paschen *et al.*, 2005). This Tom40 dimer then assembles with other dimers and other TOM complex components to form the 400 kDa core TOM complex (Dekker *et al.*, 1998; Model *et al.*, 2001; Wiedemann *et al.*, 2004). In yeast, Tom7 is required for the assembly of Tom40 assembly intermediate II into the TOM complex, possibly by complex destabilization (Model *et al.*, 2001). Tom70 and Tom20 are not part of the TOM core complex, but associate to form the TOM holo complex (600 kDa) (Dekker *et al.*, 1998; Rapaport *et al.*, 1998a; Ahting *et al.*, 1999, Model *et al.*, 2001).

The opposing functions of yeast Tom6, which stabilizes the interaction of Tom40 and the receptor proteins, and Tom7 which destabilizes those interactions, are thought to promote the cycling of new Tom subunits into the TOM complex (Model *et al.*, 2001). As observed in yeast, the loss of Tom6 in *N. crassa* resulted in destabilization of the TOM complex (Model *et al.*, 2001; Dembowski, *et al.*, 2001; Sherman *et al.*, 2005). Unlike in yeast, loss of Tom7 in *N. crassa* also destabilizes the TOM complex and the *tom6*/*tom7* double knockout has an extremely unstable TOM complex (Sherman *et al.*, 2005). Interestingly, lack of Tom7 in *N. crassa* increased the rate of assembly of Tom40 into the TOM complex but decreased the rate of porin import (Sherman *et al.*, 2005). A similar result was observed in yeast (Meisinger *et al.*, 2006). It was suggested that Tom7 interacts with Mdm10 to modulate the balance between Tom40 and porin import (see section 1.4.11.2) (Meisinger *et al.*, 2004; Meisinger *et al.*, 2006).

A number of site-directed mutations in *N. crassa* Tom40 have been examined for their effect on the assembly of the protein (Sherman *et al.*, 2006). The assembly mutants were grouped into five classes (A to E), with wildtype as class A. Class B mutants showed slightly longer accumulation at assembly intermediate I. Class C mutants were effectively stalled at assembly intermediate I with little or no assembly to later stages in the pathway. Since both B and C classes stalled in assembly intermediate I, mutations in these classes may not allow efficient insertion of the affected Tom40 precursor into the membrane by the TOB complex. Class D mutants accumulated in assembly intermediates I and II with a smear in the 100 kDa (assembly intermediate II) region, possibly due to Tom40 in various associations with TOM complex components. Class E mutants accumulated in assembly intermediates I and II, suggesting a reduced ability to interact with appropriate assembly components at both stages. The multitude of different assembly phenotypes in Tom40 mutants highlights the numerous interactions required for the functional import and assembly of Tom40 into the TOM complex.

1.4.3 Import Components of the IMS

There are two soluble complexes in the IMS which function as chaperones for the import of hydrophilic proteins: the essential Tim9-Tim10 and the non-essential Tim8-Tim13 complexes (Koehler *et al.*, 1998; Bauer *et al.*, 2000; Paschen *et al.*, 2000). All four proteins contain a twin Cx_3C motif which is involved in the formation of disulfide bonds between cysteine residues for the formation of the 70 to 80 kDa hetero-oligomeric complexes (Koehler *et al.*, 1999; Bauer *et al.*, 2000; Curran *et al.*, 2002; Hoppins and Nargang, 2004; Hell, 2007). The Tim9-Tim10 complex is thought to sequester the membrane spanning domains of carrier proteins containing multiple TMDs and other MIM proteins, such as Tim23, during transport from the *trans* site of the TOM complex to the structurally similar Tim12 of the TIM22 complex in the MIM (Koehler *et al.*, 1998; Davis *et al.*, 2000). The Tim8-Tim13 complex interacts with an additional domain of Tim23 to prevent retrograde translocation through the TOM pore and is essential for Tim23 import in the absence of a membrane potential (Davis *et al.*, 2000; Paschen *et al.*, 2000).

The Tim8-Tim13 and Tim9-Tim10 complexes are also involved in the import of beta-barrel proteins via the TOB complex. After traversing the TOM complex in both yeast and *N. crassa*, beta-barrel precursors are transferred to the TOB complex via the small Tim complexes. The small Tim complexes have been shown to interact with the Tom40 precursor at early stages of assembly and are required for the formation of Tom40 assembly intermediate I (Wiedemann *et al.*, 2004; Hoppins and Nargang, 2004; Habib *et al.*, 2005). Association of the small Tim complexes with beta-barrel proteins may be similar to their function with Tim23, to prevent retrograde translocation through the TOM pore and sequestering the hydrophobic regions until they are associated with the TOB complex (Wiedemann *et al.*, 2004; Hoppins and Nargang, 2004).

Tim8, Tim13, Tim9 and Tim10 require Tom5 for import in yeast, although this is not observed in *N. crassa* (Kurz *et al.*, 1999; Schmitt *et al.*, 2005; Sherman *et al.*, 2005). The small Tims and proteins of the IMS that carry twin Cx_3C motifs are translocated across the MOM in a loose conformation (Chacinska *et al.*, 2004). These proteins require the action of the Mia40-Erv1 disulfide relay for stable translocation into the IMS (Chacinska *et al.*, 2004; Lu *et al.*, 2004; Mesecke *et al.*, 2005). Oxidized Mia40 acts as an import receptor via transient interactions with its substrate proteins that result in their conversion from a reduced, import competent state, to a stably folded oxidized state as a result of intramolecular disulfide bond formation (Chacinska *et al.*, 2004; Grumbt *et al.*, 2007; Hell, 2007). The reaction leaves Mia40 reduced (Grumbt *et al.*, 2007; Hell, 2007). To regain its catalytic function, Mia40 is re-oxidized by Erv1 which in turn passes its electrons to molecular oxygen or oxidized cytochrome c to achieve re-oxidation (Grumbt *et al.*, 2007; Hell, 2007).

1.4.4 The TIM23 and PAM Complexes

The TIM23 complex in the MIM recognizes presequences found at the N-terminus of precursor proteins at the TOM complex *trans* site (Berthold *et al.*, 1995; Bauer *et al.*, 2000; Neupert and Herrmann, 2007). The precursor proteins are then translocated through the TIM23 complex across the MIM with the aid of PAM complex (Berthold *et al.*, 1995; Neupert and Herrmann, 2007). The TIM23 complex consists of Tim23, Tim17, Tim50, and Tim21, and the PAM complex consists of Tim44, mtHsp70,

Mge1, Tim14/Pam18, and Tim16/Pam16 (Bauer *et al.*, 2000; Neupert and Herrmann, 2007).

Tim23 and Tim17 each contain four alpha helical TMDs and form the membrane core of the twin pore TIM23 complex (Berthold *et al.*, 1995; Martinez-Caballero *et al.*, 2007). Tim23 also contains an IMS domain involved in protein recognition and Tim17 contains a smaller IMS domain thought to be involved in pore gating (Bauer *et al.*, 1996; Chacinska *et al.*, 2005; Martinez-Caballero *et al.*, 2007). Tim50 is anchored into the MIM by an alpha helix but consists mainly of an IMS domain which interacts with the precursor proteins as they emerge from the TOM complex and passes these proteins to the TIM23 pore (Mokranjac *et al.*, 2003a). Tim21 is thought to interact with the IMS domain of Tom22 and the PAM complex to regulate associations of the TIM23 complex with the TOM complex and the PAM complex (Chacinska *et al.*, 2005; Mokranjac *et al.*, 2005). The TIM23 complex is able to transfer the presequence domain of the precursor protein in the presence of membrane potential but the PAM complex is required to translocate the remainder of the protein into the matrix (Schneider *et al.*, 1994; Berthold *et al.*, 1995; Bauer *et al.*, 2000).

Tim44 is a matrix protein that binds to the MIM and forms a binding platform for other PAM complex members (Schneider *et al.*, 1994; Berthold *et al.*, 1995). A fraction of Tim44 can be co-isolated with the membrane core of the TIM23 complex (Berthold *et al.*, 1995; Mokranjac *et al.*, 2003b). MtHsp70 is an ATP binding protein in the matrix that associates with Tim44 when ATP is bound (Schneider *et al.*, 1994; Neupert and Herrmann, 2007). In this configuration, mtHsp70-Tim44 binds the incoming precursor protein (Schneider *et al.*, 1994). One model for translocation of precursors into the matrix predicts that Tim14 stimulates mtHsp70-ATP hydrolysis resulting in mtHsp70 and the bound precursor protein being released from Tim44 (Schneider *et al.*, 1994; Neupert and Brunner, 2002; Mokranjac *et al.*, 2003b; Truscott *et al.*, 2003; Neupert and Herrmann, 2007). The bound mtHsp70 prevents the precursor from sliding back out of the pore (Schneider *et al.*, 1994). Successive steps of binding the precursor by mtHsp70 result in vectorial movement into the matrix (Schneider *et al.*, 1994). Mge1, the nucleotide exchange factor, eventually releases mtHsp70 from the preprotein to allow folding and assembly (Neupert and Brunner, 2002; Neupert and Herrmann, 2007).

Tim16 functions as a negative regulator of Tim14 (Kozany *et al.*, 2004; Neupert and Herrmann, 2007).

For correct folding and assembly the N-terminal presequence must be removed by MPP in the matrix (Gakh *et al.*, 2002). This enzymatic cleavage occurs for fully translocated matrix proteins and proteins that have been arrested in translocation by the stop-transfer pathway so that only the presequence protrudes into the matrix (Gakh *et al.*, 2002; Neupert and Herrmann, 2007). Proteins arrested by the stop-transfer pathway contain a signal following the presequence which prevents further translocation (Gakh *et al.*, 2002; Neupert and Herrmann, 2007). These proteins are destined to the MIM or IMS (Gakh *et al.*, 2002). Further enzymatic cleavage processing can involve MIP (Mitochondrial Intermediate-size Peptidase) which cleaves matrix proteins after MPP to produce the mature protein (Gakh *et al.*, 2002).

1.4.5 The TIM22 Complex

The TIM22 complex is composed of Tim54, Tim22, Tim18, and Tim12 and imports the carrier proteins (such as AAC) as well as TIM complex members Tim17, Tim22, and Tim23 to the MIM (Kerscher *et al.*, 1997; Sirrenberg *et al.*, 1998; Bauer *et al.*, 2000; Rehling *et al.*, 2003). Precursor proteins are brought from the TOM complex by the Tim9-Tim10 complex to the TIM22 complex where they dock with Tim12 (see section 1.4.3) (Koehler *et al.*, 1998; Davis *et al.*, 2000). Tim22 is an essential protein and is the pore-forming component of the complex (Kercher *et al.*, 1997; Koehler *et al.*, 1998; Sirrenberg *et al.*, 1998). Tim22 mediates the insertion of the precursor protein into the MIM in the presence of membrane potential (Pfanner and Neupert, 1985; Kovermann *et al.*, 2002; Rehling *et al.*, 2003). Protein insertion into the MIM via the TIM22 complex is driven by a series of voltage-dependent steps (Kovermann *et al.*, 2002; Rehling *et al.*, 2003). Tim54 and Tim18 are non-essential proteins that are thought to be involved in TIM22 complex assembly (Kercher *et al.*, 2000; Kovermann *et al.*, 2002).

1.4.6 The TOB Complex

The TOB complex contains three proteins: Tob55 (Sam50 in yeast, Omp85 in Gram negative bacteria), Tob37 (Tom37, Sam37 or Mas37 in yeast, Mtx1 in mammals)

and Tob38 (Tom38 or Sam35 in yeast, Mtx2 in mammals) (Abdul *et al.*, 2000; Habib *et al.*, 2005; Paschen *et al.*, 2005). The TOB complex is present at a ratio of about 1:4 compared to the TOM complex in the MOM (Wiedemann *et al.*, 2003). In yeast, Tob55 and Tob38 are essential for viability (Kozjak *et al.*, 2003; Wiedemann *et al.*, 2003; Ishikawa *et al.*, 2004; Milenkovic *et al.*, 2004; Rapaport, 2005) but Tob37 is not (Gratzer *et al.*, 1995; Wiedemann *et al.*, 2003).

1.4.6.1 Tob55

Tob55 was identified in three independent laboratories by different methods: in *N. crassa*, by a proteomic screen of MOM proteins; in yeast, by purification of the TOB complex using a tagged Tob37; and in another yeast lab by sequence comparison to bacterial beta-barrel proteins (Paschen *et al.*, 2003; Kozjak *et al.*, 2003; Gentle *et al.*, 2004). Tob55 homologs are found in all mitochondria and Gram negative bacteria (Paschen *et al.*, 2003; Voulhoux and Tommassen, 2004; Gentle *et al.*, 2004). Tob55 is a beta-barrel protein, imported through the TOM complex and assembled into the MOM with its N-terminus exposed to the IMS for precursor recognition (Habib *et al.*, 2005; Paschen *et al.*, 2005; Habib *et al.*, 2007). Tob55 is essential both in yeast and *N. crassa* (Kozjak *et al.*, 2003; Hoppins *et al.*, 2007b).

In yeast, Tob55 assembly *in vitro* was decreased in mitochondria lacking Tob37, or depleted of Tob38 or Tob55, demonstrating that the TOB complex is required for the assembly of Tob55 (Habib *et al.*, 2005). Furthermore, the *in vitro* import of Tob55 was strongly reduced in the presence of excess pSu9(1-69)- dehydrofolate reductase precursor protein and in strains of Tom40 mutants produced by error-prone PCR, indicating the involvement of the TOM complex in Tob55 import (Model *et al.*, 2001; Paschen *et al.*, 2003; Habib *et al.*, 2005).

Using yeast mitochondria containing a his-tagged version of Tob38 and co-isolation from a nickel-nitrilotriacetic acid (NiNTA) column, Habib *et al.* (2005) showed that radiolabeled precursors of Tob55 and Tob37 assembled into the TOB complex. Radiolabeled precursors of porin, Tom40, Mdm10, and Tob55 were shown to co-elute with a his-tagged version of Tob55 during *in vitro* import, indicating the role of Tob55 in the import of these beta-barrel proteins (Paschen *et al* 2003). In yeast cells depleted of

Tob55, the steady state levels of all beta-barrel proteins examined were reduced while other proteins were unaffected (Paschen *et al.*, 2003; Paschen *et al.*, 2005). Similarly in *N. crassa,* depletion of Tob55 resulted in the reduction of the steady state levels of Tom40 and porin (Hoppins *et al.*, 2007b). The level of Tom22 was also reduced, but this was thought to be due to the lack of Tom40 which reduced the assembly of Tom22 (Hoppins *et al.*, 2007b). *In vitro* import of beta-barrel proteins was also reduced in Tob55 mutants with truncated N-terminal domains, the region predicted to extend into the IMS (Habib *et al.*, 2007). This N-terminal region was shown be involved in the recognition of beta-barrel precursors (Habib *et al.*, 2007). The region was proposed to facilitate the transfer of incoming precursors from the TOM to the TOB complex (Habib *et al.*, 2007).

In Neurospora, Tob55 is alternatively spliced to produce three isoforms, long, intermediate and short. Strains expressing only the long or short forms of Tob55 were indistinguishable from wildtype when grown at 30°C (Hoppins *et al.*, 2007b). Strains expressing only the long form of Tob55 showed a decreased growth rate at 37°C or under high salt conditions (Hoppins *et al.*, 2007b). Tob55 long form strains grown at 37°C also showed decreased steady state levels of Tob55, porin, Tom40 and AAC, as well as a slight increase of Tom70. Mitochondria isolated from strains expressing only the long form of Tob55 following growth at 37°C were reduced in their ability to assemble Tom40 or porin precursors (Hoppins *et al.*, 2007b). No difference in the amounts of the various Tob55 isoforms was determined when wildtype cells were analyzed following growth at three different temperatures or at three stages of growth (Hoppins *et al.*, 2007b). The reason(s) for the existence of the different forms of Tob55 remain unknown.

1.4.6.2 Tob38

Tob38 was identified by purification of the TOB complex using tagged versions of Tob55 and Tob37, and also by analysis of MOM proteins with unknown functions (Milenkovic *et al.*, 2004; Waizenegger *et al.*, 2004; Ishikawa *et al.*, 2004; Schmitt *et al.*, 2006). Using both C-terminal and N-terminal tagged versions of Tob38, protease K treatment was found to degrade both tags in isolated mitochondria (Ishikawa *et al.*, 2004; Waizenegger *et al.*, 2004; Milenkovic *et al.*, 2004). Alkali extraction removed Tob38

from the membrane whereas sonication did not (Ishikawa *et al.*, 2004; Waizenegger *et al.*, 2004). Consistent with these findings, no TMD was detected in the sequence of the protein (Ishikawa *et al.*, 2004; Milenkovic *et al.*, 2004; Waizenegger *et al.*, 2004). Thus, Tob38 is a hydrophilic, cytosolic peripheral MOM protein (Ishikawa *et al.*, 2004; Milenkovic *et al.*, 2004; Waizenegger *et al.*, 2004). Tob38 is essential for viability in yeast (Ishikawa *et al.*, 2004; Milenkovic *et al.*, 2004; Waizenegger *et al.*, 2004).

Steady state levels of Tob38 were slightly decreased in *tob37*Δ mitochondria and significantly reduced in Tob55↓ mitochondria, indicating interactions between the three complex components (Waizenegger *et al.*, 2004). In Tob38↓ mitochondria, the steady state levels of Tob37 and Tob55 were reduced to 5 to 15% of wildtype (Waizenegger *et al.*, 2004). Depletion of Tob38 also resulted in decreased steady state levels of beta-barrel proteins while levels of other classes of mitochondrial proteins were not affected (Ishikawa, *et al.*, 2004; Waizenegger *et al.*, 2004).

A his-tagged version of Tob38 was shown to bind both Tob55 and Tob37 in pull down experiments (Waizenegger *et al.*, 2004; Habib *et al.*, 2005). TOB complex purification using a Tob38-his tagged protein showed that 80% of total Tob55, but only 15% of total Tob37 was co-eluted, suggesting a stronger association between Tob38 and Tob55 than with Tob37 (Waizenegger *et al.*, 2004). Tob55 and Tob38 also co-eluted in the absence of Tob37, although not efficiently (Waizenegger *et al.*, 2004). Radiolabeled Tom40 and Mdm10 precursors were also shown to interact with Tob38-his in pull down analysis and this interaction also occurred in the absence of Tob37 (Waizenegger *et al.*, 2004).

Import of radiolabeled Tom40 and porin precursors was also decreased in isolated mitochondria from Tob38 mutant strains generated by error-prone PCR, or Tob38↓ mitochondria (Ishikawa, *et al.*, 2004; Milenkovic *et al.*, 2004). Assembly of radiolabeled Tom40 precursor was stalled at assembly intermediate I in mitochondria containing mutant Tob38 generated by error-prone PCR, while in Tob38↓ mitochondria, Tom40 precursor associated with the 400 kDa TOM complex but did not proceed further on the assembly pathway (Ishikawa, *et al.*, 2004; Milenkovic *et al.*, 2004). This radiolabeled Tom40 associating directly with the TOM complex was shown to have increased

sensitivity to trypsin digestion and alkali extraction, suggesting the topology was incorrect and the protein was not properly assembled (Ishikawa, *et al.*, 2004).

1.4.6.3 Tob37

Tob37 was identified in a yeast screen for defects in mitochondrial membrane composition and initially thought to be associated with Tom70 as an import receptor (Gratzer *et al.*, 1995). It was later shown that Tob37 and Tom70 did not interact as import receptors and that Tob37 was a component of the TOB complex (see section 1.4.13) (Ryan *et al.*, 1999; Wiedemann *et al.*, 2003; Habib *et al.*, 2005). In yeast, Tob37 is a peripheral membrane protein facing the cytosol without a predicted TMD, but in mammals Tob37 is predicted to contain a C-terminal TMD (Armstrong *et al.*, 1997; Paschen *et al.*, 2005). Tob37 is degraded by protease and is extracted from the MOM by alkali extraction in yeast, although it appears to be more tightly bound than Tob38 (Wiedemann *et al.*, 2003; Paschen *et al.*, 2005). Tob37 is not essential in yeast, but *tob37*Δ cells grew poorly at room temperature and were non-viable at 37°C (Gratzer *et al.*, 1995; Wiedemann *et al.*, 2003).

The import of Tob37 into mitochondria was found to be independent of the TOM complex, as indicated by Tob37 import in the absence of TOM receptors, strains with Tom40 mutations, and in the presence of excess precursor proteins that utilize the TOM complex (Habib *et al.*, 2005). Tob37 appears to assemble directly into the TOB complex in a manner that depends on existing Tob38 and Tob55 in the MOM but not Tob37 (Habib *et al.*, 2005). Mitochondria containing mutant Tob55 which lacked the N-terminal region known to be located in the IMS showed decreased steady state levels of Tob37, possibly due to instability of the TOB complex (Habib *et al.*, 2007). *In vitro* import of Tom40 or porin precurors into mitochondria lacking Tob37 showed decreased levels of Tom40 assembly intermediates, the TOM complex, and porin-containing complexes (Wiedemann *et al.*, 2003; Meisinger *et al.*, 2006).

1.4.7 Defining the TOB Complex and its Components

Initially, a Tob55 and Tob38 TOB core complex was predicted to combine with Tob37 to form the TOB holo complex (Paschen *et al.*, 2003; Wiedemann *et al.*, 2003;

Waizenegger *et al.*, 2004; Ishikawa *et al.*, 2004; Habib *et al.*, 2005). However, all three subunits are now considered to form the TOB core complex (Stojanovski *et al.*, 2006; Kutik *et al.*, 2007; Neupert and Hermann, 2007). The size of TOB core, holo, and putative assembly intermediates have been variable between different labs.

Analysis in yeast by the Pfanner group showed that Tob37, Tob38, and Tob55 were in a 200 kDa complex (Kozjak *et al.*, 2003; Milenkovic *et al.*, 2004; Pfanner *et al.*, 2004), and loss of Tob37 resulted in the loss of this 200 kDa complex (Wiedemann *et al.*, 2003). A larger TOB complex (350 kDa) was observed in mitochondria lacking Tom22 or Tom7 (Wiedemann *et al.*, 2003). This 350 kDa complex was later determined to contain Mdm10, and interactions between Mdm10 and the TOB complex were later shown (Meisinger *et al.*, 2004; Meisinger *et al.*, 2007). In the absence of Tom7, the amount of the 350 kDa Mdm10-TOB complex was increased, indicating a role for Tom7 in the distribution of Mdm10 (see section 1.4.11.2) (Meisinger *et al.*, 2006). This larger 350 kDa complex was later proposed to be two distinct 350 kDa TOB complexes: one containing Mdm10 and one containing Mim1 (see section 1.4.11) (Becker *et al.*, 2008). Thus, several different TOB complexes are proposed by this group, including a 200 kDa TOB core complex containing Tob37, Tob38 and Tob55, and two additional 350 kDa TOB holo complexes including either Mdm10 or Mim1 associated with the core complex.

Research by the Rapaport group in yeast initially suggested that Tob55 was present in a 220 to 250 kDa complex which was reduced by 40 kDa with the depletion of Tob37 (Paschen *et al.*, 2003). The size of the complex was later taken to be 200 kDa (Waizenegger *et al.*, 2004; Habib *et al.*, 2005). A weak 160 kDa band was also observed in control strains and it was suggested that this was likely the TOB complex lacking Tob37, as it was the only band seen in a Tob37 deletion strain and it was shown to contain Tob38 and Tob55 (Paschen *et al.*, 2003; Waizenegger *et al.*, 2004). *In vitro* import of radiolabeled Tob55 precursor into isolated mitochondria showed that the protein appeared first in a 350 kDa complex (Habib *et al.*, 2005). Three smaller complexes, including one of 200 kDa, appeared after longer import times (Habib *et al.*, 2005). The nature of the complexes has not yet been resolved. This group proposed that the TOB complex contains Tob55, Tob38 and Tob37 at 200 to 250 kDa in size. Since

Tob37 is less tightly associated than are Tob55 and Tob38, it is sometimes not present resulting in a 160 kDa complex.

Ishikawa *et al.* (2004) used a FLAG-tagged Tob38 and detected complexes of ca. 360, 290, 230, and 170 kDa following blue native gel electrophoresis (BNGE) of isolated mitochondria. The 290, 230 and 170 kDa complexes were also detected using a FLAG-tagged Tob55. The 290 and 230 kDa bands were shifted by the addition of a Tob37 antibody in both the Tob38 and Tob55 tagged experiments (Ishikawa *et al.*, 2004). The 170 kDa band was proposed to contain only Tob38 and Tob55, explaining why it did not shift with the addition of the Tob37 antibody (Ishikawa *et al.*, 2004). This suggested differences in the associations of Tob55 and Tob38 compared to Tob37 within the TOB core complex.

Taken together, the yeast data suggest the existence of a TOB core complex of 200 to 250 kDa containing Tob55, Tob38 and Tob37. Larger complexes of about 350 kDa may represent this core complex with Mim1 or Mdm10 (see section 1.4.11) (Meisinger *et al.*, 2004; Waizenegger *et al.*, 2004; Habib *et al.*, 2005; Meisinger *et al.*, 2006; Becker *et al.*, 2008). A smaller complex of 160 to 170 kDa appears to contain only Tob55 and Tob38 (Ishikawa *et al.*, 2004; Habib *et al.*, 2005). Differences in the proposed molecular weights of the complexes in different labs are most likely due to small differences in gel systems or protein standards.

1.4.8 Interaction of Incoming Tom40 Precursor Molecules with the TOB Complex to give a Tom40 Assembly Intermediate

The TOB complex is required for the assembly of beta-barrel proteins into the MOM. The most studied beta-barrel protein assembly pathway in mitochondria is that of Tom40. As mentioned in section 1.4.2, an incoming Tom40 molecules passes through the TOM complex and associates with the TOB complex to give assembly intermediate I (Fig. 2) (Paschen *et al.*, 2003; Wiedemann *et al.*, 2003; Pfanner *et al.*, 2004). When the Tom40 precursor is inserted by the TOB complex it interacts with a preexisting Tom40 molecule already in the membrane to form assembly intermediate II (Wiedemann *et al.*, 2003; Paschen *et al.*, 2005). This Tom40 dimer then assembles with other dimers and

additional TOM components to give the 400 kDa TOM complex (Dekker *et al.*, 1998; Model *et al.*, 2001; Wiedemann *et al.*, 2004).

The Pfanner group showed that in yeast mitochondria containing a mutant Tob55 generated by error-prone PCR, the levels of Tom40 assembly intermediates and the TOM complex were decreased, with most of the Tom40 precursors accumulating in assembly intermediate I (Kozjak *et al.*, 2003). Antibody shift experiments indicated the presence of Tob37 in Tom40 assembly intermediate I, but not assembly intermediate II or the final TOM complex (Wiedemann *et al.*, 2003). Further analysis showed that *tob37*Δ mitochondria accumulate a smaller form of Tom40 assembly intermediate I and do not effectively assemble the precursor into intermediate II or the TOM complex (Wiedemann *et al.*, 2003; Meisinger *et al.*, 2006). In mitochondria containing a mutant Tob38 generated by error-prone PCR, the Tom40 precursor was found at low levels in assembly intermediate I and did not progress to intermediate II or the TOM complex (Milenkovic *et al.*, 2004). Mitochondria isolated from a strain expressing a Tob38-HA showed a shift of the Tom40 assembly intermediate I to a higher molecular weight form accounted for by the HA-tag when associated with an incoming Tom40 precursor (Milenkovic *et al.*, 2004). Therefore, Tob55, Tob38 and Tob37 are all present in Tom40 assembly intermediate I.

The Rapaport group showed that Tob55↓ mitochondria had an overall reduction in Tom40 precursor *in vitro* import and a decreased amount of both assembly intermediates (Paschen *et al.*, 2003; Habib *et al.*, 2005). Waizenegger *et al.* (2004) showed that in Tob38↓ mitochondria the amount of Tom40 assembly intermediate I and an Mdm10 assembly intermediate were greatly reduced. Mitochondria containing a his-tagged version of Tob38 were used to show that Tob38 forms part of Tom40 assembly intermediate I (Waizenegger *et al.*, 2004). In mitochondria lacking Tob37, Tob38-His interacts with a smaller Tom40 assembly intermediate I, thought to contain a smaller TOB complex lacking Tob37 (Waizenegger *et al.*, 2004).

N. crassa Tob55 has also been shown to be a component of the Tom40 assembly intermediate I and a 240 kDa intermediate of porin assembly (Hoppins *et al.*, 2007b). In addition, *in vitro* import of radiolabeled Tom40 precursor into Tob55↓ mitochondria

resulted in decreased levels of the Tom40 assembly intermediates and the TOM complex, with the Tom40 assembly intermediate I the most reduced (Hoppins *et al.*, 2007b).

1.4.9 Tob38 and Tob37 Co-dependent Relationship

Characterization of *Xenopus* Tob37 and Tob38 revealed these proteins to be homologs, and analysis of human and mouse genome databases found similar results (Adolph, 2005). Tob38↓ mitochondria in both yeast and mammals showed decreased levels of Tob37 and vice versa, indicating a co-dependent relationship (Waizenegger *et al.*, 2004; Kozjak-Pavlovic *et al.*, 2007). However, the fact that the proteins have different roles is exemplified by genetic experiments done in yeast. Over-expression of Tob37 suppressed a temperature sensitive lethality in Tob38 mutants generated by low-fidelity PCR, but did not suppress the lethality of *tob38*Δ (Chan and Lithgow, 2007). The Tob38 mutant showed decreased rates of porin and Tom40 *in vitro* import, but overexpression of Tob37 in the Tob38 mutant resulted in the low levels of Tom40 precursor being assembled more quickly into the TOM complex (Chan and Lithgow, 2007). A second Tob38 mutant had reduced steady state levels of TOB components, porin, and Tom40 (Chan and Lithgow, 2007). Overexpression of Tob37 in this Tob38 mutant strain restored these proteins to wildtype levels. Although the specific locations of these mutations were not released, these results illustrated both a partial functional overlap and specificity of Tob38 and Tob37.

Overexpression of Tob38 in *tob37*Δ cells restored the growth defects observed at 30°C but did not rescue the lethality at 37°C (Chan and Lithgow, 2007). In addition, overexpression of Tob38 in *tob37*Δ cells restored wildtype mitochondrial morphology in 90% of the cells during growth at 30°C (Chan and Lithgow, 2007). The reductions of Tob38, Tob55, and TOM complex levels observed in the *tob37*Δ strain when grown at 30°C were also restored to wildtype levels with the overexpression of Tob38 (Waizenegger *et al.*, 2004; Chan and Lithgow, 2007). Restoration of wildtype levels of Tob38 and Tob55 in *tob37*Δ cells allowed for wildtype rates of Tom40 assembly in isolated mitochondria, indicating that Tob38 and Tob55 do not require Tob37 for the import and assembly of Tom40 and that the import defects observed in *tob37*Δ are partially due to the lack of Tob38.

1.4.10 Mammalian Metaxin1 and Metaxin2

Metaxin1 (Mtx1, Tob37) is ubiquitously expressed in all mouse tissues with subcellular localization to mitochondria (Bornstein *et al.*, 1995; Armstrong *et al.*, 1997). Mice lacking Mtx1 show an early embryonic lethal phenotype (Bornstein *et al.*, 1995). Attempts to rescue the *tob37*Δ in yeast with the mammalian *mtx1* cDNA were unsuccessful (Armstrong *et al.*, 1997).

Protease susceptibility studies showed that Mtx1 is located on the cytosolic side of the MOM (Armstrong *et al.*, 1997). It is anchored to the membrane by a TMD that ends 22 amino acids prior to the C-terminus and is resistant to membrane extraction by carbonate (at pH 11.5) (Armstrong *et al.*, 1999). Two Mtx1 deletion constructs where created, one missing 15 amino acids from the C-terminus (Mtx1ΔC) (not predicted to contain the TMD), and one missing 48 amino acids predicted to contain the TMD (Mtx1ΔTM/C) (Armstrong *et al.*, 1997). Only Mtx1ΔTM/C had decreased association with mitochondria (Armstrong *et al.*, 1997). The TM/C region was shown to be necessary but not entirely sufficient to target a heterologous protein completely to mitochondria (Armstrong *et al.*, 1997).

Metaxin2 (Mtx2, Tob38) is ubiquitously expressed in all mouse tissues and its localized to mitochondria (Armstrong *et al.*, 1999). The protein does not contain a predicted TMD (Armstrong *et al.*, 1999). Following carbonate extraction (at pH 11.5) Mtx2 is found in the supernatant, indicating that Mtx2 is a peripheral membrane protein (Armstrong *et al.*, 1999). Like Mtx1, Mtx2 is sensitive to externally added protease, supporting its localization on the cytosolic side of the MOM (Armstrong *et al.*, 1997; Armstrong *et al.*, 1999).

The addition of Mtx1 antibodies to isolated mitochondria resulted in decreased import of the mitochondrial precursor preadrenodoxin, a protein that uses the TOM complex for import, in a dose-dependent manner (Armstrong *et al.*, 1997). Overexpression of Mtx1 inhibited precursor protein import via the TOM complex as observed with Tom20 overexpression, but not as severely (Abdul *et al.*, 2000). Overexpression of both Tom20 and Mtx1 inhibited precursor protein import to a level similar to that of Tom20 alone, indicating the proteins were likely affecting the same

process (Abdul *et al.*, 2000). These results suggest that Mtx1 may have a role as a TOM complex receptor in mammals.

Kozjak-Pavlovic *et al.* (2007) analyzed RNAi knockdowns of Tom40, Tom70, Sam50 (Tob55) and Mtx2 in human cell lines. Tom40↓ mitochondria had reduced steady state levels of Tom20, Tom22 and Tom70, but other mitochondrial proteins including Voltage Dependent Anion Channel (VDAC, also known as porin), Sam50, Mtx1, and Mtx2 were present at wildtype levels (Kozjak-Pavlovic *et al.*, 2007). Sam50↓ mitochondria showed decreased steady state levels of Tom40, VDAC, Mtx1 and Mtx2 (Kozjak-Pavlovic *et al.*, 2007). Mtx2↓ mitochondria showed decreased steady state levels of Mtx1 but had little effect on the levels of VDAC and Tom40 (Kozjak-Pavlovic *et al.*, 2007). However, examination of import in mitochondria depleted of Mtx2 showed strong defects of the assembly of VDAC and Tom40 *in vitro* (Kozjak-Pavlovic *et al.*, 2007). Depletion of Mtx2 and Mtx1 had no affect on matrix targeted precursors (Kozjak-Pavlovic *et al.*, 2007).

Although Tom40 assembly intermediate I is not normally seen upon analysis of import in human mitochondria, a mutant form of the human Tom40 precursor can be stalled in assembly intermediate I (Humphries *et al.*, 2005). This intermediate complex was shown to contain Sam50 but not Mtx1 by supershift assays (Humphries *et al.*, 2005). Neither Mtx1 nor Sam50 antibodies shifted the Tom40 assembly intermediate II or the TOM complex (Humphries *et al.*, 2005). Sam50 is found in a 200 kDa complex but Mtx2 is found in a distinct 600 kDa com[illegible]umphries *et al.*, 2005; Kozjak-Pavlovic *et al.*, 2007). A small amount of Mtx1 associated with the 600 kDa Mtx2-containing complex with a smear down to 200 kDa (Kozjak-Pavlovic *et al.*, 2007). These data indicate that in mammals, Sam50 is not in a complex with Mtx2 and Mtx1, although Mtx1 may be in a loosely associated 600 kDa complex with Mtx2 (Kozjak-Pavlovic *et al.*, 2007).

1.4.11 Additional Proteins Interacting with the TOB Complex

In addition to the TOM complex, the IMS small Tims, and the TOB core complex, other proteins are thought to be involved in beta-barrel protein import and assembly by functioning either with the TOB complex or at a subsequent step in

pathways specific for different beta-barrel precursors. The precise functions of two of these proteins, Mim1 and Mdm10, are not yet clarified.

1.4.11.1 Mim1

Mim1 is a non-essential, integral MOM protein with an N-terminal cytosolic domain, a TMD, and a C-terminal IMS domain (Ishikawa *et al.*, 2004). It is proposed to be involved in Tom40 assembly via the TOB complex (Ishikawa *et al.*, 2004; Waizenegger *et al.*, 2005). Mim1 was found in three different studies, in three different complexes: a 180 kDa complex that did not contain Tob38 or Tob55 (Ishikawa *et al.*, 2004), a 400 to 450 kDa complex with Tob38 (Waizenegger *et al.*, 2005), and in a 300 kDa complex (Hulett *et al.*, 2008). In *mim1*Δ mitochondria, steady state levels of Tom40, Tom22, and Tom20 were reduced while other mitochondrial proteins were present in wildtype amounts (Ishikawa *et al.*, 2004; Waizenegger *et al.*, 2005; Becker *et al.*, 2008). Analysis of TOM complex steady state levels in mitochondria depleted in Mim1, revealed a portion of Tom40 exists in a 100 kDa complex (Waizenegger *et al.*, 2005; Popov-Celeketic *et al.*, 2007; Becker *et al.*, 2008). Since the steady state levels of porin and TOB complexes in Mim1↓ cells were unaffected, Mim1 involvement appeared to be specific for Tom40 assembly (Ishikawa *et al.*, 2004; Waizenegger *et al.*, 2005).

Two groups showed that import of Tom40 precursor into Mim1↓ mitochondria was characterized by a decreased amount of the TOM complex but little to no change in the amount of assembly intermediate I (Ishikawa *et al.*, 2004; Waizenegger *et al.*, 2005). The two groups had opposite findings with respect to the levels of Tom40 assembly intermediate II. Ishikawa *et al.* (2004) saw no affect on the amount of assembly intermediate II but Waizenegger *et al.* (2005) saw no assembly intermediate II formed. Subsequent studies using *mim1*Δ strains showed the near absence of assembly intermediate II and the fully formed TOM complex as well as a slight reduction of assembly intermediate I (Becker *et al.*, 2008; Hulett *et al.*, 2008). The differences in results may be attributed to differences in the methods of producing Mim1 deficient cells and residual amounts of Mim1 in the different studies (Ishikawa *et al.*, 2004; Becker *et al.*, 2008). Mim1 appears to be involved in the Tom40 assembly pathway at a point after the association of the precursors with the TOB complex.

Mim1 and Mdm10 (section 1.4.7) were shown to separately co-purify with the TOB components in 350 kDa complexes since they did not co-purify with each other (Becker *et al.*, 2008). This supports the presence of two 350 kDa TOB complexes, one associated with Mdm10 and one associated with Mim1.

Mim1 has also been shown to be involved in the assembly of Tom20 and Tom70 into the TOM complex. The import and membrane insertion of radiolabeled Tom20 or Tom70 precursors into *mim1*Δ mitochondria was strongly reduced while the import of Tom22 was unaffected (Becker *et al.*, 2008). Later research showed that Tom20 was efficiently imported into mitochondria lacking Mim1 but assembly into the TOM complex was strongly reduced (Hulett *et al.*, 2008). Mim1 homo-oligomerizes via a TMD which is required for the interaction with the Tom20 TMD for Tom20 assembly into the TOM complex (Popov-Celeketic *et al.*, 2007; Hulett *et al.*, 2008). The import of Tom20 and Tom70 did not require the TOB complex or Mdm10, indicating a specific role of Mim1 in the assembly of the TOM complex receptors (Popov-Celeketic *et al.*, 2007; Becker *et al.*, 2008; Hulett *et al.*, 2008).

1.4.11.2 Mdm10

Mdm10 is a non-essential beta-barrel protein in the MOM initially classified as a protein required for mitochondrial morphology that was involved in actin binding in yeast (see section 1.3) (Boldogh *et al.*, 1998; Boldogh *et al.*, 2003). Further research has indicated a possible involvement of Mdm10 in small Tom associations with Tom40 and interactions with TOB complex components (Meisinger *et al.*, 2004; Meisinger *et al.*, 2006). Mitochondria lacking Mdm10 are deficient in Tom40 assembly (Meisinger *et al.*, 2004; Meisinger *et al.*, 2006). It has been suggested that Mdm10 participates in later stages of Tom40 assembly, enabling the small Toms to associate into the complex (Meisinger *et al.*, 2004; Meisinger *et al.*, 2006). Mdm10 is found in a 140 kDa complex and a 350 kDa complex containing the TOB complex (Meisinger *et al.*, 2004; Meisinger *et al.*, 2006). In addition, Mdm10 and a small amount of Tom7 were shown to co-migrate on 2D BNGE (Meisinger *et al.*, 2006). In *tom7*Δ mitochondria, the amount of Mdm10 in the 350 kDa complex was significantly increased and the 140 kDa complex

decreased, indicating a role of Tom7 in the distribution of Mdm10 (Meisinger *et al.*, 2006).

Tom7, which is thought to participate in the formation of the TOM complex *trans* site, is thought to have a role in beta-barrel protein import because *tom7*Δ mitochondria have the unusual phenotype of decreased porin but increased Tom40 precursor import (Honlinger *et al.*, 1996; Meisinger *et al.*, 2006). Mitochondrial proteins involved in import were present in wildtype steady state amounts in *tom7*Δ mitochondria, including Mdm10 (Meisinger *et al.*, 2006). Meisinger *et al.* (2006) suggested that Tom7 interacts with Mdm10 to prevent the formation of the Mdm10-350 kDa TOB complex needed for Tom40 precursor import. The assembly of Tom40 in *mdm10Δ* mitochondria was blocked at assembly intermediate I, whereas *tom7*Δ mitochondria showed an increase in the rate of TOM complex formation (Meisinger *et al.*, 2006). The opposite occurs for porin, with *tom7*Δ mitochondria showing decreased and *mdm10*Δ mitochondria showing increased porin assembly (Meisinger *et al.*, 2006). Mdm10 is not thought to be part of the TOB core complex involved in Tom40 assembly intermediate I, but is thought to associate after Tom40 membrane integration to favour Tom40 import and assembly over porin import and assembly (Meisinger *et al.*, 2006).

Deletion of Mdm12 and Mmm1 also reduce the assembly of all beta-barrel proteins (Meisinger *et al.*, 2007). These proteins are thought to act in a general beta-barrel assembly pathway with Mdm10 following the action of the TOB complex (Meisinger *et al.*, 2007).

1.4.12 The TOB Complex and Alpha Helical Proteins

Recently, a role for TOB complex components in the integration of alpha-helical TMD proteins into the MOM has been shown (Stojanovski *et al.*, 2007). Mitochondria depleted in Tob55, Tob38 or Tob37 showed decreased steady state levels of Tom22 and decreased Tom22 import and assembly (Paschen *et al.*, 2003; Ishikawa *et al.*, 2004; Paschen *et al.*, 2005; Stojanovski *et al.*, 2007). Though Tom22 assembly was not dependent on IMS chaperones as observed for beta-barrel precursors, further analysis showed that the integration of Tom22 into the MOM was less efficient in mitochondria depleted of TOB complex components (Stojanovski *et al.*, 2007). Other alpha helical

anchored MOM proteins (Fis1, Fzo1 ,Ugo1, Gem1, and OM45) did not show a dependence of the TOB complex for import or integration into the MOM (Stojanovski *et al.*, 2007). The small Toms (Tom5, 6, and 7) are also anchored into the MOM via alpha helical TMDs (Künkele *et al.*, 1998; Model *et al.*, 2001). Integration of the small Toms into the MOM was shown to require Tob37 but not Tob55 or Tob38, indicating a specific role for Tob37 (Stojanovski *et al.*, 2007).

1.4.13 The Tob37 and Tom70 Interaction

Double knockouts of *tob37*/*tom70* and *tob37*/*tom20* both stopped growth after 8 to 10 divisions in yeast and showed aberrant mitochondrial morphology (Gratzer *et al.*, 1995). Later studies showed that single mutant *tob37*Δ cells also contained aberrant giant mitochondria (Stojanovski *et al.*, 2006; Altmann and Westermann, 2005). Tob37 (first named Tom37) was initially thought to associate with Tom70 in a MOM receptor complex as they were co-isolated on a sucrose gradient at approximately 100 to 110 kDa (Gratzer *et al.*, 1995). Furthermore, Tob37 and Tom70 antibodies blocked ATP-mediated transfer of a precursor from MSF to the import receptors, MSF-bound precursor co-immunoprecipitated Tom70 and Tob37, and Tom70 antibodies immunoprecipitated Tob37 (Hachiya *et al.*, 1995). Therefore, Tob37 was initially thought to be involved in mitochondrial import in a heterodimer receptor complex with Tom70. Interaction with a protease-sensitive 37 kDa MOM protein (possibly Tob37) was also shown to be important for the assembly of Tom70 into the TOM complex, but not Tom70 membrane integration (Schlossmann and Neupert, 1995).

However, Komiya *et al.*, (1997) provided evidence that Tom70 was able to effectively bind MSF without Tob37. Furthermore, Tom70 and Tob37 were later shown not to co-migrate on BNGE in contrast to the previous sucrose gradient data (Ryan *et al.*, 1999). Finally, *tob37*Δ showed no affect on AAC precursor binding to the MOM, a precursor known to utilize Tom70 as an import receptor (Ryan *et al.*, 1999).

1.5 Objectives of this Analysis

Currently, the precise roles of Tob37 and Tob38 are unknown in both yeast and *N. crassa*. Possibilities for their roles might include promoting interactions of the TOB complex with cytosolic chaperones, mediating a transient association between the TOB and TOM complexes to transfer beta-barrel precursor proteins, regulating the Tob55 pore structure, interacting with beta-barrel protein assembly intermediates within the Tob55 pore for folding, releasing substrates from the complex, and/or interacting with additional proteins required for import of specific beta-barrel proteins.

The initial goal of this study was to characterize the effects of Tob38 and Tob37 depletion at the mitochondrial and cellular level in *N. crassa*. This included analyzing porin and Tom40 import and assembly. Further details of Tob38 and Tob37 function were investigated by mutating conserved regions of each protein. A second goal was to determine the interactions among the *N. crassa* TOB complex components Tob55, Tob38 and Tob37. A third goal, initiated late in this study, was to determine if there was any relationship between Tom70 and the TOB complex.

2. Materials and Methods

2.1 Growth of *N. crassa*

The growth and care of *N. crassa* followed standard protocols as described in Davis and De Serres (1970). Strains used in this analysis are listed in Table 1. Typically, strains were grown in 1 L liquid medium (Vogel's medium plus any required supplements, inoculated at 1 x 10^6 conidia/ml) by shaking overnight (16 to 18 hr) at 30°C with the following exceptions. Tob38↓ and Tob37↓ cultures were produced in histidine (his) plus p-fluoro-DL-phenyl-alanine (fpa) medium (Vogel's medium containing 200 mg /L his, 68 mg/L fpa) for 40 to 42 hr in 1 L liquid medium inoculated at 5 x 10^6 conidia/ml. Strains Tob37-15-3 and Tob37-20-1 in L liquid minimal medium with his for 40 to 42 hr, inoculated at 5 x 10^6 conidia/ml. Yields of mycelium for all cultures following the specified growth conditions were 5 to 10 g/L (wet weight). The measurement of growth rate by colony size was done by spotting 10 µl of suspended conidia at concentrations of 1 x 10^7, 1 x 10^6, 1 x 10^5, and 1 x 10^4 conidia/ml onto plates containing minimal medium with sorbose and the appropriate supplements and inhibitors. Spot plates were grown at 30°C or 37°C for 48 hr, or for 96 hr at 18°C.

2.2 Sequence Alignment and Phylogeny Construction

Sequence similarity of Tob38 proteins and Tob37 proteins between different species is relatively poor. Maximum likelihood alignments were done using an unrooted Jones-Taylor-Thornton (JTT) substitution matrix of amino acid change using Bioedit Sequence Alignment Editor (Isis Pharmaceuticals Inc., Carlsbad, CA). The JTT substitution matrix uses a large collection of global alignments of closely related sequences to determine evolutionary distance based on amino acid substitution rates (Jones *et al.*, 1992). Once the homologs were defined, ungapped local alignments were performed using the ClustalW2 program to identify conserved regions in Tob38 and Tob37 (Chenna *et al.*, 2003).

Table 1: Strains used in this analysis

Strain	Genotype	Origin or Source
Stock Strains		
76-26	*his-3 fpa*^{R}	R.L. Metzenberg
HP1	*his-3 fpa*^{R} + *pan-2 ben*^{R}	Heterokaryon of 76-26 and Fungal Stock Center # 7118
Tob37 Strains		
*tob37*KO-5	Sheltered heterokaryon. As HP1 with replacement of the *tob37* gene in the *his-3 fpa*^{R} nucleus with a hygromycin cassette	Nancy Go
Tob37-His$_6$	*his-3 fpa*^{R} *hyg*^{R} *bleo*^{R} with an ectopic copy of *tob37* with six his residues added to the C-terminus	Transformation of Tob37KO-5 with the pBS520-T37-his plasmid
Tob37-15	*his-3 fpa*^{R} *hyg*^{R} *bleo*^{R} with an ectopic copy of *tob37* with a premature stop codon at amino acid 337 removing both predicted transmembrane domains	Transformation of Tob37KO-5 with the pBS520-T37-15 plasmid
Tob37-20	*his-3 fpa*^{R} *hyg*^{R} *bleo*^{R} with an ectopic copy of *tob37* with is a deletion of LP at amino acids 52 - 53	Transformation of Tob37KO-5 with the pBS520-T37-20 plasmid
Tob37-21	*his-3 fpa*^{R} *hyg*^{R} *bleo*^{R} with an ectopic copy of *tob37* with a substitution of the L52→A	Transformation of Tob37KO-5 with the pBS520-T37-21 plasmid

Tob37-22	*his-3 fpa*^{R} *hyg*^{R} *bleo*^{R} with an ectopic copy of *tob37* with is a substitution of the P53→A	Transformation of Tob37KO-5 with the pBS520-T37-22 plasmid
Tob37-23	*his-3 fpa*^{R} *hyg*^{R} *bleo*^{R} with an ectopic copy of *tob37* with a deletion of a 17 amino acid glutamic rich region 236 – 253	Transformation of Tob37KO-5 with the pBS520-T37-23 plasmid
Tob37-35	*his-3 fpa*^{R} *hyg*^{R} *bleo*^{R} with an ectopic copy of *tob37* with an eight amino acid deletion LAINVAGL in the first putative transmembrane domain	Transformation of Tob37KO-5 with the pBS520-T37-35 plasmid
Tob37-36	*his-3 fpa*^{R} *hyg*^{R} *bleo*^{R} with an ectopic copy of *tob37* with a premature stop codon at amino acid 425, removing the second putative transmembrane domain	Transformation of Tob37KO-5 with the pBS520-T37-36 plasmid

Tob38 Strains

*tob38*KO-6	Sheltered heterokaryon. As HP1 with replacement of the *tob38* gene in the *his-3 fpa*^{R} nucleus with a hygromycin cassette	Nancy Go
Tob38-His_6	*his-3 fpa*^{R} *hyg*^{R} *bleo*^{R} with an ectopic copy of *tob38* with six his residues added to the C-terminus	Transformation of Tob38KO-6 with the pBS520-T38-his plasmid
Tob38-27	*his-3 fpa*^{R} *hyg*^{R} *bleo*^{R} with an ectopic copy of *tob38* with a single amino acid substitution of D25 → A	Transformation of Tob38KO-6 with the pBS520-T38-27 plasmid

Tob38-30	*his-3 fpa*^{R} *hyg*^{R} *bleo*^{R} with an ectopic copy of *tob38* with a deletion of FDTFP at amino acids 24 – 28	Transformation of Tob38KO-6 with the pBS520-T38-30 plasmid

Tob55 Strains

*tob55*KO-3	Sheltered heterokaryon. As HP1 with replacement of the *tob55* gene in the *his-3 Fpa*^{R} nucleus with a hygromycin cassette	Nancy Go
His_9-Tob55	*his-3 fpa*^{R} *hyg*^{R} *bleo*^{R} with an ectopic copy of *tob55* with nine his residues added to the N-terminus	Nancy Go
ST55	*his-3 fpa*^{R} *hyg*^{R} *bleo*^{R} with an ectopic copy of the short version of *tob55*	Nancy Go
LT55	*his-3 fpa*^{R} *hyg*^{R} *bleo*^{R} with an ectopic copy of the long version of *tob55*	Nancy Go

Other Strains

tom70^{RIP}	Ascospore isolate of NCN235 and SU-1-1 cross; contains two RIPed alleles of *tom70*; *pan-2 ben*^{R} *hyg*^{R}	Lesley Grad

2.3 Oligonucleotides and Plasmids

Oligonucleotides and plasmids used in this study are listed in Tables 2 and 3, respectively.

2.4 Transformation of *N. crassa*

Plasmid DNA that had been linearized by digestion with one or more restriction enzymes was transformed into conidia of *tob38*KO or *tob37*KO sheltered heterokaryon as previously described (Margolin *et al.*, 1997; Margolin *et al.*, 2000) with slight modifications. 5 to 7 day old conidia were harvested in 50 ml sterile distilled water (sdH_2O) and washed three times with 50 ml of ice cold 1 M sorbitol. Conidia were resuspended in 1 M sorbitol at 2.5×10^9 conidia/ml and kept on ice. Previously isolated plasmid DNA containing a bleomycin resistance marker and genomic *tob38* or *tob37* carrying site-directed mutations (with a minimum of 500 bp upstream and downstream of the coding sequence) was linearized and brought to a concentration of 1μg/μl. 40 μl of the conidial suspension, containing 1×10^8 of conidia, was combined with 8 μg (1 μg/μl) of linearized DNA and chilled on ice in the electroporation cuvette for 15 min. Electroporation was performed at 2.1 kV with a resistance of 475 Ohms using a BTX ECM 630 electroporator (Genetronics, San Diego, CA), or at 1.5 kV with a resistance of 480 Ohms on a BTX ECM 600 electroporator (Genetronics, San Diego, CA), both at 25°C for 11 to 12 milliseconds. 1 ml of ice cold 1 M sorbitol was directly added to the electroporation cuvettes and samples were incubated at 30°C for 45 min. Aliquots of 10, 50, and 100 μl were mixed gently in 10 ml of top agar (Vogel's sorbose medium, 1.5% agar, 1 M sorbitol) containing 200 mg/L his, 68 mg/L fpa, and 1.5 ml/L bleomycin (1.7 units/ml) at 48°C and spread onto plates containing the same medium except lacking the 1 M sorbitol and only 1 ml/L bleomycin (1.7 units/ml). Plates were then incubated at 30°C for 7 to 10 days until colonies formed. Single colonies were picked to slants of Vogel's medium containing 200 mg/L his, 68 mg/L fpa and 0.5 ml/L bleomycin (1.7 units/ml). This is half of the bleomycin concentration used for selection on plates to allow for better growth and conidiation. Slants were grown at 30°C for 3 to 4 days and removed to room temperature for one week to allow maximal conidiation. To isolate

Table 2: Oligonucleotides used in this analysis

Name	Sequence (5' – 3')	Function
	PCR and sequencing primers	
Met2KO5F	GTAACGCCAGGGTTTTCCCAGTCACGACGTTTAGAACTAAGAACCGGCA	To amplify the 5' UTR of Tob38 for the knockout protocol and to amplify probes for Southern analysis
Met2KO5R	ACCGGGATCCACTTAACGTTACTGAAATCGGTTGCGAATCGACCTGGTA	
Met2KO3F	CGTTCTATAGTGTCACCTTAAATCGTATGTCTCATGACGAAGGCTACGAC	To amplify the 3' UTR of Tob38 for the knockout protocol and to amplify probes for Southern analysis
Met2KO3R	GCGGATAACAATTTCACACAGGAAACAGCTGGAGGTGAAAGAGTGACGG	
SmaI-met2-NF	GCTATCGACCCGGGATTTCCTCTTCTCGCCTACG	Amplification of the N-terminal half of Tob38 for expression
PstI-met2-NR	GAACTCACCTGCAGGCATTTCGGATAGGGACATC	
EKR3	GAAGCGTCATCGCTTCAGTTGTC	Tob38 sequencing primer
EKR4	AATAGGCCTTCCTCAAGCTTGCC	Tob38 sequencing primer
EKR5	TAGGTTGCCCTCTGTTTATCCGG	Tob38 sequencing primer
EKR8	CCAACGACAACAACCCATCCATC	Tob37 sequencing primer
EKR9	CTATCGTCAACTATCTCTCCACCC	Tob37 sequencing primer
EKR10	CATCCGTTCTCGTATCATTCC	Tob37 sequencing primer

Tag creation or mutagenic primers

EKR12	GCCTTCGTCATGAGTTTCCATGTC AATGGTGATGGTGATGGTGAGCT TGATGCTGAAATTGCA	Tob38 his-6 tag
EKR14	GGTTCTCTACCCTCAACGTCTTCA ATCGTGATGGTGATGGTGTGCAA GACCAGCGAACATGGCTCCTG	Tob37 his-6 tag
EKR15	CAATTACGGCCCTCACAAACCGT CAAACGATACTGAGCGCCGAG	Tob37 premature stop at G337
EKR17	GCCCGCTCCAGAAGGTCTTCCCTC TTCTCGCCTACGACGT	Tob38 deletion of DTF 25-27
EKR19	CTCCAGAAGGTCTTCGATACAGCT CCTCTTCTCGCCTACGACG	Tob38 F27A
EKR20	CATTCATCTCGATACAGATCACGC ACTCTACAACCCCTCCAC	Tob37 deletion of LP 52-53
EKR21	CATCTCGATACAGATCACGCCCC GGCACTCTACAACCCCTCC	Tob37 L52A
EKR22	CATCTCGATACAGATCACCTCGCG GCACTCTACAACCCCTCC	Tob37 P53A
EKR23	GATGTGCTTGGGGAAGTTGATTTC CTGGCTAAAGAGGGCGGTGCAAG GATCAAGG	Tob37 deletion of EEE DGEEEEEEEEE 235 – 248
EKR27	GTAGGCGAGAAGAGGGAAGACCT TCTGGAG	Tob38 D25A
EKR30	CGAGAAGAGGGGCTGTATCGAAG	Tob38 deletion of FDTFP 24 – 28
EKR35	GTATCGGTACCAGTAAATACCCA GAGTCAACCCGGCACCAG	Tob37 deletion of LAINVAGL 397 – 404
EKR36	GCCTACCAGTCACCTATGCCAC	Tob37 premature stop P425

cDNA amplification and sequencing

EKR37	GGATCCATGACGCTAGAGCTCC	Tob37 at the start codon with 5' BamHI cut site
EKR38	GAATTCTCATGCAAGACCAGCG	Tob37 at the stop codon with 3' EcoRI cut site
EKR44	CCGGGAGGTGATCTGTATCG	Tob37 internal primer to sequence cDNA start codon
EKR45	CTCTGCCGAGACACAGCTCG	Tob37 internal primer to sequence cDNA stop codon

Table 3: Plasmids used in this analysis

Plasmid	Source	Description
		Stock plasmids
pBS520	This study	pBSK with the bleomycin cassette inserted into the *Not*I of the MCS
		Tob37 plasmids
pBS520-T37	Nancy Go	Genomic copy of *tob37* with 500 bp upstream and 500 bp downstream cloned into pBS520
pBS520-T37-his	This study	As for pBS520-T37 with six his residues added to the C-terminus
pBS520-T37-15	This study	As for pBS520-T37 with a premature stop codon at amino acid 337 removing both predicted TMDs
pBS520-T37-20	This study	As for pBS520-T37 with a deletion of LP at amino acids 52 to 53
pBS520-T37-21	This study	As for pBS520-T37 with a substitution of the L52A
pBS520-T37-22	This study	As for pBS520-T37 with a substitution of the P53A
pBS520-T37-23	This study	As for pBS520-T37 with a deletion of a 17 amino acid glutamic rich region amino acids 236 to 253
pBS520-T37-35	This study	As for pBS520-T37 with an eight amino acid deletion (LAINVAGL) in the first putative TMD at amino acids 396 to 404
pBS520-T37-36	This study	As for pBS520-T37 with a premature stop codon at amino acid 425, removing the second putative TMD

pGEM-T37-10	Nancy Go	pGEM®-7Zf(+) with *tob37* cDNA, isoform lacking 9 bp in the glutamic acid rich region
pGEM-T37-4	This study	pGEM®-7Zf(+) with *tob37* cDNA isolate 4, full length with two missense mutations

Tob38 Plasmids

pBS520-T38	This study	Genomic copy of *tob38* with 1213 bp upstream and 2088 bp downstream cloned into pBS520
pBS520-T38-his	This study	As for pBS520-T38 with six his residues added to the C-terminus
pBS520-T38-27	This study	As for pBS520-T38 with a single amino acid substitution of D25A
pBS520-T38-30	This study	As for pBS520-T38 with a deletion of FDTFP at amino acids 24 to 28
pGEM-T38	D. Rapaport	pGEM®-4Zf(+) (Promega, Madison, WI) with *tob38* cDNA
pGEM-T38-17	This study	As for pGEM-T38 with a deletion of FDT at amino acids 24 to 26
pGEM-T38-19	This study	As for pGEM-T38 with a single amino acid substitution of F27A
pGEM-T38-27	This study	As for pGEM-T38 with a single amino acid substitution of D25 A
pGEM-T38-30	This study	As for pGEM-T38 with a deletion of FDTFP at amino acids 24 to 28
pQE40-T38-N1	This study	pGE40 (Qiagen Inc., Mississauga, ON) with the 50% N-terminal region of *tob38*

single colonies, conidia were streaked on plates containing 200 mg/L his, 68 mg/L fpa and 1 ml/L bleomycin (1.7 units/ml) and grown at 30°C until colonies formed. Single colonies were picked to Vogel's medium containing 200 mg / ml his without inhibitors and allowed to grow and conidiate. Transformants were then tested for nutritional requirements to ensure that they were homokaryons.

2.5 Knockout of Tob38 and Tob37 Using the Split Marker Approach

A split marker approach to knocking out essential genes in *N. crassa* heterokaryons was used. Knockouts were created by replacing the target gene with the hygromycin resistance marker in one nucleus of the heterokaryon. To ensure homologous recombination, two transforming constructs were used in a split marker approach. One construct contained 3 kb upstream of the target gene and the N-terminal half of the hygromycin resistance marker while the second construct contained the C-terminal half of the hygromycin resistance marker and 3 kb downstream of the target gene. Both constructs were transformed into the heterokaryotic HP1 strain. Only when both constructs are inserted at the target site to replace the gene by homologous recombination does hygromycin resistance occur. Colonies arising on hygromycin containing medium were purified in the same fashion as described for bleomycin resistant strains in section 2.4. This was done for both *tob37* and *tob38* by Nancy Go, the lab technician.

To test if the knockouts were lethal, and to determine which nucleus contained the knockout, conidia were plated on medium containing nutrients that would allow homokaryons of each nucleus to grow. Colonies were then isolated and tested for nutrient requirements to determine if the knockout nucleus can grow as a homokaryon (non-essential) or only as a heterokaryon with the control sheltering nucleus (essential gene). This strategy is discussed further in section 3.1 and shown in Fig. 3A using the *tob38*KO as an example. Strains were also tested by Southern and Western blot analysis for the predicted DNA integration pattern and for decreases in the levels of the appropriate protein. Nancy Go tested the *tob37*KO and I tested the *tob38*KO.

2.6 Creation of Tob38 and Tob37 Mutant Alleles

Tob38 and Tob37 mutant alleles were created by site-directed PCR mutagenesis of plasmids containing wildtype genomic or cDNA versions of the target genes on a plasmid that also carried bleomycin and ampicillin resistance markers. Primers with 10 to 20 nucleotides upstream and downstream of the site to be mutagenized were used and are listed in Table 2. 16 µg of primer was phosphorylated using 10 units of T4 polynucleotide kinase (Invitrogen, Carlsbad, CA) and 1 mM ATP. This reaction was incubated at 37 °C for 3 hr, extracted once with phenol, once with phenol:chloroform (1:1), once with chloroform, and then ethanol precipitated and resuspended in 10 µl sdH_2O. 1.5 µg of phosphorylated mutagenic primers were then used in a PCR reaction containing 0.5 to 1 µg of wildtype plasmid, 17 µl PT1.1x mastermix (50 mM KCl, 10 mM Tris HCl pH 8.5, 1.5 mM $MgCl_2$, 0.01% bovine serum albumin (BSA), 2 mM dNTPs), 0.5 mM NAD, 0.5 µl dimethylsulfoxide (DMSO), and 5 units of Taq DNA ligase. 2.5 units of Pfu polymerase were added to the reaction during the initial denaturation step of the PCR protocol. This reaction underwent PCR consisting of 2 min at 95°C (initial denaturation step), then thirty repeats of a 1 min at 95°C (denaturation), 1 min at 55°C (annealing), and 10 min at 65°C (extension). The final PCR products were digested overnight using 10 units of DpnI (New England Biolabs Ltd., Pickering, ON) to remove the wildtype methylated DNA of the original template plasmid and leave only the *in vitro* synthesized mutation-containing DNA intact. The final mixture was then transformed into *Escherichia coli* XL2 or XL10 competent cells and plated onto L-agar plates containing ampicilin. Plasmids were isolated from individual colonies and screened by sequence analysis. Before being used in *N. crassa* transformations, the mutagenized genes were sequenced entirely to insure that no additional mutations had arisen as a result of PCR.

Mutant plasmids were linearized and used to transform the respective *N. crassa* sheltered knockout heterokaryon strains. Mutant alleles that maintain a minimal level of function should rescue the lethal phenotype of the knockouts. Transformation selection and purification of strains was as described in section 2.4. In addition, bleomycin was added to the medium to select for transformation with plasmids carrying the mutant allele. Once strains were purified, nutrient testing for the *his-3 fpa*^{R} nucleus was done to

ensure the transformants were homokaryons of the nucleus that contained the original knockout version of the gene. Four strains for each mutation were spotted at specific concentrations to test for growth defects. Conformation of the mutant strains was done by sequence analysis. Primers in the 5' and 3' untranslated region (UTR) region were used to amplify the gene from genomic DNA by PCR, resulting in amplification of both the ectopically integrated mutant allele and the hygromycin resistance marker of the original knockout at the endogenous locus. The band of the appropriate size was isolated following gel electrophoresis. The mutant genes were entirely sequenced using gene specific primers. For mutations in which more than one growth rate was observed in isolated strains, multiple strains were sequenced to confirm the mutation. Since integration of the mutant allele was at ectopic sites, poor growth rates could be due to secondary effects at a given random insertion site. Mutants are named from the primers used to create the mutation.

2.7 Tob38 Antibody Production

The antigen for the generation of the Tob38 antibody was made by inserting the N-terminal half (residues 1 to 185) of the Tob38 protein into a pQE-40 (Qiagen Inc., Mississauga, ON) vector for overexpression in BL21 *E. coli* cells. The overexpressed protein contained (in order) dehydrofolate reductase (DHFR), the N-terminal 50% of Tob38, and a hexa-his tag and was roughly 49 kDa in size. Expression was induced with 1 mM IPTG for 4 hr at 37°C. Cells were then harvested by centrifugation and the overexpressed protein was isolated according to QIAexpressionist protocol 17 (Batch purification of 6xhis-tagged proteins from *E. coli* under denaturing conditions) (Qiagen Inc., Mississauga, ON). The elutions with the majority of the overexpressed protein (elution 2 to 6, of 8) were combined and concentrated approximately 15-fold using a Centriplus (Millipore, Bedford, MA) centrifugal filter device YM-30 (filter molecular weight cut off 30 kDa). The concentration of the sample was then determined using the Bio-Rad Bradford protein assay (Bio-Rad, Mississauga, ON). Two rabbits and two guinea pigs were each injected initially with 500 µg of expressed protein in 250 µl elution buffer suspended in an equal volume of Freund's Complete Adjuvant (Difco, Kansas, MO). The subsequent injections contained 250 µg of expressed protein in 250 µl elution

buffer suspended in an equal volume of Freund's Incomplete Adjuvant (Difco, Kansas, MO). After nine injections, guinea pig N3-2 was the only animal found to produce a useable Tob38 antibody. The animal was euthanized and the serum was collected.

Serum was isolated from test bleeds and the final bleed of N3-2 by allowing the blood to clot at room temperature for 2 to 3 hr. This was centrifuged at 5000 rpm in a SA-600 rotor in a Sorvall RC5C Plus centrifuge (Mandel Scientific Company, Guelph, ON) for 10 min at 4°C to remove the clot and then at 13000 rpm for 30 min at 4°C to remove the remaining blood cells. The serum was then inactivated by incubation at 56°C for 30 min. The serum was aliquoted and stored at -80°C.

2.8 Preparation of *N. crassa* for Transmission Electron Microscopy

Control conidia (HP1) were grown in 1 L liquid Vogel's medium containing either 200 mg/L his, 68 mg/L fpa, or without supplements. This provided control mycelia for mutants grown in either condition. HP1 was inoculated with 1 x 10^6 conidia / ml and grown for 10 hr. Knockout strains were grown in 1 L Vogel's liquid medium containing 200 mg/L his and 68 mg/L fpa to produce Tob37↓ and Tob38↓ cultures. For growth in fpa containing medium, the knockouts were inoculated with 5 x 10^6 conidia/ml and grown for 36 hr. The knockouts were also grown as heterokaryons in 1 L liquid Vogel's medium without supplements, inoculated with 1 x 10^6 conidia/ml for 10 hr. All cultures had less than 5 g wet weight of mycelium per liter when harvested. Prior to harvesting, 2 to 5 ml of culture was pelleted at 7000 rpm in a Sorvall Pico centrifuge (Mandel Scientific Company, Guelph, ON) and washed with 1 ml milliQ H_2O. Mycelium was re-pelleted, resuspended in 1 ml 1.5% $KMnO_4$, and incubated at room temperature for 30 min with gentle mixing every 5 min. Mycelium was then pelleted again and washed 6 to 8 times with 1 ml milliQ H_2O until the solution was clear. The final pellet was resuspended in 1 ml gluteraldehyde cacodylate buffer (0.05 M cacodylate buffer: 25 ml 0.2 M Na cacodylate, 2.1 ml 0.1% HCl pH 7.2, containing 15% sucrose and 2% gluteraldehyde) for 30 min on ice with gentle mixing every 5 min. Mycelium was then pelleted, resuspended in 1 ml 1% OsO_4 1.5% $K_2Cr_2O_7$, and incubated on ice for 90 min with occasional mixing. Mycelium was pelleted and resuspended in 1% uranyl acetate for 16 to 24 hr. Finally, mycelium was pelleted and resuspended in 1 ml milliQ

H_2O. A dehydration series of 20, 30, 40, 60, 80, 90 and 100% absolute alcohol was performed with incubations of at least 15 min at each concentration, no further centrifugation steps were necessary as the pellets settled to the bottom of the tubes. Mycelium was then resuspended in 1:1 propylene oxide and absolute ethanol for 15 min, then in propylene oxide for 15 min, then in a 1:1 propylene oxide and spur resin mixture for 16 to 24 hr. The mycelium was then set in pure spur resin and solidified in a 60°C oven for 24 to 72 hr. Samples were sectioned and further stained by the Microscopy Unit, Department of Biological Sciences. Sections were examined by transmission electron microscopy at a magnification of 22,000.

2.9 Preparation of *N. crassa* for Fluorescence Microscopy

Control conidia (HP1) were grown in 500 ml liquid Vogel's medium containing either 200 mg/L his, 68 mg/L fpa, or without supplements. This provided control mycelium for mutants grown in either condition. HP1 was inoculated with 1 x 10^6 conidia/ml and grown for 6 hr. Tob38 and Tob37 knockout strains were grown in 500 ml Vogel's liquid medium containing 200 mg/L his and 68 mg/L fpa to produce Tob37↓ and Tob38↓ cultures. For growth in fpa containing medium, the knockouts were inoculated with 5 x 10^6 conidia/ml and grown for 24 hr. The *tom70*^{RIP} strain was grown in 500 ml liquid Vogel's medium with 10 μg/L pantothenate (pan). The strain was inoculated with 1 x 10^6 conidia/ml and grown for 6 hr. 150 ml of each culture was concentrated to 2 ml and washed in fresh Vogel's medium (pH 7.4) with appropriate supplements. Cultures were then resuspended in fresh Vogel's medium (pH 7.4) with the appropriate supplements and 100 nM Green-Fluorescent MitoTracker ® Green FM, made from a 100 mM stock in DMSO, and incubated at 30°C for 30 min. Samples were washed with fresh Vogel's medium (pH 7.4) with appropriate supplements and mounted on slides. Samples were imaged using a Zeiss Axioskop2 MOT microscope (Carl Zeiss Ltd., Welwyn Garden City, UK) and images were taken at a wavelength of 490 nm using a Zeiss Axiocam and Axiovision software (Carl Zeiss Ltd., Welwyn Garden City, UK).

2.10 Isolation of Mitochondrial and Whole Cell Protein

Mitochondrial isolation was as described in Mayer *et al.* (1993). Briefly, cells were grown in medium as described in section 2.1 and mycelium was isolated by vacuum filtration. The mycelium was ground with an equal mass of quartz sand (white quartz, 50-70 mesh, Sigma-Aldrich, Oakville, ON) and one volume of SEMP (0.25 M sucrose, 1 mM ethylendinitrilo tetra acetic acid (EDTA-$Na_2 \cdot H_2O$), 10 mM 4-morpholine propanesulfonic acid (MOPS) pH 7.2, 1 mM phenylmethylsulfonyl fluoride (PMSF)) for 1 min on ice. An additional volume of SEMP was added following the grinding and the resulting slurry was centrifuged twice at 5000 rpm in a SLC-1500 rotor in a Sorvall RC5C Plus centrifuge (Mandel Scientific Company, Guelph, ON) for 10 min at 4°C to remove cellular debris. The resulting supernatant was centrifuged at 12000 rpm for 20 min at 4°C to pellet mitochondria. The mitochondrial pellet was washed with 10 ml SEM (0.25 M sucrose, 1 mM EDTA-$Na_2 \cdot H_2O$, 10 mM MOPS pH 7.2) and re-pelleted. The pellet was resuspended in SEM or SEMP and assayed for protein concentration

For whole cell protein isolation, cells were grown in medium as described in section 2.1 and mycelium was isolated by vacuum filtration. The mycelium was ground with an equal mass of quartz sand (white quartz, -50-70 mesh, Sigma-Aldrich, Oakville, ON) and one volume of whole cell protein isolation buffer (1 mM EDTA-$Na_2 \cdot H_2O$, 10 mM MOPS pH 7.2, 1% sodium dodecyl sulfate (SDS), 1 mM PMSF) for 2 to 4 min on ice. An additional volume of whole cell protein isolation buffer was added and the resulting slurry was centrifuged at 5000 rpm for 20 min at 4°C in a SLC-1500 rotor in a Sorvall RC5C Plus centrifuge (Mandel Scientific Company, Guelph, ON) remove cellular debris. The supernatant was then centrifuged at 10000 rpm for 20 min at 4°C to further remove cellular debris. The supernatant was then assayed for protein concentration.

2.11 Alkaline Extraction of Membranes and Proteinase K Treatment

Mitochondria were isolated as described in section 2.10. 30 µg of mitochondria were suspended in 50 µl of sdH2O and 1 ml fresh ice-cold 0.1 M Na_2CO_3 was added. The unadjusted pH was 10.8, but in some experiments the pH was raised to 11.5 or 12.0 using NaOH. The mixture was incubated on ice for 30 min. Samples were then centrifuged at 50000 rpm in a TLA55 rotor in a Beckman Optima Table Top

Ultracentrifuge (Beckman, Mississauga, ON) for 1 hr at 4°C. Pellets were resuspended in cracking buffer (0.06 M Tris-HCl pH 6.8, 2.5% SDS, 5% β-mercaptoethanol, 5% sucrose). To precipitate the proteins in the supernatants, 210 µl of 72% trichloroacetic acid (TCA) (11% final w/vol) was added. The mixture was incubated on ice for 1 hr. Samples were pelleted by centrifugation at 13000 rpm in a Sorvall Pico centrifuge (Mandel Scientific Company, Guelph, ON) for 30 min at 4°C. The pellet was then washed in 1 ml acetone for 5 min at room temperature with shaking and re-pelleted for 30 min at 4°C. This pellet was left to dry overnight at room temperature and then resuspended in cracking buffer. The pellet and supernatant fractions were then analyzed by Western blot analysis.

Isolated mitochondria were also subjected to proteinase K treatment. 8 µl of 2 mg/ml proteinase K was added to 30 µg of intact mitochondria in 140 µl SEM (0.25 M sucrose, 1 mM EDTA-$Na_2 \cdot H_2O$, 10 mM MOPS pH 7.2) and incubated on ice for 20 min. 1 µl of PMSF (35 mg/ml in 95% ethanol) and 1 ml of SEMP (0.25 M sucrose, 1 mM EDTA-$Na_2 \cdot H_2O$, 10 mM MOPS pH 7.2, 1 mM PMSF) were then added to stop the protease assay. Samples were then pelleted for 30 min at 4°C and pellets were resuspended in cracking buffer and analyzed by Western blot analysis.

2.12 Outer Membrane Vesicle (OMV) Isolation

Isolation of purified mitochondrial outer membrane vesicles (OMVs) was performed as described in Mayer *et al.* (1995). 150 gm of mycelium was isolated from 8 L of liquid control (HP1) culture grown overnight. Mitochondria were isolated by mixing the mycelium at 4°C in a blender with 150 g of quartz sand (white quartz, 50-70 mesh, Sigma-Aldrich, Oakville, ON) and 600 ml OMP buffer (0.085 M sucrose, 2.5 mM EDTA, 10 mM MOPS pH 7.2, 1 mM PMSF) for 1 min until a uniform mixture was obtained. Cells were then broken twice by running through a grind mill at 4°C. The resulting slurry was centrifuged twice at 4000 rpm in a SLC-1500 rotor in a Sorvall RC5C Plus centrifuge (Mandel Scientific Company, Guelph, ON) for 5 min at 4°C. The supernatant was collected and centrifuged at 10000 rpm in a SLC-600 rotor in a Sorvall RC5C Plus centrifuge (Mandel Scientific Company, Guelph, ON) for 30 min at 4°C. The supernatant was removed by suction to avoid disturbing the mitochondrial pellet. The

pellet was washed with 200 ml OMP buffer, centrifuged at 10000 rpm for 30 min at 4°C, and resuspended in 10 ml swelling buffer (5 mM KPO_4 pH 7.2, 5 mM EDTA-$Na_2 \cdot H_2O$, 1 mM PMSF). Following even suspension, 600 ml of swelling buffer was added and the mixture was incubated at 4°C for 30 min to generate mitoplasts. The mixture was then centrifuged at 10000 rpm for 30 min at 4°C and the supernatant was removed by suction. Mitoplasts were resuspended in 60 ml of swelling buffer and dounced at 80 rpm on ice for 45 min to remove the outer membrane from the mitoplasts. The mixture was then stored over night at 4°C.

The OMV fraction was isolated on sucrose gradients in a SW28 swinging bucket rotor in a Beckman L8-8OM Ultracentrifuge. The first gradient consisted of a 13 ml bottom layer of 32% SEMP (0.32 M sucrose, 2.5 mM EDTA-$Na_2 \cdot H_2O$, 10 mM MOPS pH 7.2, 1 mM PMSF), a 9 ml middle layer of OMP buffer, and 15 ml of the dounced mitochondrial solution in swelling buffer as the top layer. This gradient was centrifuged at 26000 rpm for 1 hr at 4°C. The middle and top layers were aspirated off and the fraction at the lowest interface was collected in about 20 ml of the lower solution. 20 ml 70% SEMP (0.7 M sucrose, 2.5 mM EDTA-$Na_2 \cdot H_2O$, 10 mM MOPS pH 7.2, 1 mM PMSF) was added to the collected fraction and loaded as the bottom layer for a new gradient. The middle layer was 20 ml 25% SEMP (0.25 M sucrose, 2.5 mM EDTA-$Na_2 \cdot H_2O$, 10 mM MOPS pH 7.2, 1 mM PMSF), and the top layer consisted of 3 ml EMP buffer (2.5 mM EDTA-$Na_2 \cdot H_2O$, 10 mM MOPS pH 7.2, 1 mM PMSF). This gradient was centrifuged at 26000 rpm for 16 hr at 4°C. The top interface was collected and contained the OMV fraction. The purity of the OMVs was checked by Western blot analysis using markers for the outer membrane (Tom70 and porin), the intermembrane space (cytochrome *c* heme lyase and Tim8), the inner membrane (ADP/ATP carrier (AAC)), and the matrix (Hsp70).

2.13 Pulldown Analysis

Mitochondria from strains expressing His_9-Tob55, Tob38-His_6, or Tob37-His_6, as well as from the control (76-26) strain were isolated as described in section 2.10. The His_9-Tob55 protein is tagged at the N-terminus and the Tob38-His_6 and Tob37-His_6 proteins are both tagged at the C-terminus. 300 µg of isolated mitochondria were

resuspended in 1.5 ml of pulldown buffer (1% digitonin, 1 mM PMSF, 20 mM Tris HCl pH 7.4, 50 mM NaCl, 10% glycerol, 10 mM imidazole) and rocked gently for 45 min at 4°C. Samples were then centrifuged at 20000 rpm in a TLA55 rotor in a Beckman Optima Table Top Centrifuge (Beckman) for 20 min at 4°C and the supernatant was collected. 100 µl of supernatant was kept for analysis and the rest was combined in a ratio 1 vol nickel-nitrilotriacetic acid (NiNTA) resin (Qiagen Inc., Mississauga, ON) to 2 vol lysate. This solution was mixed by rotation at 4°C for 2 to 3 hr then added to an open top column at 4°C. The column was washed once with 10 ml (10 column volumes) of wash 1 (1mM PMSF, 20 mM Tris HCl pH 7.4, 50 mM NaCl, 10% glycerol, 10 mM imidazole) and once with 10 ml (10 column volumes) of wash 2 (1 mM PMSF, 20 mM Tris HCl pH 7.4, 50 mM NaCl, 10% glycerol, 20 mM imidazole). Samples were eluted five times with 1 ml (one column volume) of native elution buffer (1 mM PMSF, 20 mM Tris HCl pH 7.4, 50 mM NaCl, 400 mM imidazole). 1 ml of each wash and 0.5 ml of each elution were concentrated by TCA precipitation (see section 2.11) and analyzed by Western blot analysis. The washes and elutions were compared to 30 µg of mitochondria protein, the pellet of 50 µg mitochondrial protein following digitonin lysis and the centrifugation step, 20 µl of the supernatant following digitonin lysis and centrifugation step, and 20 µl of the runoff from the column.

2.14 Blue Native Gel Electrophoresis (BNGE)

Mitochondria were isolated as described in section 2.10, suspended in SEMP at a concentration of 1 to 4 µg/µl, aliquoted into 50 µg amounts, and either used fresh or frozen once at -80°C. Mitochondria in the 50 µg aliquot were pelleted at 13000 rpm in a Sorvall Pico Centrifuge (Mandel Scientific Company, Guelph, ON) for 30 min at 4°C, resuspended in 50 µl of digitonin buffer (1% digitonin, 1 mM PMSF, 20 mM Tris HCl pH 7.4, 0.1 mM EDTA-$Na_2 \cdot H_2O$, 50 mM NaCl, 1% glycerol) and rocked gently at 4°C for 15 min. The sample was centrifuged at 13000 rpm for 30 min at 4°C, and the resulting supernatant was added to 5 µl of sample buffer (5% coomassie brilliant blue G-250 in 100 mM Bis-Tris, 500 mM 6-aminocaproic acid pH 7.0) and rocked gently at 4°C for 15 min. A native ladder was made containing 40 µl the digitonin buffer, 100 µg BSA (68 kDa), 50 µg apoferritin (440 kDa), 20 µg β-amylase (200 kDa), and 5 µl sample

buffer. Samples were then analyzed on a 6 to 13% gradient blue native gel at 4°C as previously described (Schagger and von Jagow, 1991; Schagger *et al.*, 1994) except that the gel was electrophoresed overnight (18 hr) at 80 V whereafter primary cathode buffer was changed to the secondary cathode buffer. Electrophoresis was then continued for 3 to 4 hr at 500 V. The gel was the blotted to a polyvinylidene fluoride (PVDF) membrane. The blot was stained for 10 min in coomassie buffer (0.1% coomassie brilliant blue G-250, 24% methanol, 6% glacial acetic acid) and then destained in methanol to visualize the ladder.

2.15 *In vitro* Import of Radioactive Tom40, porin, Tob55, Tob38 and Tob37 into Isolated Mitochondria

Mitochondria were isolated as described in section 2.10. Wildtype and mutant radioactive precursor proteins were transcribed and translated *in vitro* using the TnT reticulocyte lysate system (Promega, Madison, WI) in the presence of [^{35}S]-methionine (Amersham, Piscataway, NJ). The amount of each lysate to use in import reactions was roughly equalized by electrophoresis of 1 µl samples of the lysates on SDS-polyacrylamide gel electrophoresis (PAGE) gels, blotting to nitrocellulose and examining the intensity of each band following autoradiography. Radiolabeled precursor proteins were imported into fresh mitochondria for the indicated time points at 25°C as described by Harkness *et al.* (1994), except that after import, mitochondria were not treated with proteinase K but resuspended in 1 ml ice cold SEMK buffer (SEMP buffer, 80 mM KCl) (Rapaport *et al.*, 2001). Mitochondria were then pelleted at 13000 rpm in a Sorvall Pico Centrifuge (Mandel Scientific Company, Guelph, ON) for 30 min at 4°C and processed with the BNGE protocol described in section 2.14. Samples were analyzed by BNGE and viewed by autoradiography.

2.16 Pulse import of Tom40, Tob38, and Tob55 Wildtype Precursors

Mitochondria were isolated as described in section 2.10 and radioactive precursor proteins were imported for 1 min at 25°C (Harkness *et al.*, 1994, Rapaport *et al.*, 2001). Mitochondria were then washed with SEMP buffer, isolated by centrifugation at 13000 rpm in a Sorvall Pico Centrifuge (Mandel Scientific Company, Guelph, ON) for 30 min

at 4°C, and resuspended in 100 µl of fresh import buffer (0.25% BSA, [w/vol], 250 mM sucrose, 80 mM KCl, 5 mM $MgCl_2$, 2 mM ATP, 2 mM NADH, 14 mM PCre, 15 µg CreK, 10 mM MOPS, pH 7.2). Samples were incubated for 1, 2, 5, 30 min, and 1, 2, 4, and 8 hr at 25°C. Mitochondria were then resuspended in 1 ml ice cold SEMK buffer (SEMP buffer, 80 mM KCl) and pelleted at 13000 rpm for 30 min at 4° C. Samples were analyzed by BNGE and viewed by autoradiography.

2.17 Other techniques

Standard protocols for agarose gel electrophoresis, *E. coli* transformation, cloning, restriction digests, PCR using *Taq* and *Pfu* polymerases, genomic DNA isolation, Southern blotting of agarose gels, and the preparation of radioactive DNA probes were all performed as described in Ausubel *et al.* (1992) or Sambrook and Russell (2001).

The following procedures were performed as previously described or in accordance with the suppliers instructions: isolation of plasmid DNA on QIA columns (Qiagen, Mississauga, ON), amplification of cDNA from first strand synthesis using SuperScript™ II reverse transcriptase (Invitrogen, Carlsbad, CA), automated sequencing using a BigDye Terminator Cycle sequencing kit (version 3.1), separation of mitochondrial proteins by SDS-PAGE (Laemmli, 1970), protein concentration determination with the Coomassie dye binding assay (Bio-Rad, Mississauga, ON), the Pierce BCA protein assay (Pierce, Rockford, IL), or Ponceau S stain, Western blotting (Good and Crosby, 1989), and Western blot enhanced chemiluminescence (ECL) detection using LumiGLO chemiluminescent substrate (Kirkegaard and Perry Laboratories, Gaithersburg, MD).

3. Results

3.1 Sheltered Heterokaryon Knockout Strains in *N. crassa*

Knockouts of both *tob37* and *tob38* were created by Nancy Go, the lab technician, prior to my arrival in the lab using a split marker approach (see section 2.5). The knockouts were verified by Southern and Western blot analysis (*tob37*KO Southern analysis by Nancy Go, see later in this section for Southern analysis of *tob38*KO by me, and section 3.2 and 3.3 for Western blot analysis of both mutants by me). Nancy also performed genetic tests with the *tob37*KO strain. I used the same approach to examine the *tob38*KO strain. A special technique called sheltered disruption was used to create the knockouts since it was possible that *tob37* and *tob38* were essential genes. The filamentous fungus *Neurospora crassa* can be maintained as a heterokaryon (two distinct nuclei in the same cytoplasm) in the asexual lifecycle. Thus, an essential gene can be knocked out in one nucleus while the second nucleus maintains a functional copy, enabling survival of the knockout nucleus. The resulting construct is termed a sheltered heterokaryon. Appropriate genetic markers allow the maintenance of both nuclei in the sheltered heterokaryon by growth on minimal medium which forces nutritional complementation (Fig. 3A). If marked with appropriate resistance markers, the sheltered heterokaryon can be grown under conditions that result in numerical superiority of the knockout nucleus, increasing the ratio of knockout to control nucleus (Fig. 3B). These cultures are essentially knockdowns of the specific gene since some proportion of the essential wildtype protein must be produced for growth. Cultures in which the level of Tob37 was reduced by this method will be referred to as Tob37↓ and similarly for Tob38↓ (Fig. 3B).

To determine if Tob38 was indeed essential for growth, nutritional analysis was performed on strains arising from asexual spores (conidia) produced by the sheltered heterokaryon. Conidia are produced in a developmentally controlled process (Lowry *et al.*, 1967; Davis, 2000) that randomly segregates one or more nuclei (typically two to five) into the asexual spores. Thus, three types of conidia were expected: the heterokaryon and the two possible homokaryons (Fig. 3A). 398 colonies were isolated from plates containing both histidine (his) and pantothenate (pan) and tested for nutrient

Figure 3: Sheltered heterokaryon *tob38*KO strain. **A.** An essential gene can be knocked out in one nucleus of a heterokaryon. In the example shown, the his-requiring fpa-resistant nucleus of heterokaryon HP1 undergoes knock-out of the *tob38* gene to give the sheltered heterokaryon *tob38*KO. The second nucleus (pan-requiring, fpa-sensitive) is unaffected. Growth on medium lacking his or pan forces nutritional complementation of the two nuclei and insures the maintenance of the *tob38*KO nucleus. *N. crassa* strains (homokaryons or heterokaryons) give rise to asexual conidia spores that typically contain two to five nuclei that have segregated randomly into the conidia. Thus, three possible types of conidia are formed from the *tob38*KO sheltered heterokaryon: homokaryons (if viable) which contain only the *tob38*KO nucleus, homokaryons of the *tob38*$^+$ nucleus, or heterokaryons containing both nuclei. The three different types can be distinguished by their nutritional requirements. **B.** The *tob38*KO strain can be grown under conditions that favour numerical superiority of the *tob38*KO nucleus. In this example, this is accomplished by growth in the presence of his and fpa. The reduction in relative number of the *tob38*$^+$ nucleus results in a Tob38↓ culture. If *tob38* is an essential gene, the *tob38*$^+$ nucleus can never be totally eliminated. A Tob37↓ culture is produced by treatment of the *tob37*KO strain in the same fashion since the nutritional and resistance markers in the *tob37*KO and *tob38*KO sheltered heterokaryons are identical.

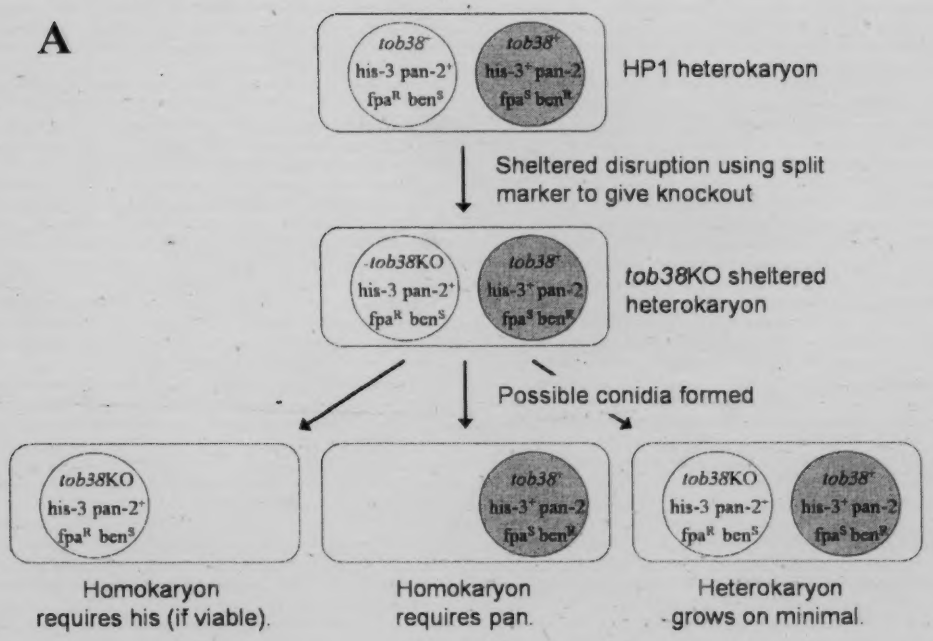
A
tob38⁻
his-3 pan-2⁺
fpa^R ben^S
tob38⁺
his-3⁺ pan-2
fpa^S ben^R
HP1 heterokaryon
Sheltered disruption using split marker to give knockout
tob38KO
his-3 pan-2⁺
fpa^R ben^S
tob38⁺
his-3⁺ pan-2
fpa^S ben^R
tob38KO sheltered heterokaryon
Possible conidia formed
tob38KO
his-3 pan-2⁺
fpa^R ben^S
Homokaryon requires his (if viable).
tob38⁺
his-3⁺ pan-2
fpa^S ben^R
Homokaryon requires pan.
tob38KO
his-3 pan-2⁺
fpa^R ben^S
tob38⁺
his-3⁺ pan-2
fpa^S ben^R
Heterokaryon - grows on minimal.

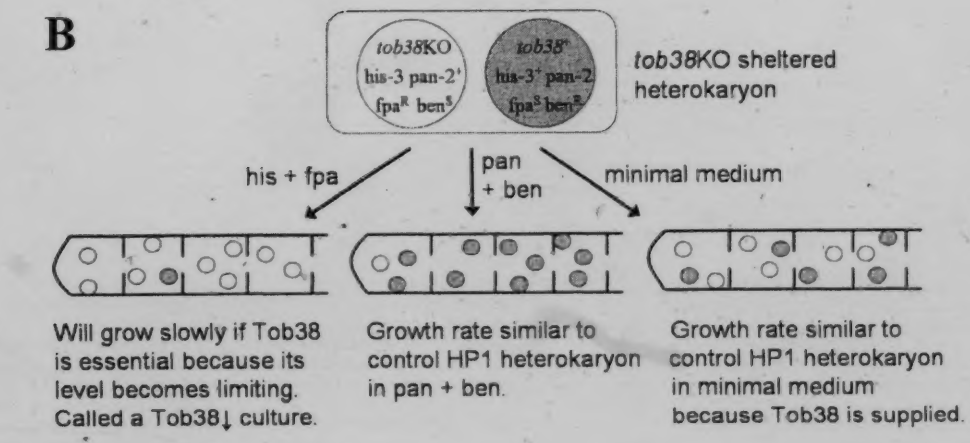
B
tob38KO
his-3 pan-2⁺
fpa^R ben^S
tob38⁺
his-3⁺ pan-2
fpa^S ben^R
tob38KO sheltered heterokaryon
his + fpa
pan + ben
minimal medium
Will grow slowly if Tob38 is essential because its level becomes limiting. Called a Tob38↓ culture.
Growth rate similar to control HP1 heterokaryon in pan + ben.
Growth rate similar to control HP1 heterokaryon in minimal medium because Tob38 is supplied.

requirements. 225 grew on minimal medium (heterokaryons), none were histidine requiring (homokaryons of the his-3 nucleus), and 173 required pan (homokaryons of the pan$^-$/ben^R nucleus) (Fig. 4). These data demonstrate that the his-3 nucleus carrying the *tob38*KO is not capable of producing viable conidia. Similar results were obtained by Nancy Go for the *tob37*KO strain (N. Go, personal communication). To determine if slow growth occurs when the *tob38*KO strain is grown under conditions that favour the knockout nucleus (Tob38↓ as shown in Fig. 3B), conidia from the sheltered heterokaryon were plated on medium that contained histidine (his) and p-fluoro-DL-phenyl-alanine (fpa). Under these conditions, the knockout has a much slower growth rate than the control heterokaryon or rescued homokaryons (Fig. 4B). Similar results are shown for the *tob37*KO strain. Therefore, the knockouts in both the *tob37*KO and *tob38*KO sheltered heterokaryons were in the his-3 nucleus and both *tob37 and tob38* are essential genes in *N. crassa*.

To confirm the genomic location of the *tob38*KO gene replacement, total genomic DNA was digested by *Kpn*I to determine if the hygromycin resistance marker had replaced *tob38* (section 2.5) as predicted (Fig. 5 A and B). Nancy Go initially used a 2 kb probe immediately upstream of the *tob38* coding region to determine the restriction patterns, but unexpected extra bands were present on her Southern blots. I repeated her experiment and confirmed the results (Fig. 5C, D). Upon comparison of the *N. crassa* genome sequence with the 2 kb upstream region used for the probe, four other regions were found in the genome that displayed 67 to 85% identity with a 3' region of the upstream probe (http://www.broad.mit.edu/annotation/ genome/neurospora /Home.html; Galagan *et al.*, 2003). Based on sequence analysis and the size of the additional bands, it seems likely that these regions produced the additional bands on the Southern blot (Fig. 5D, Table 4).

The *tob38* gene is found on chromosome V contig 14. Regions with identity to the upstream *tob38* sequence were found on chromosome II contig 5, chromosome V contig 37, and chromosome VII contigs 52 and 21 (Table 4). The origin of the five related sequences is not known, but one possibility is sequence duplication within the genome. The sequence differences between the five regions appear to be the result of natural RIP (repeat induced point mutation). This is suggested by dinucleotide

Figure 4: Tob38 is essential for viability. **A.** Conidia from the *tob38*KO heterokaryon were spread on medium containing both his and pan and colonies were picked to slants containing his and pan. These colonies were tested for nutritional requirements. Numbers indicate the number of colonies of each type from a total of 398 colonies tested. No colonies with only the *tob38*KO nucleus (his-3) were found, indicating that the loss of *tob38* is lethal. **B.** Growth of various *tob37* and *tob38* strains. Serial dilutions of conidia were spotted on the indicated medium and allowed to grow. The control is the heterokaryon HP1 used to create the knockout, *tob38*KO is the *tob38* sheltered heterokaryon knockout strain with the knockout in the his-3 nucleus, *tob37*KO is the *tob37* sheltered heterokaryon knockout strain with the knockout in the his-3 nucleus, Tob38-His_6 is the *tob38*KO strain rescued with a hexa-his tag version of Tob38, and Tob37-His_6 is the *tob37*KO strain rescued with a hexa-his tag version of Tob37. The rescued strains are viable homokaryons of the his-3 nucleus.

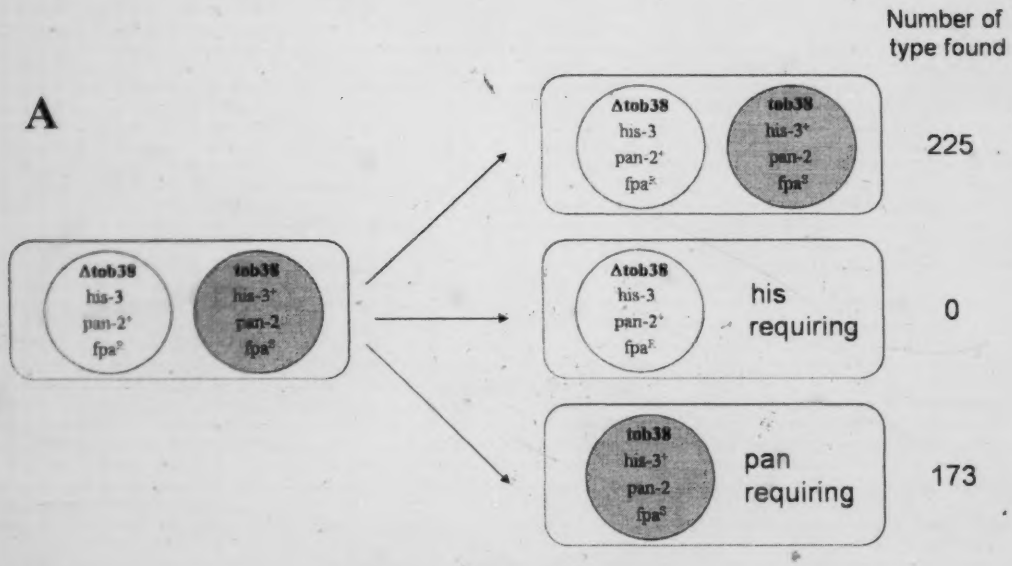
A
Number of type found
Δtob38
his-3
pan-2+
fpa-
tob38
his-3+
pan-2
fpa+
225
his requiring
0
pan requiring
173

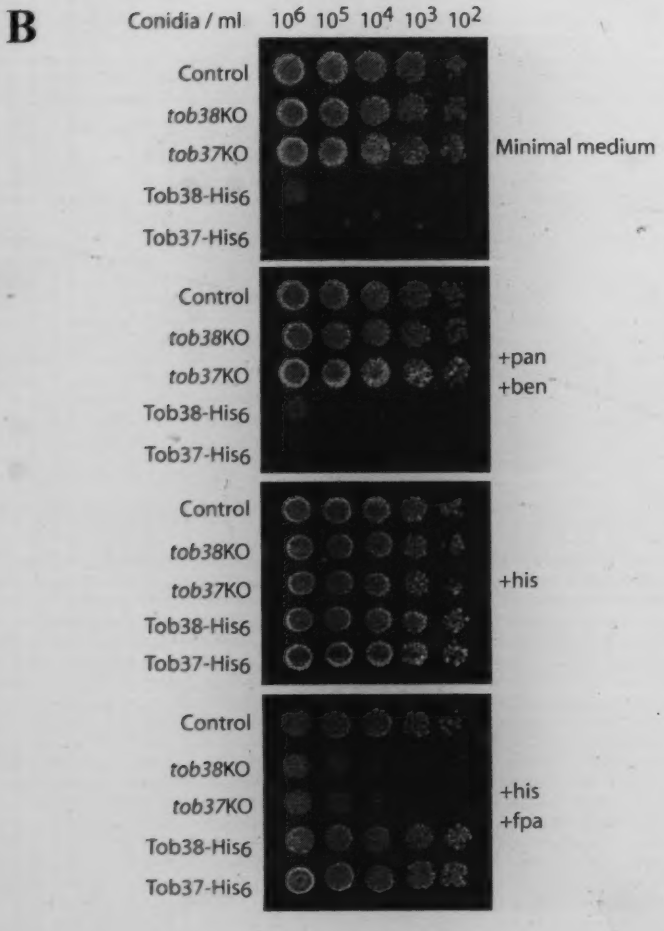
B
Conidia / ml
10^6 10^5 10^4 10^3 10^2
Control
tob38KO
tob37KO
Tob38-His6
Tob37-His6
Minimal medium
+pan
+ben
+his
+fpa

Figure 5: Southern blot analysis of the *tob38*KO strain. **A.** The knockout allele in the sheltered heterokaryon was created using a split-marker approach to transform the heterokaryon HP1. If both components of the split marker recombined at the endogenous location, the *tob38* gene would be replaced by the hygromycin resistance marker. This would give rise to a different restriction pattern between heterokaryons with both the knockout and wildtype alleles, and the HP1 control heterokaryon with two wildtype *tob38* alleles (see Fig. 3A). **B.** A schematic illustrating the different restriction pattern expected from a strain containing only the wildtype *tob38* gene compared to a heterokaryon containing both the wildtype and knockout alleles. **C.** Ethidium bromide stained agarose gel following *Kpn*I genomic digest of control strain (HP1, lane 1) and *tob38* knockout strains 6 to 10 (lanes 2 to 6, respectively). **D.** Southern blot probed with the 2 kb probe upstream of *tob38*. The upstream probe was expected to hybridize to a 2.5 kb fragment in the control strain and to 2.5 and 9.3 kb fragments in the heterokaryotic knockout strains. However, unexpected bands were also present (extra). **E.** Southern blot probed with the 3 kb probe downstream of *tob38*. The downstream probe hybridized to the fragments of expected sizes as predicted by analysis of sequence from the *Neurospora* genome project: 6.6 kb in the control strain and 6.6 and 9.3 kb in the heterokaryotic knockout strains. **F.** The location of the homologous RIPed regions relative to coding sequences. Proteins were identified using the *N. crassa* genome database and are indicated by their accession number. The length of the RIPed region, distances between regions, and the length of the predicted proteins near the RIPed regions are indicated in kilobases. The direction of transcription for the predicted protein mRNAs is indicated by an arrow accompanying the protein name.

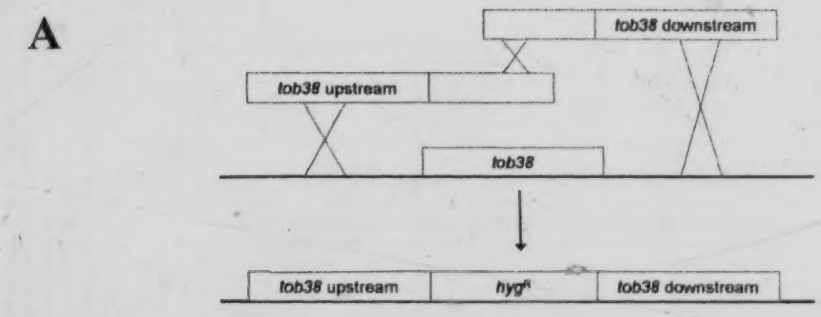
A
tob38 downstream
tob38 upstream
tob38
tob38 upstream
hyg^R
tob38 downstream

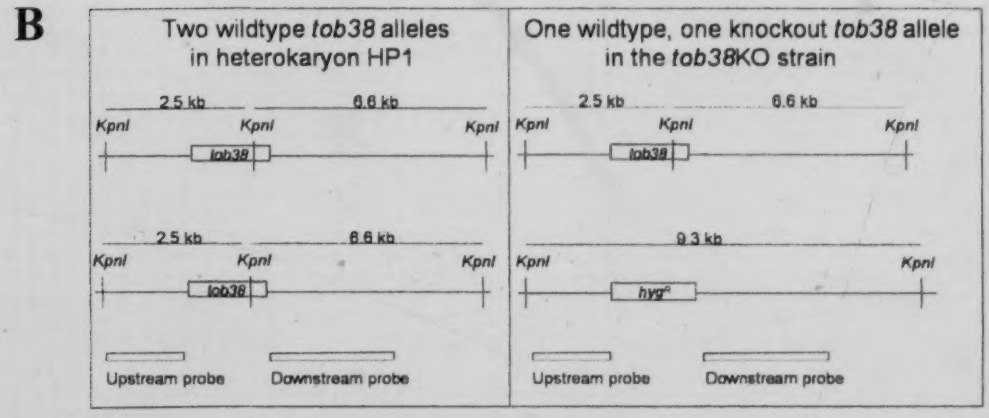
B
Two wildtype tob38 alleles in heterokaryon HP1
One wildtype, one knockout tob38 allele in the tob38KO strain
2.5 kb
6.6 kb
KpnI
KpnI
KpnI
tob38
9.3 kb
hyg^R
Upstream probe
Downstream probe

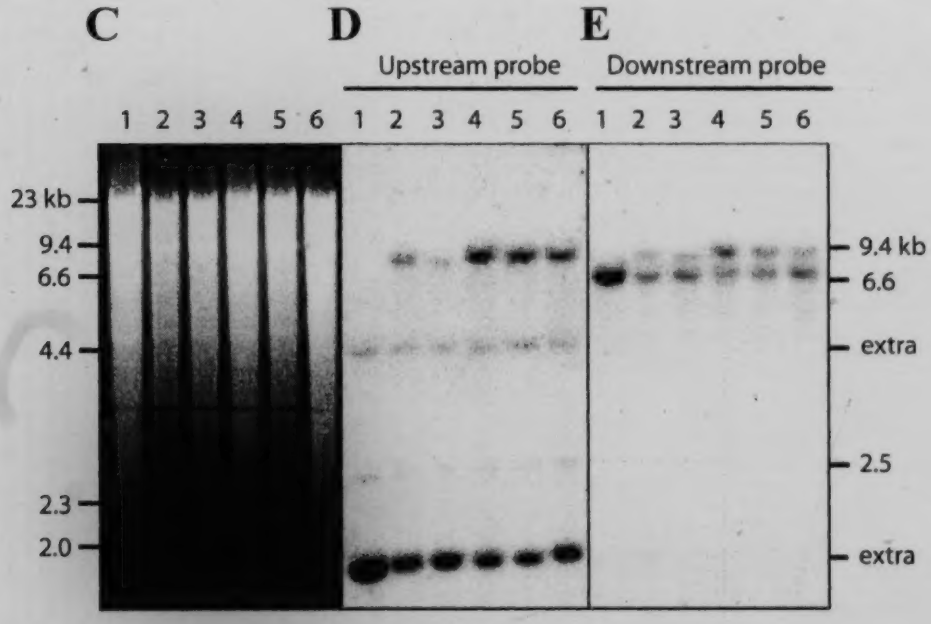
C
D
E
Upstream probe
Downstream probe
1 2 3 4 5 6 1 2 3 4 5 6 1 2 3 4 5 6
23 kb
9.4
6.6
4.4
2.3
2.0
9.4 kb
6.6
extra
2.5
extra

F

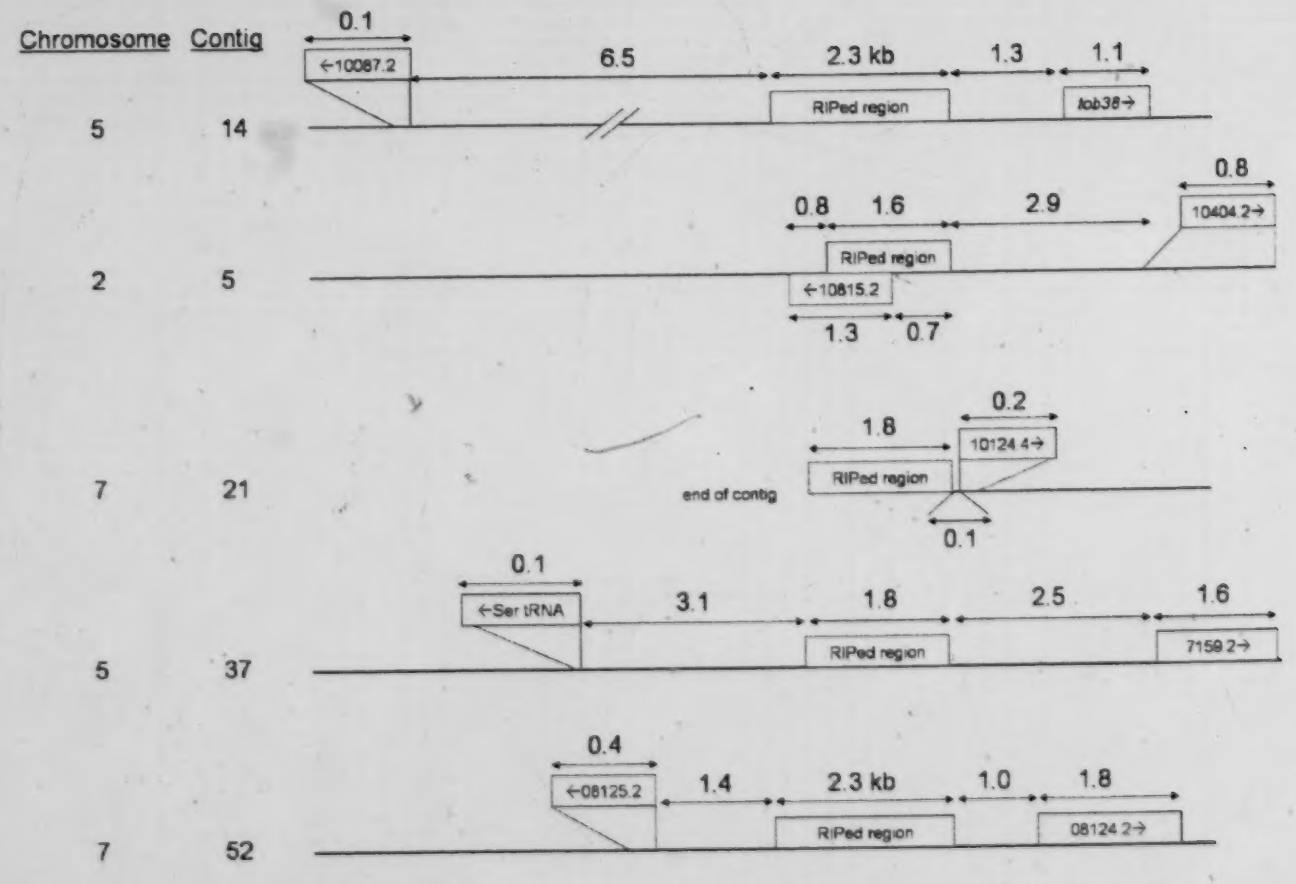
Chromosome
Contig
5
14
0.1
←10087.2
6.5
2.3 kb
1.3
1.1
RIPed region
tob38→
2
5
0.8
0.8
1.6
2.9
10404.2→
RIPed region
←10815.2
1.3
0.7
7
21
0.2
1.8
10124.4→
RIPed region
end of contig
0.1
5
37
0.1
←Ser tRNA
3.1
1.8
2.5
1.6
RIPed region
7159.2→
7
52
0.4
←08125.2
1.4
2.3 kb
1.0
1.8
RIPed region
08124.2→

Table 4: Comparison of five similar sequences in *N. crassa* (Genome release 7)

Linkage group. Contig	Location on contig	Size (bp)	+/-	A+T [a]	TpA / ApT [b]	CpA + TpG / ApC + GpT [c]	Identity to 5.14 [d]	Identity to 2.5 [d]	Identity to 7.21 [d]	Identity to 5.37 [d]
5.14 (upstream *tob38*)	105294 - 107625	2331	-	67.6	1.493	0.447	-	-	-	-
2.5	402461 – 404098	1638	-	62.8	1.497	0.440	0.67	-	-	-
7.21[e]	636959 – 638750	1792	+	67.4	1.423	0.350	0.85	0.70		-
5.37	300764 – 302608	1845	-	67.9	1.382	0.493	0.70	0.85	0.69	-
7.52	22071 – 24364	2294	+	71.8	1.455	0.313	0.81	0.68	0.80	0.69
tob38	102886 – 103984	1098	-	46.2	0.869	1.079	-	-	-	-

[a] A+T content of non-coding *N. crassa* sequence average is 51%, A+T content of coding sequence average is 41%.

[b] High TpA/ApT indicates sequence in A+T rich sequence with higher than normal TpA composition. The average TpA/ApT of non-RIPed *N. crassa* sequence was shown to be 0.66 $\pm$ 0.23; high ratios indicate RIPed sequence (Margolin *et al*, 1998).

[c] This ratio compares the frequency of RIP target dinucleotides CpA and TpG to dinucleotides of the same frequency (ApC and GpT) which are not common targets of RIP. The average ratio of these dinucleotide frequencies in non-RIPed sequences was shown to be 1.21 $\pm$ 0.18; a decrease in the ratio indicates the occurrence of RIP (Margolin *et al*, 1998).

[d] Identity determined using ClustalW pairwise alignment to regions of overlapping sequence per pair, not complete regions.

[e] Similarity in 7.21 up to 107144 on contig 5.14, at which point contig 7.21 ends, similarity might continue if contig 7.21 was extended.

frequencies (Table 4) consistent with known RIPed targets (Margolin *et al.*, 1998). RIP is a natural process affecting duplications in Neurospora that results in changing G/C base pairs to A/T base pairs (Selker, 1990). The duplicated region occurs 1.3 kb upstream of the *tob38* coding sequence. There is no consistency in the location of the other regions relative to the coding sequences at the other loci (Fig. 5F). The potential importance of this repeated region is unknown. To avoid the additional bands in the Southern analysis, a 3 kb downstream probe was chosen which does not have regions of similarity in the genome. This probe detected the expected 6.6 kb fragment from strains containing only the wildtype *tob38* gene and the 6.6 kb and 9.3 kb fragments from heterokaryons that contain both the knockout and wildtype versions of *tob38* (Fig. 5D).

3.2 Antibody Production and Testing

For further analysis of the *tob38*KO strain, I wished to develop a Tob38 antibody. The N-terminal half (amino acid residues 1 to 185) of the *tob38* coding sequence was inserted into a pQE-40 vector for overexpression in *E. coli*. The overexpressed protein contained DHFR, the N-terminal 50% of Tob38, and a C-terminal hexa-his tag. This protein was purified on a Ni-NTA column and the elutions were injected into two rabbits and two guinea pigs. Translation of the *tob38* coding sequence using Compute pI/MW Tool predicted a molecular weight of 37.3 kDa for the protein (Bjellqvist *et al.*, 1993; Galagan *et al.*, 2003). One guinea pig, N3-2, produced a useable antibody which identified *N. crassa* Tob38 as a 37 kDa protein present in control (HP1) mitochondria, absent in Tob38↓ mitochondria, present in *in vitro* reticulocyte lysates in which Tob38 was translated, and present in control (HP1) outer membrane vesicles (OMVs) (Fig. 6A). The antibody also reacted with the antigen fusion protein with a predicted molecular weight of 41 kDa (Fig. 6B). The α-Tob38 N3-2 antibody gave high levels of background when used to probe blots of blue native gel electrophoresis (BNGE) (data not shown) and was therefore not used for BNGE analysis.

A Tob37 mouse antibody was developed by Nancy Go using the peptide TFPDSGKVLPWADRE (Fig. 7A). There was only a small amount of this antibody serum available and it did not work to probe blots of BNGE (not shown). Translation of

Figure 6: Western blot analysis using Tob38 antibodies. Mitochondrial proteins were electrophoresed on SDS-PAGE gels, blotted to nitrocellulose, and probed with specific antibodies. **A.** Western blot probed with the α-Tob38 N-terminal (N3-2) antibody produced in house from guinea pig, final bleed (bleed 7) (see section 3.2). Tob38 is present at 38 kDa in the control (HP1) strain and the *tob38*KO heterokaryon strain grown in minimal medium (*tob38*KO min), but absent in Tob38↓ mitochondria (*tob38*KO fpa). Strains were grown as described in Fig. 3. Mitochondria carrying a his-tagged version of the protein (Tob38-His_6) contain a slightly larger version of Tob38. The protein was also seen in *in vitro* transcription/translation lysates of a Tob38 cDNA, and in OMVs isolated from a control (HP1) strain. **B.** Western blot probed with an earlier N3-2 bleed (bleed 3 of 7). The blot contained the Tob38 N-terminal antigen fused to DHFR (see section 2.7) (ca. 41 kDa) and OMVs isolated from a control (HP1) strain. **C.** Western blot probed with the α-Tob38 GenScript antibody. Lanes are as in panel A except that *tob38*KO min is missing and a lane containing mitochondria isolated from a strain carrying a Tob38 mutant protein (Tob38-30-2) lacking five amino acids is added. All lanes contain 30 μg of mitochondrial protein or 5 μg of control (HP1) OMV protein. Lanes with *in vitro* transcription/translation products contain 2 to 4 μl of lysate.

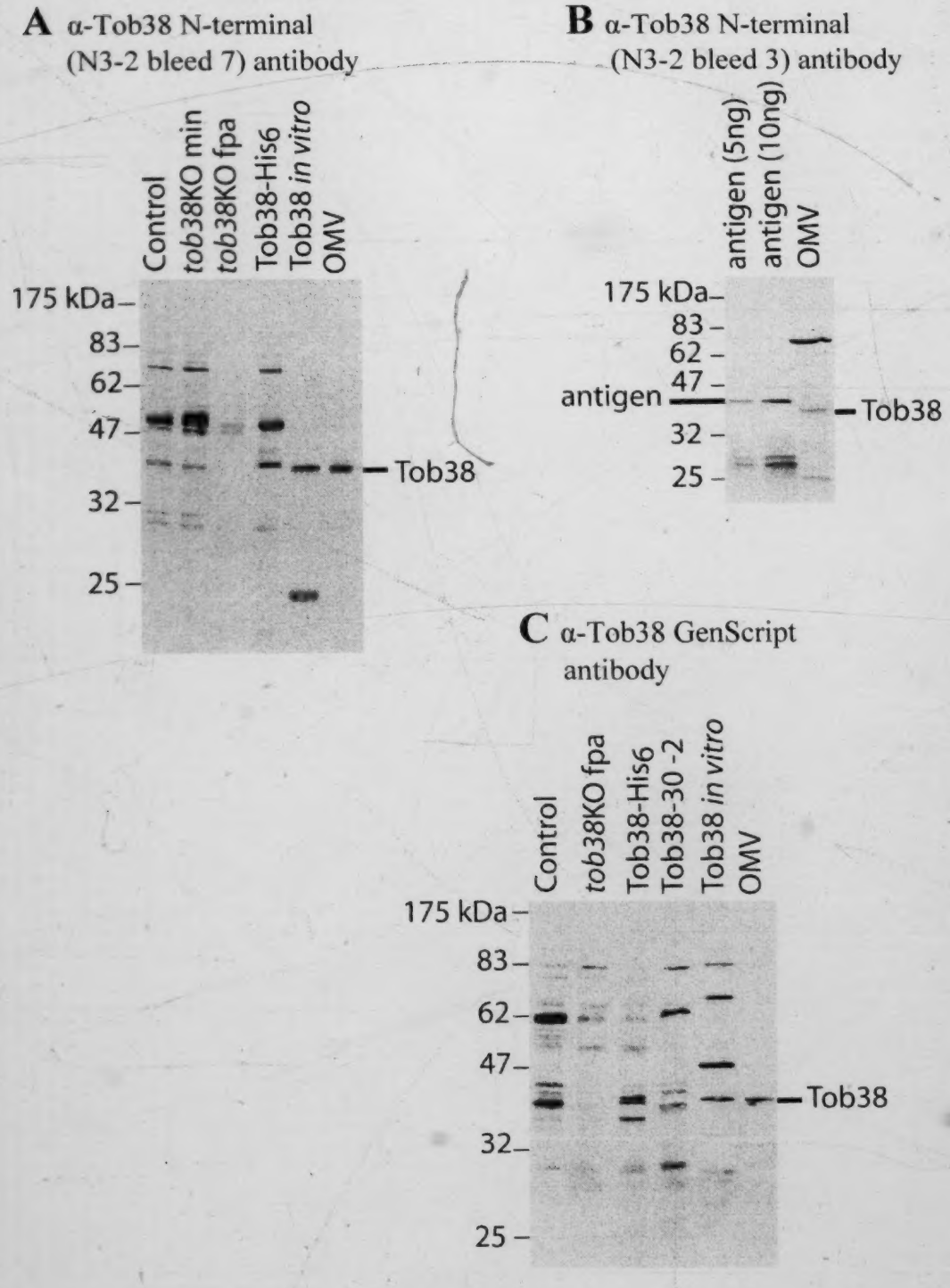
A α-Tob38 N-terminal (N3-2 bleed 7) antibody
Control
tob38KO min
tob38KO fpa
Tob38-His6
Tob38 in vitro
OMV
175 kDa
83
62
47
32
25
Tob38
B α-Tob38 N-terminal (N3-2 bleed 3) antibody
antigen (5ng)
antigen (10ng)
OMV
175 kDa
83
62
47
antigen
32
25
Tob38
C α-Tob38 GenScript antibody
Control
tob38KO fpa
Tob38-His6
Tob38-30 -2
Tob38 in vitro
OMV
175 kDa
83
62
47
32
25
Tob38

Figure 7: Western blot analysis using Tob37 antibodies. Mitochondrial proteins were electrophoresed on SDS-PAGE gels, blotted to nitrocellulose, and probed with specific antibodies. **A.** Western blot probed with the Tob37 mouse antibody produced in house (see section 3.2). Tob37 is present at 49 kDa in the control (HP1) mitochondria, the *tob37*KO strain grown in minimal medium (*tob37*KO min), the Tob37-His_6 tag strain, and control (HP1) OMVs. Strains were grown as described in Fig. 3. Tob37 was not observed in Tob37↓ (*tob37*KO fpa) mitochondria. The antibody detects a larger Tob37 protein produced via *in vitro* transcription/translation of a Tob37 cDNA-Δ9. **B.** Western blot probed with the affinity purified α-Tob37 peptide 1 GenScript antibody (1/100 dilution), made to the same epitope as the α-Tob37 mouse antibody used in panel A. Lanes are as in panel A except *tob37*KO min is not present. **C.** Western blot probed with the affinity purified α-Tob37 peptide 2 GenScript antibody (1/100 dilution). Lanes are as in panel B. **D.** Autoradiography of blot following an SDS-PAGE gel of *in vitro* transcription/translation products produced from Tob37 cDNA-Δ9 and Tob37 cDNA-4. **E.** Western analysis of panel D with the α-Tob37 peptide I GenScript antibody. Detection of the Tob37 protein was inefficient and background bands are visible (**a**, larger Tob37 produced from *in vitro* translation of Tob37 cDNA-Δ9; **b**, non-specific bands; **c**, correct size Tob37 produced from *in vitro* translation of Tob37 cDNA-4). Lanes containing control (HP1) mitochondria and OMVs are shown for reference. All lanes contain 30 μg of mitochondrial protein or 5 μg of control (HP1) OMV protein. Lanes with *in vitro* transcription/translation products contain 2 to 4 μl of lysate.

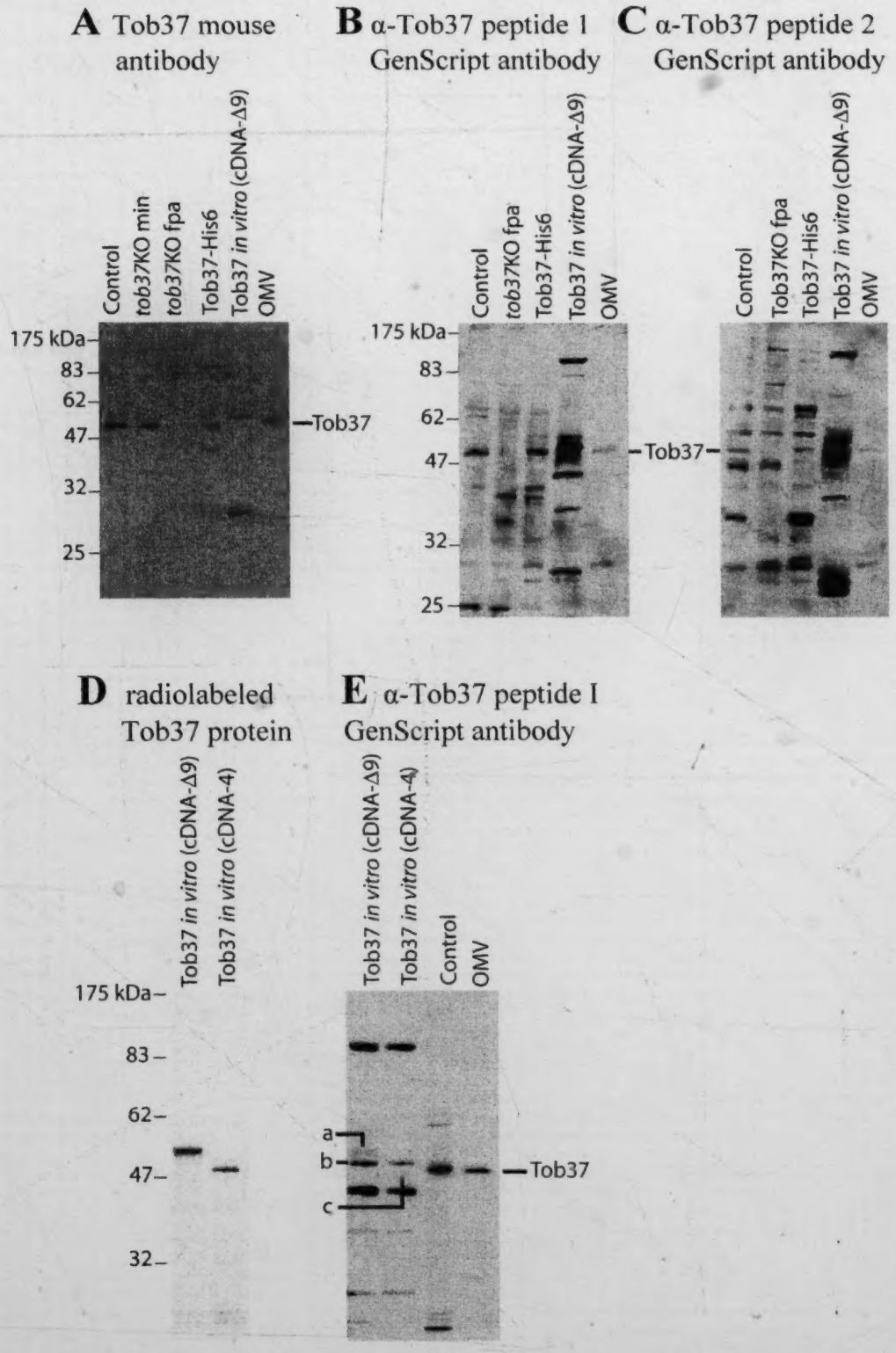
A Tob37 mouse antibody
Control
tob37KO min
tob37KO fpa
Tob37-His6
Tob37 in vitro (cDNA-Δ9)
OMV
175 kDa
83
62
47
32
25
Tob37
B α-Tob37 peptide 1 GenScript antibody
Control
tob37KO fpa
Tob37-His6
Tob37 in vitro (cDNA-Δ9)
OMV
175 kDa
83
62
47
32
25
Tob37
C α-Tob37 peptide 2 GenScript antibody
Control
Tob37KO fpa
Tob37-His6
Tob37 in vitro (cDNA-Δ9)
OMV
Tob37
D radiolabeled Tob37 protein
Tob37 in vitro (cDNA-Δ9)
Tob37 in vitro (cDNA-4)
175 kDa
83
62
47
32
E α-Tob37 peptide I GenScript antibody
Tob37 in vitro (cDNA-Δ9)
Tob37 in vitro (cDNA-4)
Control
OMV
a
b
c
Tob37

the *tob37* coding sequence using Compute pI/MW Tool predicted a molecular weight of 48.6 kDa for the protein (Bjellqvist *et al.*, 1993; Galagan *et al.*, 2003).

Commercial antibodies were ordered for Tob38 and Tob37 because of the high background when using the α-Tob38 N3-2 antibody and the need for more α-Tob37 mouse antibody. One Tob38 peptide (LYRDPEYTDLLDRFC) and two Tob37 peptides (peptide 1 = TFPDSGKVLPWADRES) (peptide 2 = ALRKAVGGQNCGVKC) were synthesized by GenScript (GenScript Corporation, Piscataway, NJ) and injected into two rabbits each. The Tob37 peptide 1 is the same peptide as used to create the previous mouse Tob37 antibody that was produced in house. The blood from both rabbits injected with the same antigen was combined and affinity purified by GenScript (GenScript Corporation, Piscataway, NJ). The purified antibodies only worked at a high concentration (1/100) to detect Tob38 (Fig. 6C) and Tob37 (Fig. 7B and C) proteins in control (HP1) mitochondria and in control (HP1) OMVs. Background with both GenScript antibodies was high.

As seen in Fig. 7A, the Tob37 *in vitro* transcription/translation product was increased in size relative to the *in vivo* proteins detected by Western blot analysis (Fig. 7). The cDNA encoding this version of Tob37 (cDNA-Δ9) was isolated by Nancy Go and contained a 9 bp deletion relative to the coding sequence predicted by the Neurospora genome sequence project (http://www.broad.mit.edu/annotation/genome/neurospora /Home.html; Galagan *et al.*, 2003). This deletion was in a region of the gene encoding 12 glutamic acid residues in a row. It is difficult to reconcile the observation of a protein with a higher apparent molecular weight resulting from a cDNA containing a 9 base pair deletion. Perhaps an additional upstream initiation site exists in this clone, or there may be an unexpected effect on electrophoretic mobility due to the loss of these three acidic residues from the highly acidic region. Since our cDNA sequence differed from the predicted coding sequence, I re-amplified Tob37 cDNA from purified mRNA using reverse transcription. Of the 10 cDNAs found, two contained a 5 bp deletion in the glutamic acid codon region, one contained a 1 bp deletion in the glutamic acid codon region, and four contained no deletions relative to the predicted mRNA sequence. The variation in this region is likely caused by slippage of the polymerase on the highly repetitive glutamic acid codon region. Tob37 cDNA-4 was chosen for further research as

it does not contain any deletions relative to the predicted coding sequence. Though it was later discovered that this cDNA contains two missense mutations, the *in vitro* translated Tob37 from cDNA-4 was the same size as Tob37 in control (HP1) mitochondria and OMVs (Fig. 7D and E). The darkest bands near the position predicted for Tob37 present in Figure 7E are non-specific bands as they were also visible when a Tob55 *in vitro* translated lysate was probed with the α-Tob37 GenScript peptide 1 antibody (data not shown). A faint band present at the appropriate size in the Tob37 cDNA-4 lysate sample is considered to be Tob37 (Fig. 7E). In conclusion, it appears that all of the antibodies described above do recognize the appropriate Tob proteins, but background due to non-specific interactions is relatively high.

3.3 Analysis of Knockout Mitochondria

Mitochondria were isolated from control (HP1), Tob38↓ and Tob37↓ strains. Mitochondrial proteins were then examined by Western blot analysis (Fig. 8A) with a coomassie blue stained gel serving as a loading control (Fig. 8B). Differences in the intensities of some bands on the coomassie stained gel were obvious, suggesting up or down regulation of various proteins in response to the deficiency of Tob37 or Tob38. However, this result was not pursued further. Tob38↓ and Tob37↓ mitochondria had greatly reduced levels of Tom6, Tom5, Tob38, Tob37, Tob55, Tom40, porin and Tim13. Levels of the other mitochondrial proteins analyzed also appeared to be slightly reduced (Fig. 8A).

The observed differences in all mitochondrial proteins analyzed could have been directly due to the lack of Tob38 or Tob37. Alternatively, changes in mitochondria due to the lack of one of these proteins could have resulted in artifacts during the isolation of the mitochondria. Therefore, whole cell protein was analyzed by Western blot analysis to avoid the mitochondrial isolation step (Fig. 9A). A coomassie stained gel was used as a loading control (Fig. 9B). Tob37 and Tim23 could not be identified in whole cell protein isolates due to increased background of the blots using antibodies directed against these proteins. Tom70, Hsp70 and actin levels were at similar levels in control and mutant mitochondria. Porin, Tom40, Tim8 and Tim13 were slightly reduced in Tob37↓ or Tob38↓ whole cell protein. Tob38 and Tob55 were reduced to a much greater extent in

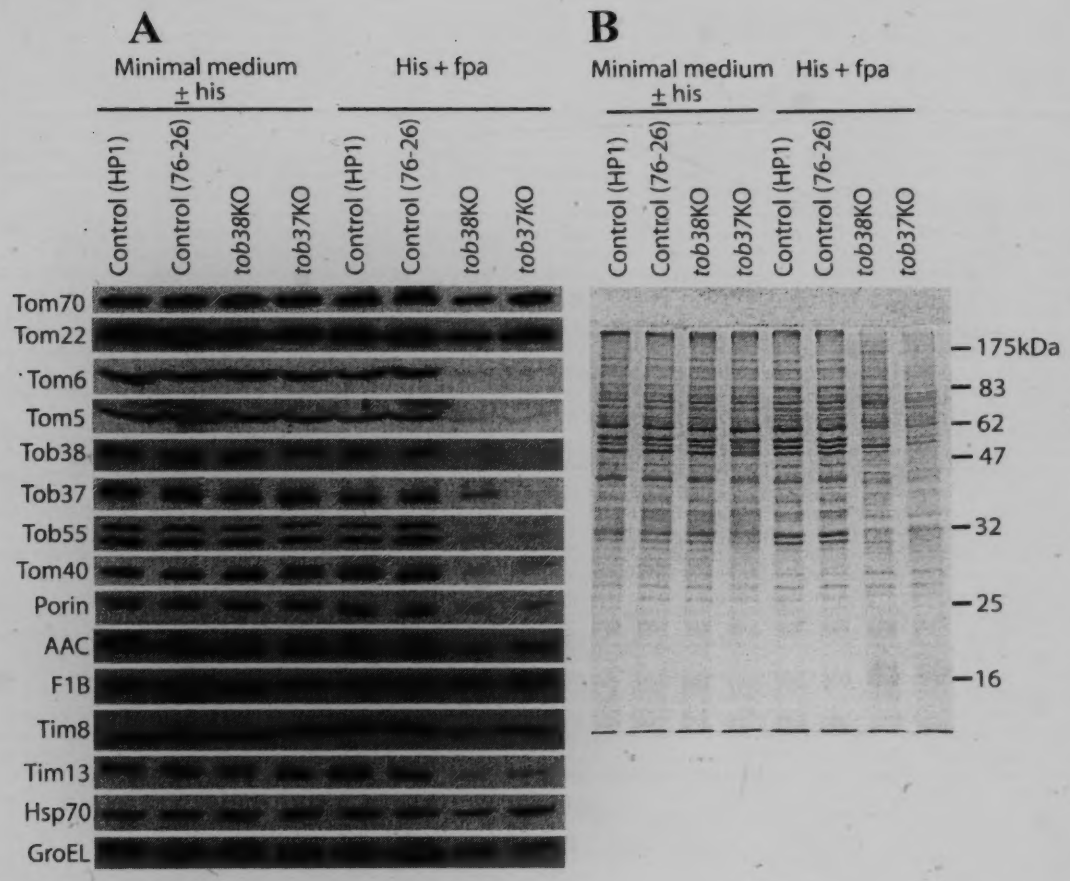

Figure 8: Mitochondrial proteins in knockout strains. **A.** Mitochondrial proteins in control strains HP1 and 76-26 are shown along with the *tob37*KO and *tob38*KO strains. Strains were grown as described in Fig. 3. The 76-26 strain is the his-3 fpa^R homokaryon that was used in the construction of HP1. Growth in the presence of his and fpa produce the Tob37↓ and Tob38↓ conditions in the knockout strains. Mitochondrial proteins were electrophoresed on SDS-PAGE gels, blotted to nitrocellulose, and probed with specific antibodies. **B.** Coomassie blue stained gel of the same lanes as panel A. All lanes contain 30 μg of mitochondrial protein.

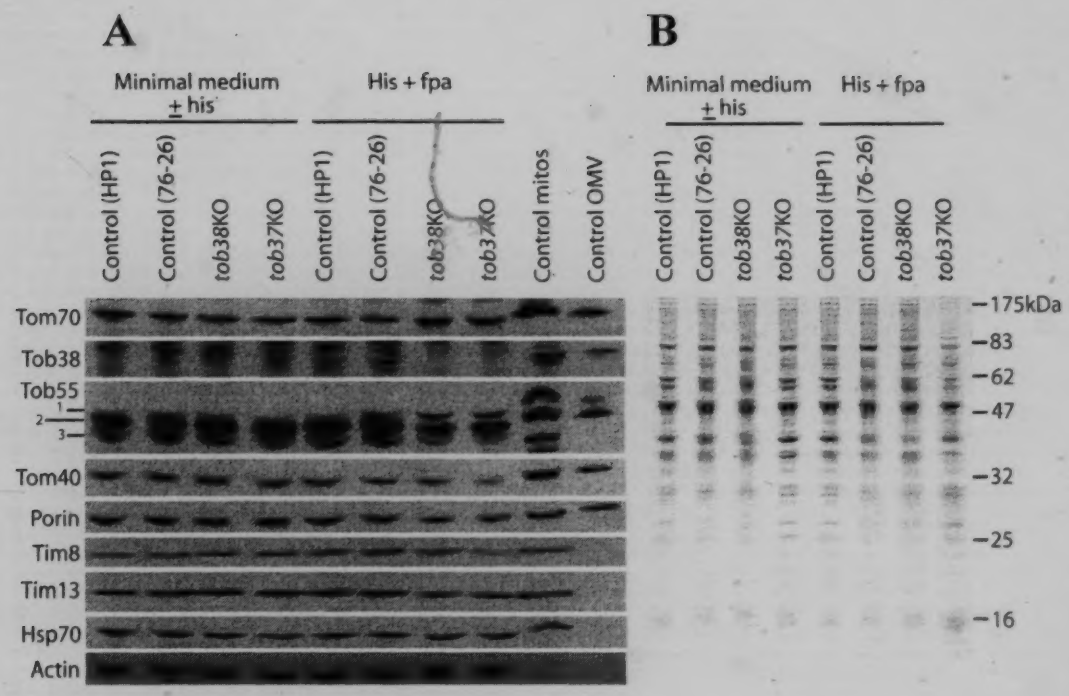

Figure 9: Analysis of protein in whole cell extracts and OMVs. **A.** Western blot of whole cell protein from the strains described in Fig. 8. 200 μg of whole cell protein was loaded in each lane. As controls, 30 μg of control mitochondrial proteins (HP1 strain) (Control mitos) and 5 μg of control OMVs (HP1 strain) (Control OMV) were included. Proteins were electrophoresed on SDS-PAGE gels, blotted to nitrocellulose, and probed with specific antibodies. The Tob55 antibody blot shows three bands representing: band 1, long and intermediate isoforms of Tob55; band 2, the short Tob55 isoform; and band 3, background contaminant. **B.** Coomassie stained gel of the same samples loaded in panel A except without the control mitochondria and OMVs.

Tob37↓ or Tob38↓ whole cell protein, similar to the reduction observed when isolated mitochondria were examined. The differences in the amounts of reduction of IMS proteins (Tim8 and Tim13) observed in the whole cell protein analysis of Tob37↓ and Tob38↓ cultures in comparison to the mitochondrial isolates suggest that these proteins are lost during mitochondrial isolation. This may be due to increased fragility of the MOM in the knockout mitochondria that allows the IMS proteins to leak out during isolation. However, the differences observed for other mitochondrial proteins such as Hsp70, porin, and Tom40 are more difficult to explain. It appears that there may be differences in the mitochondria isolated from control cultures versus Tob37↓ and Tob38↓ cultures.

3.4 Sequence and Phylogeny Construction

Alignment of *N. crassa, S. cerevisiae*, and *Homo sapien* Tob37 and Tob38 are shown in Figures 10 and 11, respectively. Overall, similarity is quite poor. When aligned individually, the *N. crassa* Tob37 protein is 15% identical and 46% similar to the *S. cerevisiae* protein and 21% identical and 53% similar to the *H. sapien* protein. For Tob38, the *N. crassa* protein is 15% identical and 48% similar to the *S. cerevisiae* protein and 19% identical and 50% similar to the *H. sapien* protein.

I wished to determine the conserved regions of Tob38 and Tob37 by sequence alignment and began the study by identifying their respective homologs in the National Center for Biotechnology Information (NCBI) and the Broad Institute databases (as described in section 2.2). Potential homologs to *N. crassa* Tob37 or Tob38 were identified in *Neurospora crassa*, *Chaetomium globosum*, *Magnaporthe grisea*, *Saccharomyces cerevisiae*, *Gibberella zeae*, *Aspergillus fumigatus*, *Schizosaccharomyces pombe*, *Kluyveromyces lactis*, *Ashbya gossypii*, *Debaryomyces hansenii*, *Candida albicans*, *Yarrowia lipolytica*, *Xenopus tropicalis*, *Drosophila melanogaster*, *Caenorhabditis elegans*, *Homo sapiens*, *Danio rerio* and *Mus musculus*. Their evolutionary relationship is shown in Fig. 12. As noted previously (Adolph, 2005), Tob37 and Tob38 are homologs of each other. The relationships between the homologs of Tob37 and Tob38 determined using another maximum likelihood algorithm (Fitch-Margoliash matrix), a protein parsimony algorithm, or by aligning the Tob37 or the

Figure 10: Multiple sequence alignment of Tob37 from *N. crassa* (Nc), *S. cerevisiae* (Sc), and *H. sapiens* (Hs) using ClustalW2 (Chenna *et al.*, 2003). "*" indicates identical residues, ":" indicates conserved substitutions, "." indicates semiconserved substitutions. Mutations created that affects the protein are named above the *N. crassa* sequence (see section 3.11), residues affected are shown in boxes. EKR20 was designed to create a deletion of the LP residues at positions 52 to 53 (but see section 3.12), EKR21 is a single substitution of L52A, and EKR22 is a single substitution of P53A. EKR23 is a deletion of 17 amino acids of the glutamic acid rich region encompasing amino acids 236 to 253. Tob37 contains two predicted TMDs in the C-terminus. EKR15 is a premature stop codon at amino acid 337 which removes both predicted TMDs. EKR35 is an eight amino acid deletion (LAINVAGL) in the first putative TMD at amino acids 396 to 404. EKR36 is a premature stop codon at amino acid 425, removing the second putative TMD. Peptide 1 and peptide 2 from GenScript, which were used as antigens for antibody production, are indicated in bold. The peptide used to produce an in-house antibody in mouse was identical to the GenScript peptide 1 except that it lacked the last two amino acids. TMDs in *N. crassa* and *H. sapiens* (Armstrong *et al.*, 1997) are indicated in bold and by shading.

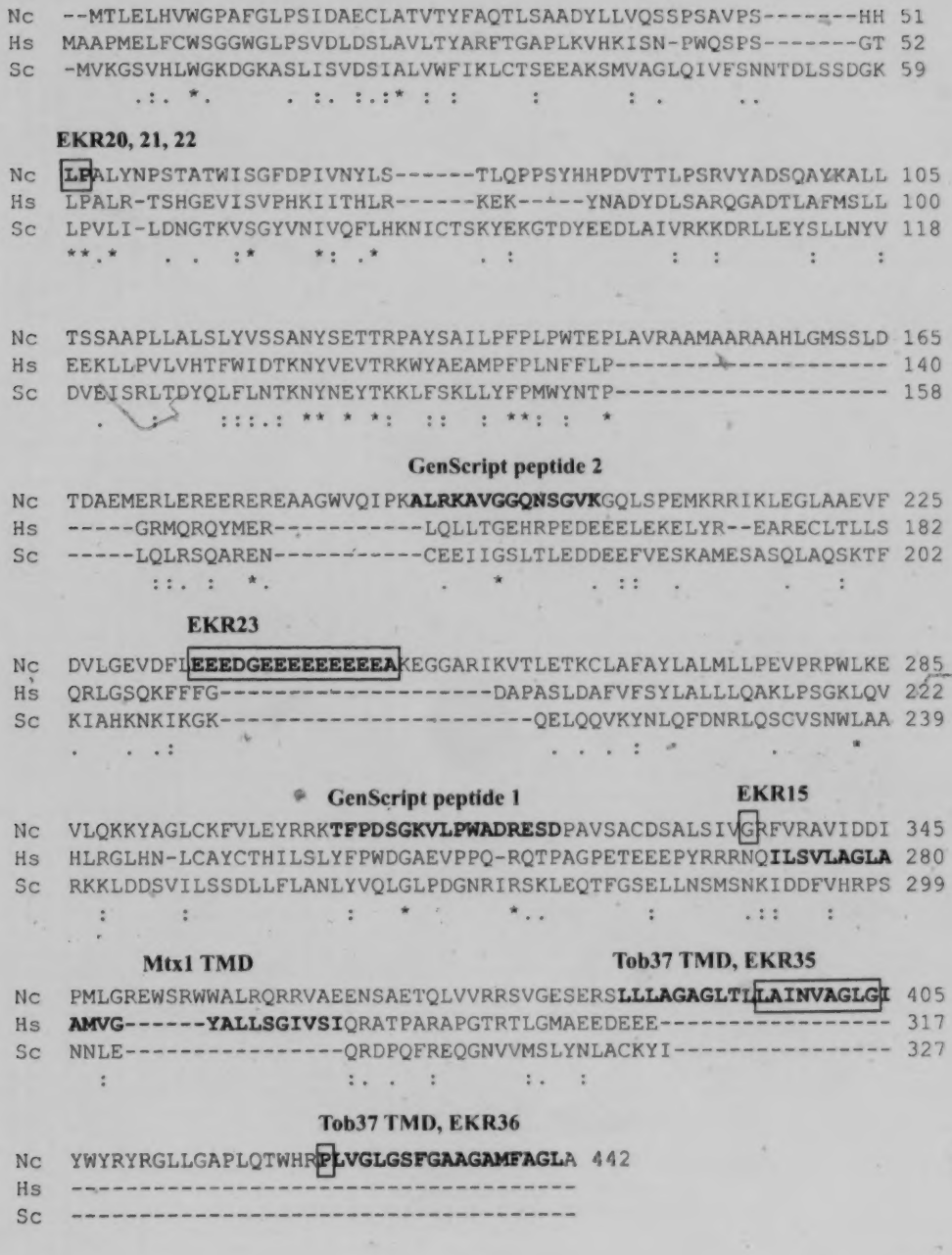
Nc --MTLELHVWGPAFGLPSIDAECLATVTYFAQTLSAADYLLVQSSPSAVPS-------HH 51
Hs MAAPMELFCWSGGWGLPSVDLDSLAVLTYARFTGAPLKVHKISN-PWQSPS-------GT 52
Sc -MVKGSVHLWGKDGKASLISVDSIALVWFIKLCTSEEAKSMVAGLQIVFSNNTDLSSDGK 59
EKR20, 21, 22
Nc LPALYNPSTATWISGFDPIVNYLS------TLQPPSYHHPDVTTLPSRVYADSQAYKALL 105
Hs LPALR-TSHGEVISVPHKIITHLR------KEK-----YNADYDLSARQGADTLAFMSLL 100
Sc LPVLI-LDNGTKVSGYVNIVQFLHKNICTSKYEKGTDYEEDLAIVRKKDRLLEYSLLNYV 118
Nc TSSAAPLLALSLYVSSANYSETTRPAYSAILPFPLPWTEPLAVRAAMAARAAHLGMSSLD 165
Hs EEKLLPVLVHTFWIDTKNYVEVTRKWYAEAMPFPLNFFLP---------------------- 140
Sc DVEISRLTDYQLFLNTKNYNEYTKKLFSKLLYFPMWYNTP---------------------- 158
GenScript peptide 2
Nc TDAEMERLEREEREREAAGWVQIPKALRKAVGGQNSGVKGQLSPEMKRRIKLEGLAAEVF 225
Hs -----GRMQRQYMER-----------LQLLTGEHRPEDEEELEKELYR--EARECLTLLS 182
Sc -----LQLRSQAREN-----------CEEIIGSLTLEDDEEFVESKAMESASQLAQSKTF 202
EKR23
Nc DVLGEVDFIEEEDGEEEEEEEEEAKEGGARIKVTLETKCLAFAYLALMLLPEVPRPWLKE 285
Hs QRLGSQKFFFG---------------------DAPASLDAFVFSYLALLLQAKLPSGKLQV 222
Sc KIAHKNKIKGK-----------------------QELQQVKYNLQFDNRLQSCVSNWLAA 239
GenScript peptide 1
EKR15
Nc VLQKKYAGLCKFVLEYRRKTFPDSGKVLPWADRESDPAVSACDSALSIVGRFVRAVIDDI 345
Hs HLRGLHN-LCAYCTHILSLYFPWDGAEVPPQ-RQTPAGPETEEEPYRRRNQILSVLAGLA 280
Sc RKKLDDSVILSSDLLFLANLYVQLGLPDGNRIRSKLEQTFGSELLNSMSNKIDDFVHRPS 299
Mtx1 TMD
Tob37 TMD, EKR35
Nc PMLGREWSRWWALRQRRVAEENSAETQLVVRRSVGESERSLLLAGAGLTLLAINVAGLGI 405
Hs AMVG------YALLSGIVSIQRATPARAPGTRTLGMAEEDEEE----------------- 317
Sc NNLE----------------QRDPQFREQGNVVMSLYNLACKYI----------------- 327
Tob37 TMD, EKR36
Nc YWYRYRGLLGAPLQTWHRPLVGLGSFGAAGAMFAGLA 442
Hs ----------
Sc ----------

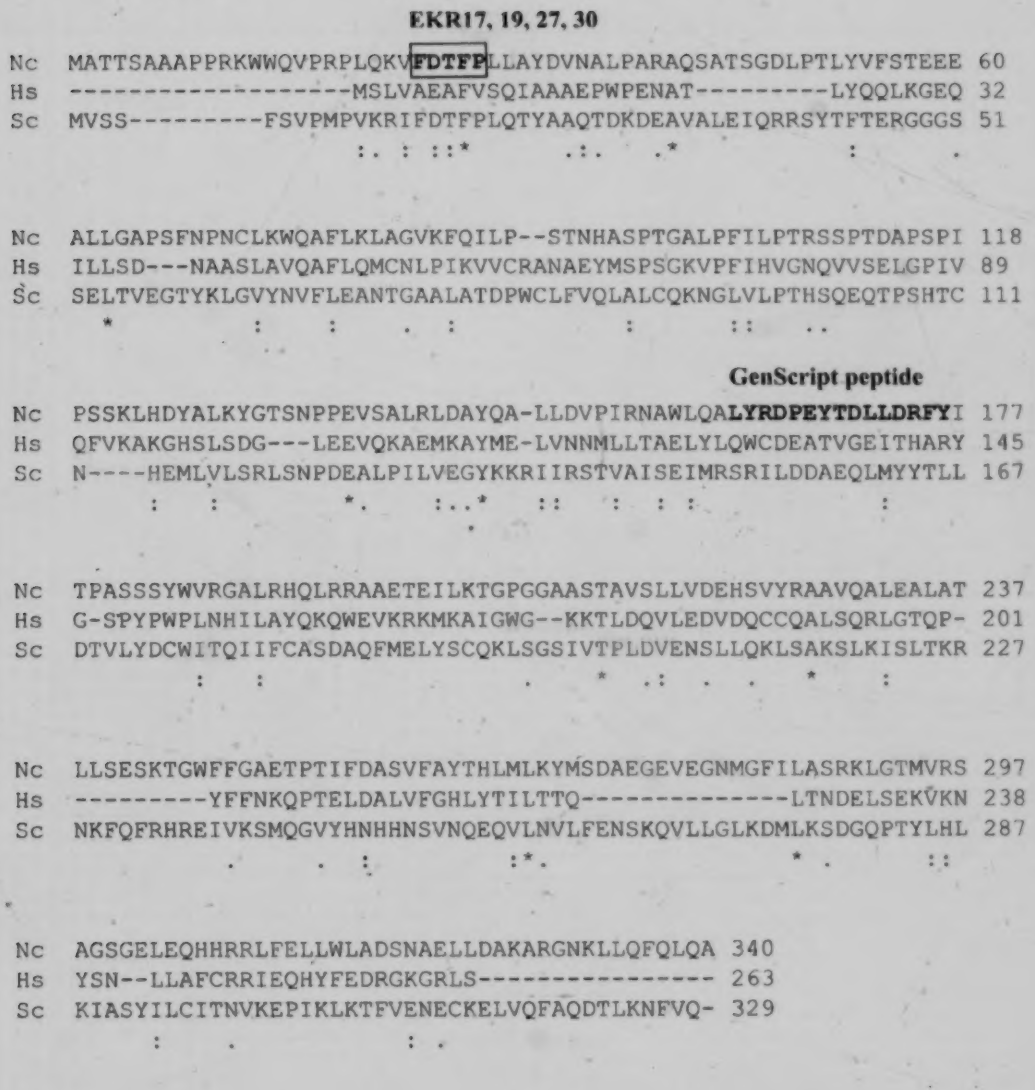

Figure 11: Multiple sequence alignment of Tob38 from *N. crassa* (Nc), *S. cerevisiae* (Sc), and *H. sapiens* (Hs) using ClustalW2 (Chenna *et al.*, 2003). "*" indicates identical residues, ":" indicates conserved substitutions, "." indicates semi-conserved substitutions. Mutations created in the protein (see section 3.9) are shown above the sequence. Residues affected are indicated in boxes. The mutation EKR17 is a deletion of FDT at amino acids 24 to 26, EKR19 is a single substitution of D25A, EKR27 is a single substitution of F27A, and EKR30 is a deletion of FDTFP at amino acids 24 to 28. The GenScript peptide used as an antigen for antibody production is indicated in bold. The in-house antibody to *N. crassa* Tob38 was raised in a guinea pig to a fusion protein containing residues 1 to 185 of Tob38.

Figure 12: An unrooted maximum likelihood tree of Tob37 and Tob38 protein homologs using the JTT matrix with the following species: *Neurospora crassa* (Nc), *Chaetomium globosum* (Cg), *Magnaporthe grisea* (Mg), *Saccharomyces cerevisiae* (Sc), *Gibberella zeae* (Gz), *Aspergillus fumigatus* (Af), *Schizosaccharomyces pombe* (Sp), *Kluyveromyces lactis* (Kl), *Ashbya gossypii* (Ag), *Debaryomyces hansenii* (Dh), *Candida albicans* (Ca), *Yarrowia lipolytica* (Yl), *Xenopus tropicalis* (Xt), *Drosophila melanogaster* (Dm), *Caenorhabditis elegans* (Ce), *Homo sapiens* (Hs), *Danio rerio* (Dr), and *Mus musculus* (Mm). Tob38 homologs are indicated by the shaded background. Mtx1 is the name used in animal species for Tob37. Mtx2 is the name used for in animals Tob38.

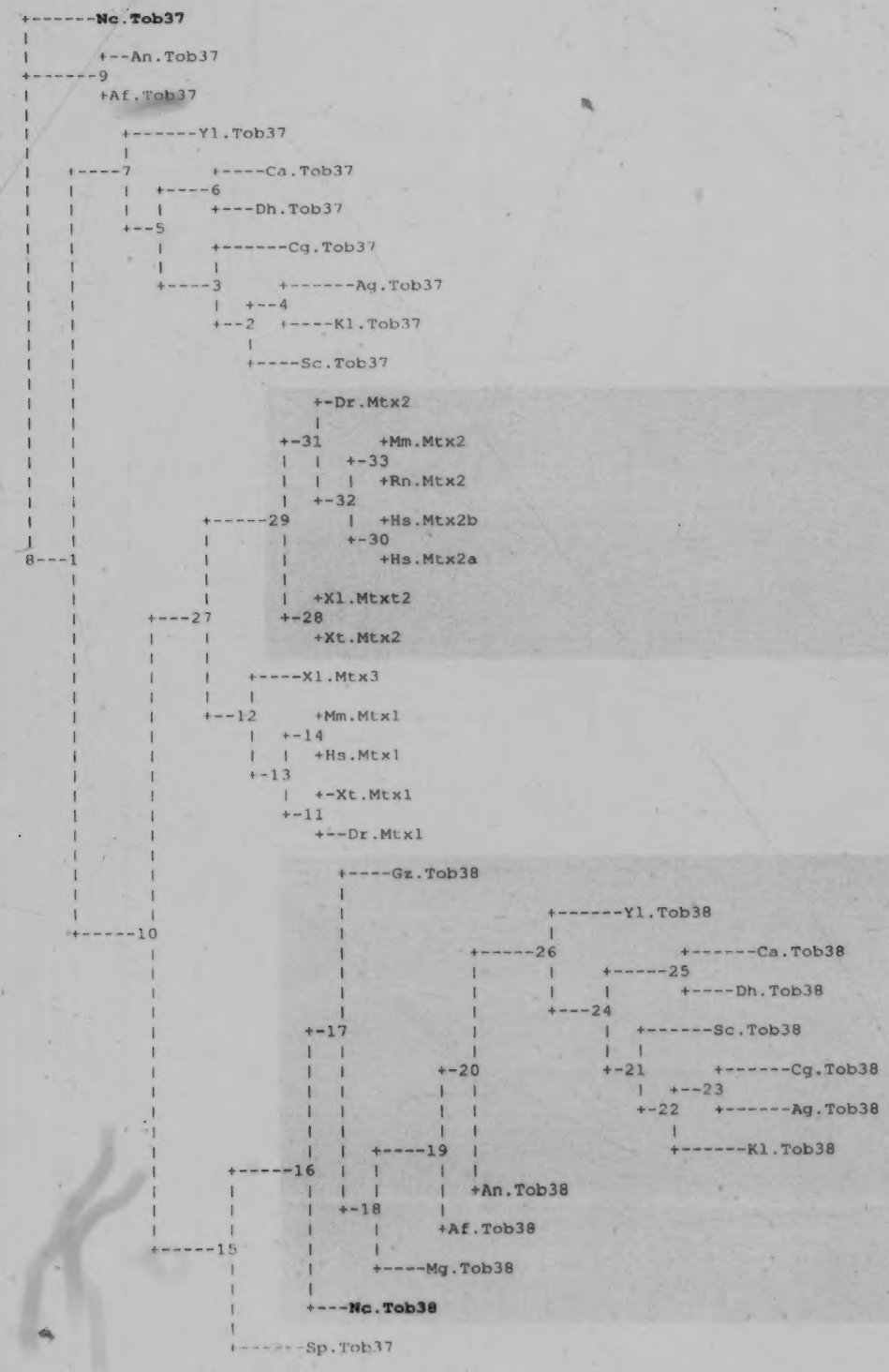

Ln Likelihood = -22220.41164

Tob38 homologs separately with the same algorithms, were similar to those found with the JTT maximum likelihood matrix (Eck and Dayhoff, 1966; Fitch and Margoliash, 1967; Fitch, 1971; Sankoff, 1975; Jones *et al.*, 1992).

3.5 Location and Topology of *N. crassa* Tob37 and Tob38

Amino acid sequence analysis using HMMTOP and TopPredII, computer programs for the prediction of transmembrane helices and topology of proteins, was performed on the predicted sequences of the *N. crassa* Tob38 and Tob37 proteins (Claros and von Heijne, 1994; Tusnady and Simon, 1998). In *N. crassa*, Tob37 is predicted to be an integral membrane protein with two putative transmembrane domains (TMD) near the C-terminus located at amino acids 386 to 405 and 424 to 441 of the 442 amino acid protein based on computer prediction (Fig. 10). Neither of the two putative C-terminal TMDs in Tob37 were predicted in the yeast protein (Fig. 10A), though a single C-terminal TMS is predicted in the mammalian version of Tob37 (Armstrong *et al.*, 1997). The mammalian TMD corresponds to the first *N. crassa* TMD with respect to distance from the C-terminus. Previous results with the yeast homolog predict the majority of Tob37 is on the cytosolic side of the MOM (Wiedemann *et al.*, 2003; Paschen *et al.*, 2005). An attempt was made to determine if either of the TMDs was functional by creating mutations in the C-terminal end of the *N. crassa* protein (see section 3.11). Another putative TMD was predicted at amino acids 102 to 122 in *N. crassa* Tob37. However, due to the low prediction score and no previous indication TMD in other species at this location, this domain was not investigated further.

Tob38 does not contain any regions predicted to be TMDs in any species examined (Fig. 11). Tob38 in yeast is predicted to be a peripheral MOM protein (Milenkovic *et al.*, 2004; Ishikawa *et al.*, 2004; Waizenegger *et al.*, 2004).

Proteinase K treatment of isolated mitochondria was used to determine if *N. crassa* Tob37 and Tob38 were located on the cytosolic side of the MOM. Several proteins were examined as controls. The known MOM protein Tom70, which contains a large cytosolic domain, is known to be sensitive to proteinase K (Hines *et al.*, 1990; Lithgow *et al.*, 1994). Tob55 is an integral beta-barrel protein with loops exposed to the cytosol and was known to be sensitive to proteinase K, as shown by a shift to a lower

molecular weight following treatment (Habib *et al.*, 2005; Paschen *et al.*, 2005; Habib *et al.*, 2007). The IMS protein Tim8 and matrix protein Hsp70 are insensitive to the proteinase K since the MOM protects them from the action of the enzyme (Schneider *et al.*, 1994; Hoppins *et al.*, 2004). Each of the controls behaved as expected following proteinase K treatment (Fig. 13A). Tob37 and Tob38 were degraded by externally added proteinase K, suggesting that they are at least partially exposed on the cytosolic side of the MOM.

Carbonate extraction was used to determine if Tob37 and Tob38 were peripheral or integral membrane proteins (Fig. 13B). Several proteins were used as controls. Tom70 is a MOM protein with a single TMD anchoring it to the membrane (Hines *et al.*, 1990; Lithgow *et al.*, 1994), Tob55 is an integral beta-barrel protein (Habib *et al.*, 2005; Paschen *et al.*, 2005; Habib *et al.*, 2007), and Tim8 and Hsp70 are not integrated in a membrane (Schneider *et al.*, 1994; Hoppins *et al.*, 2004). Carbonate extraction showed Tob38 was not extracted at pH 10.8 but the majority of the protein was removed from the membrane at pH 11.5. At pH 12.0, all Tob38 was removed from the membrane. For Tob37, a small amount of the protein was removed at pH 10.8 and pH 11.5, but greater dissociation from the membrane was observed at pH 12.0. Interestingly, this pattern resembles that for Tom70, a protein with a single known TMD. Taken together, these results indicate that Tob37 is probably anchored in the MOM by at least a single TMD and that Tob38 is peripherally associated with the MOM by relatively strong interactions with other components of the MOM.

3.6 Microscopy of Tob38↓, Tob37↓ and *tom70*^{RIP} Mitochondria

Fluorescence microscopy of yeast Tob38↓, Mim1↓, Tob55↓, temperature sensitive Tom40 mutants generated by error prone PCR, temperature sensitive Tob55 mutants generated by error prone PCR, *mdm10*Δ, *tob37*Δ, *tom5*Δ, *tom6*Δ, and *tom7*Δ cells have all shown aberrant mitochondrial morphology including enlarged mitochondria, to different extents in the various strains (Meisinger *et al.*, 2004; Altmann and Westermann, 2005; Meisinger *et al.*, 2006; Stojanovski *et al.*, 2006). Yeast cells lacking Tob37 showed enlarged mitochondria in 86 to 95% of the cells at 37°C (Meisinger *et al.*, 2004; Meisinger *et al.*, 2006). The percentage of cells with abnormal

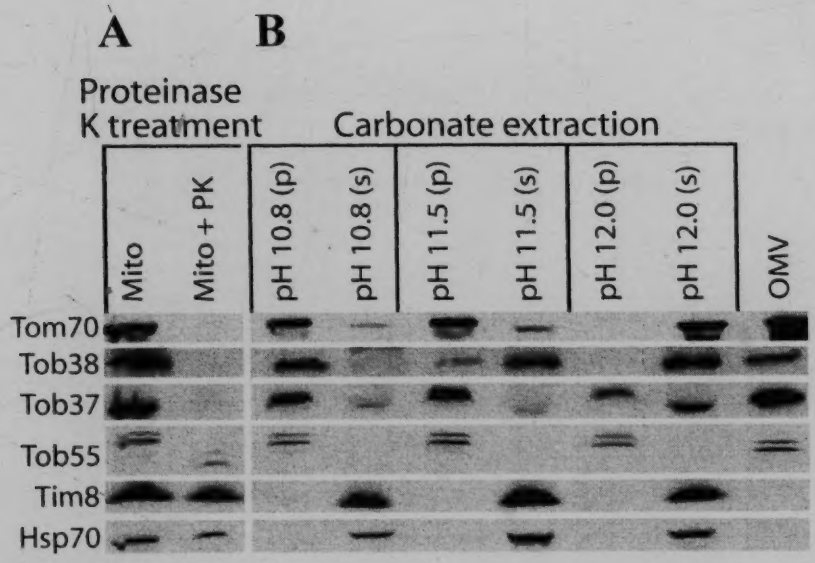

Figure 13: Behaviour of Tob38 and Tob37 following proteinase K treatment and carbonate extraction of mitochondria. **A.** 30 μg of control (76-26) mitochondria were either untreated (Mito) or treated with proteinase K (Mito + PK). Mitochondrial proteins were electrophoresed on SDS-PAGE gels, blotted to nitrocellulose, and probed with specific antibodies. **B.** 30 μg of control (76-26) mitochondria were extracted with sodium carbonate at different pHs as indicated on the figure. The pellet (p) and supernatant (s) were obtained as described section 2.11 and examined on Western blots. OMVs from control (HP1) mitochondria were used as a control on the same blots.

mitochondrial morphology was not published for Tob38↓ cells (Altmann and Westermann, 2005). The average size of ellipsoidal mitochondria as viewed by electron microscopy in *N. crassa* is 600 to 1500 nm (Nicastro *et al.*, 2000). TEM of control and the knockout strains grown as heterokaryons in minimal medium, and Tob37↓ or Tob38↓ cultures all showed well formed mitochondria with observable cristae and double membranes (Fig. 14). Tob38↓, Tob37↓, and also *tob38*KO grown as a heterokaryon in minimal medium showed some enlarged mitochondria as compared to the control (HP1) mitochondria. Thus, there may be slight effects on mitochondrial morphology in these mutants.

Fluorescence microscopy of *N. crassa* control (HP1), Tob38↓, Tob37↓ and *tom70*^{RIP} cells stained with MitoTracker green was attempted. A Tom70 mutant strain was deemed to be a good control as it had previously been shown to have enlarged mitochondria by TEM (Grad *et al.*, 1999). Unfortunately, the interpretation of the results of this experiment was hindered by high background and low resolution (Fig. 15). Thus, conclusions on the relative size and arrangement of mitochondria in the wildtype, Tob37↓, Tob38↓, or *tom70*^{RIP} strains were not possible based on this method.

3.7 TOB Complex Interactions

Tob55, Tob38 and Tob37 are considered to be the components of the core TOB complex in yeast (Meisinger *et al.*, 2007; Neupert and Herrmann, 2007). To determine if these proteins associate as a complex in *N. crassa*, the knockout strains were rescued with C-terminal his_6-tagged versions of Tob37 and Tob38 for use in pulldown experiments. Mitochondria containing an N-terminal His_9-Tob55 (supplied by Nancy Go) were also used. When mitochondria containing His_9-Tob55 were analyzed by Ni-NTA chromatography, Tob37 and Tob38 co-eluted from the column with Tob55 as indicated by Western blot analysis of the eluted proteins (Fig. 16). Similar experiments with Tob38-His_6 showed that Tob55 and Tob37 both co-eluted from the column with Tob38. When mitochondria containing Tob37-His_6 were analyzed by Ni-NTA chromatography, very low amounts of Tob55 and Tob38 were observed. However, even Tob37-His_6 was barely detectable in these experiments, and the low levels of other TOB components observed might be due to poor binding of the tagged Tob37 protein to the nickel-

Figure 14: Transmission electron microscopy of mitochondria. **A.** Control strain (HP1) was grown in the presence of his and fpa. The *tob38*KO strain was grown in minimal medium (*tob38*KO min) or medium containing his and fpa (*tob38*KO fpa) to generate Tob38↓ cells as described in Fig. 3. The scale bars represent 500 nm. **B.** As in panel A except with the *tob37*KO strain.

A

Control (his + fpa) *tob38*KO min *tob38*KO fpa

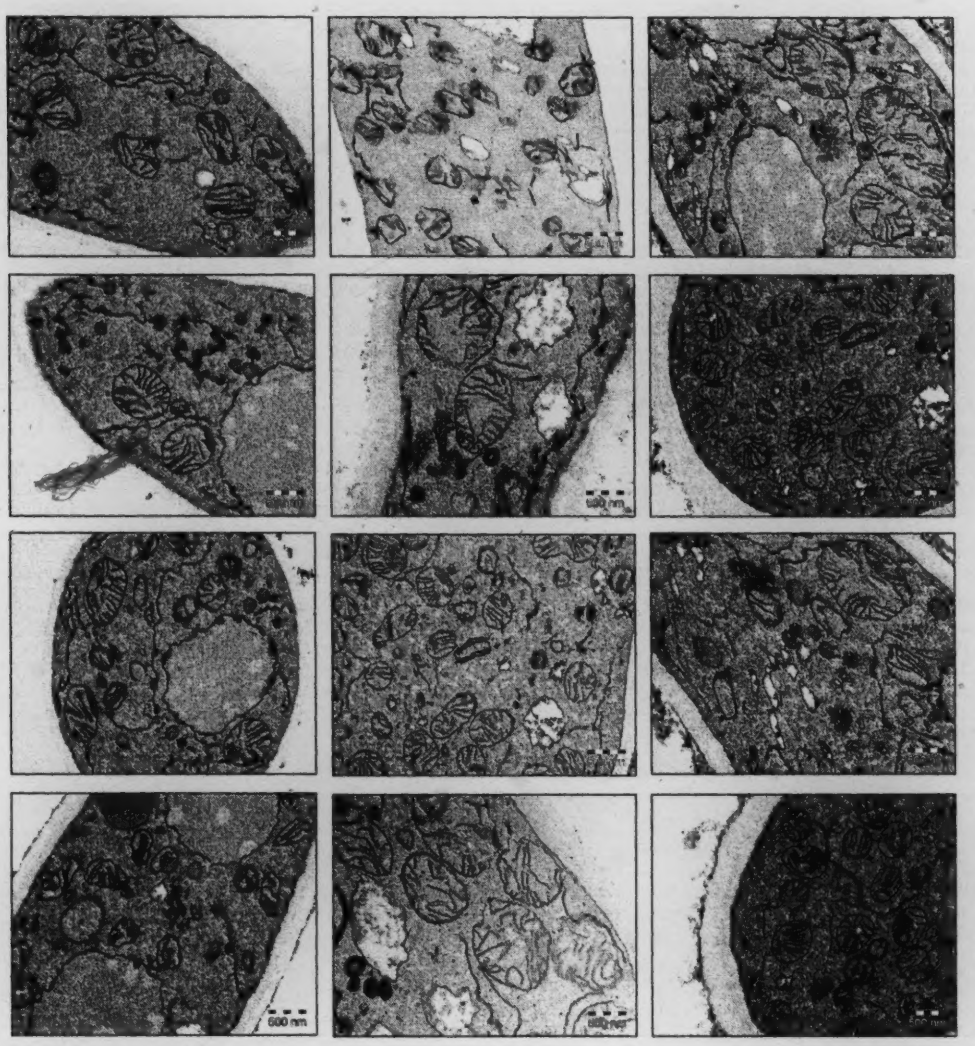

B

Control (his + fpa) *tob37*KO min *tob37*KO fpa

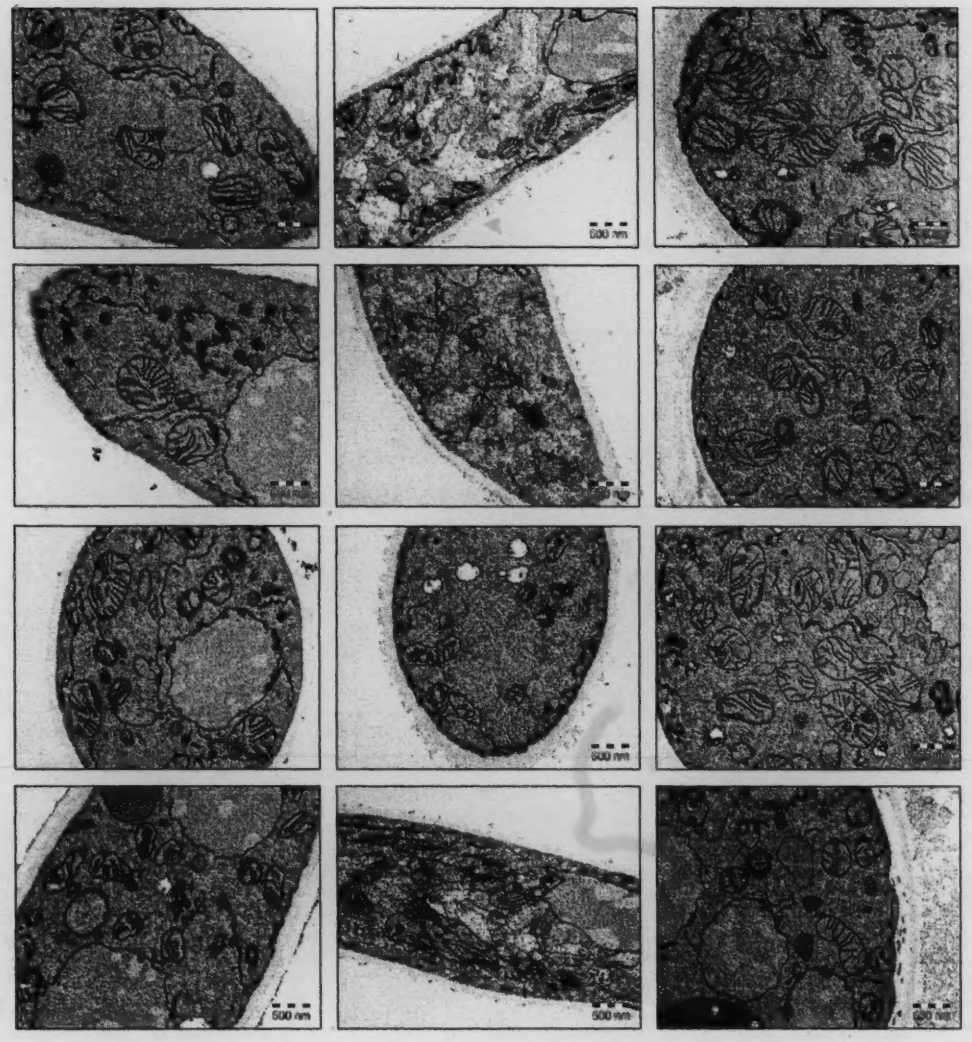

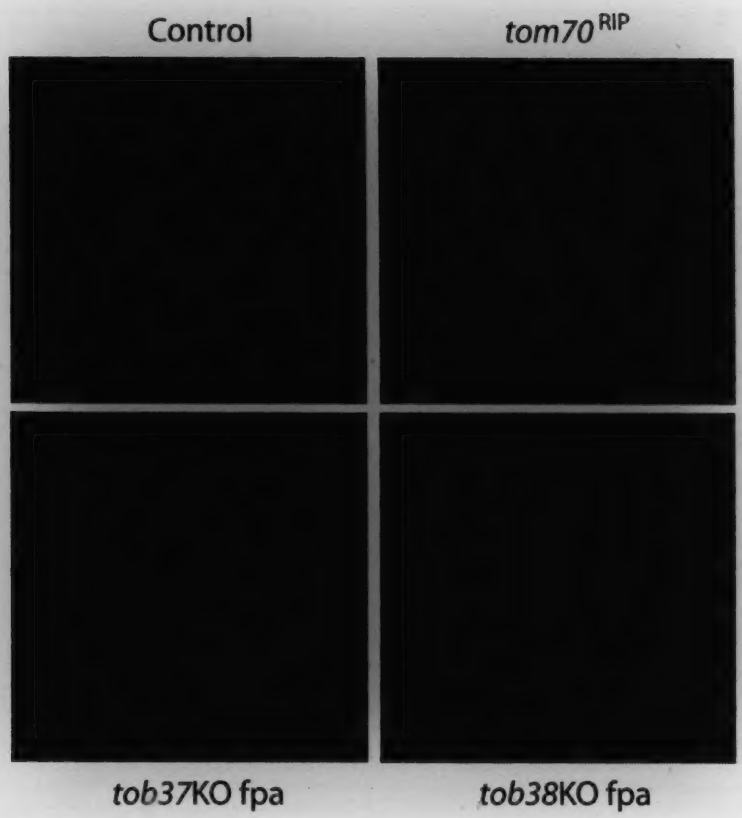

Figure 15: Fluorescence microscopy of mitochondria. Control (HP1), *tom70*^{RIP}, Tob37↓ (*tob37*KO fpa) and Tob38↓ (*tob38*KO fpa) cells were stained with MitoTracker green and analyzed by fluorescence microscopy at 1000x magnification. Strains were grown as described in Fig. 3.

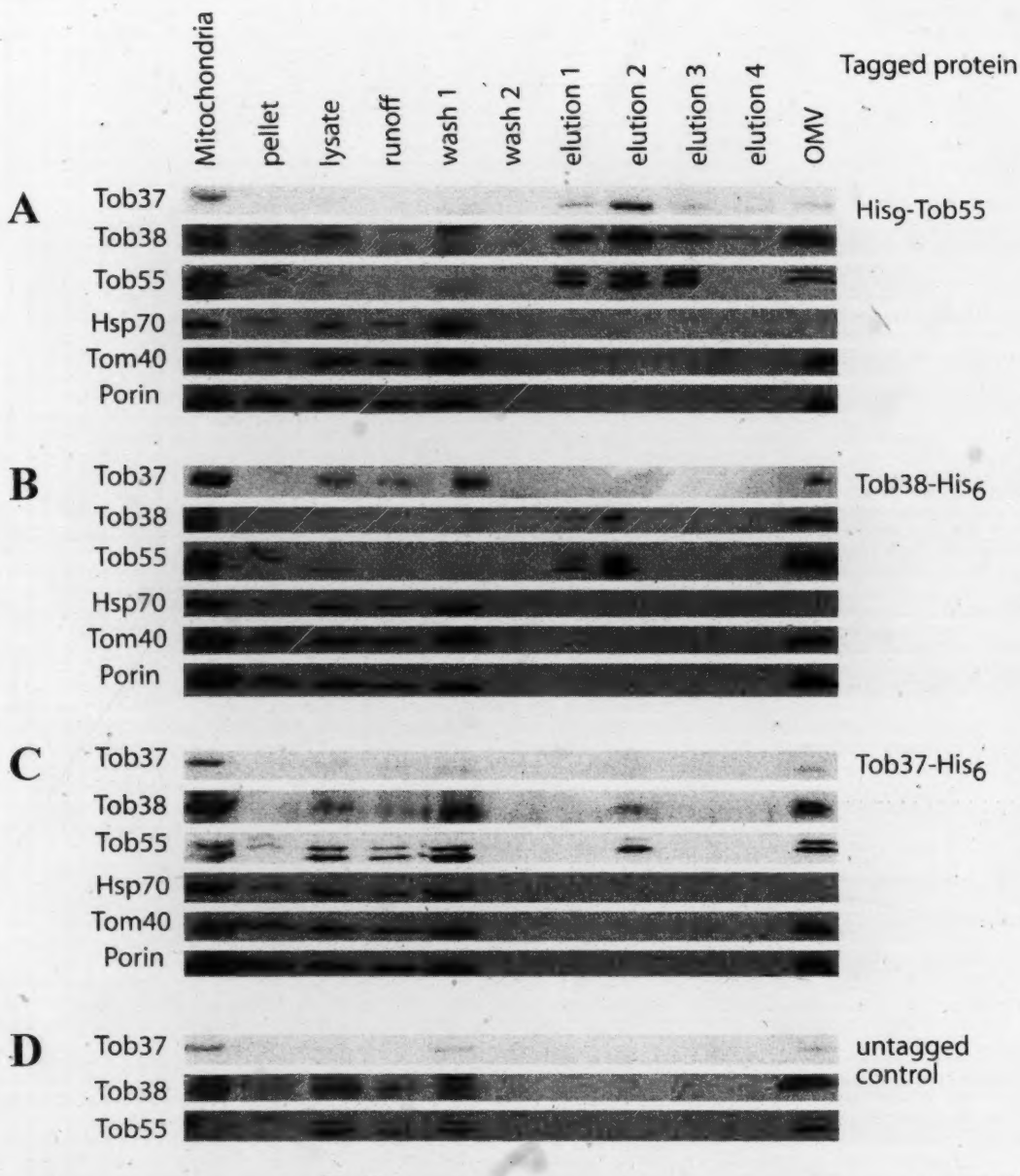

Figure 16: Binding of his-tagged TOB complex proteins to Ni-NTA resin and identification of interacting proteins. Isolated mitochondria (300 μg) from strains carrying Tob37-His_6 (**A**), Tob38-His_6 (**B**), His_9-Tob55 (**C**), and an untagged control (76-26) strain (**D**) were lysed with 1% digitonin and soluble proteins were subjected to Ni-NTA chromatography. The column was washed once with 10 vol of 10 mM imidazole buffer, once with 10 vol of 20 mM imidazole buffer, then eluted four times with a buffer containing 400 mM imidazole. Samples were electrophoresed on SDS-PAGE gels, blotted to nitrocellulose, and probed with specific antibodies. 5 μg of control (HP1) OMVs are included as a control in each panel.

nitrilotriacetic acid (NiNTA) column. None of the proteins analyzed were detected in column elutions when proteins from control (76-26) mitochondria, containing no his-tagged proteins, were loaded onto the column (Fig. 16D).

Further analysis of the TOB complex was done using BNGE to determine the size of the complex(s) and the effect of decreased levels of individual Tob components on TOB complex formation. The TOM complex was also examined to look for quantitative differences in the mutant mitochondria. Mitochondria isolated from control (HP1) and cultures deficient in various Tob proteins were probed with antibodies against Tom40 and Tob55. The α-Tom40 antibody detected the TOM complex of 400 kDa in all strains examined (Fig. 17). The TOM complex was present at decreased levels in all strains with reduced Tob components. This was expected due to the deficiency of TOM complex components seen in SDS-PAGE analysis (Fig. 8). Surprisingly, in the Tob55↓ and Tob37↓ mitochondria the TOM complex appeared to be of a slightly higher molecular weight (Fig. 17). This increase in size was not due to the amount of protein present per lane of the gel, as decreasing concentrations of wildtype mitochondria analyzed by BNGE revealed no changes in size (data not shown). The α-Tob55 antibody detected 50, 100, 140, 185 and 250 kDa bands representing putative TOB complexes (Fig. 17). The 50 and 100 kDa bands may represent Tob55 monomers, dimers, or trimers respectively. However, it is not expected that an excess of Tob55 monomer be present in Tob55↓ mitochondria. An alternative explanation is that a non-specific protein is overproduced in all three mutants and reacts with the antibody. The 185 and 250 kDa complexes are virtually eliminated in Tob38↓, Tob37↓ and Tob55↓ mitochondria. The 140 kDa band was only a very minor band in OMVs and only appeared in the control sample to any extent. Its significance is unknown. The compact 160 kDa band was not substantially reduced in the knockdowns and was not present in OMVs. This band is thought to be due to non-specific binding. Curiously, the mitochondria lacking Tom70 appeared to have reduced levels of the TOB complex. This is discussed further in section 3.13. The Tob38 and Tob37 antibodies used in this study were not useful for probing native gels

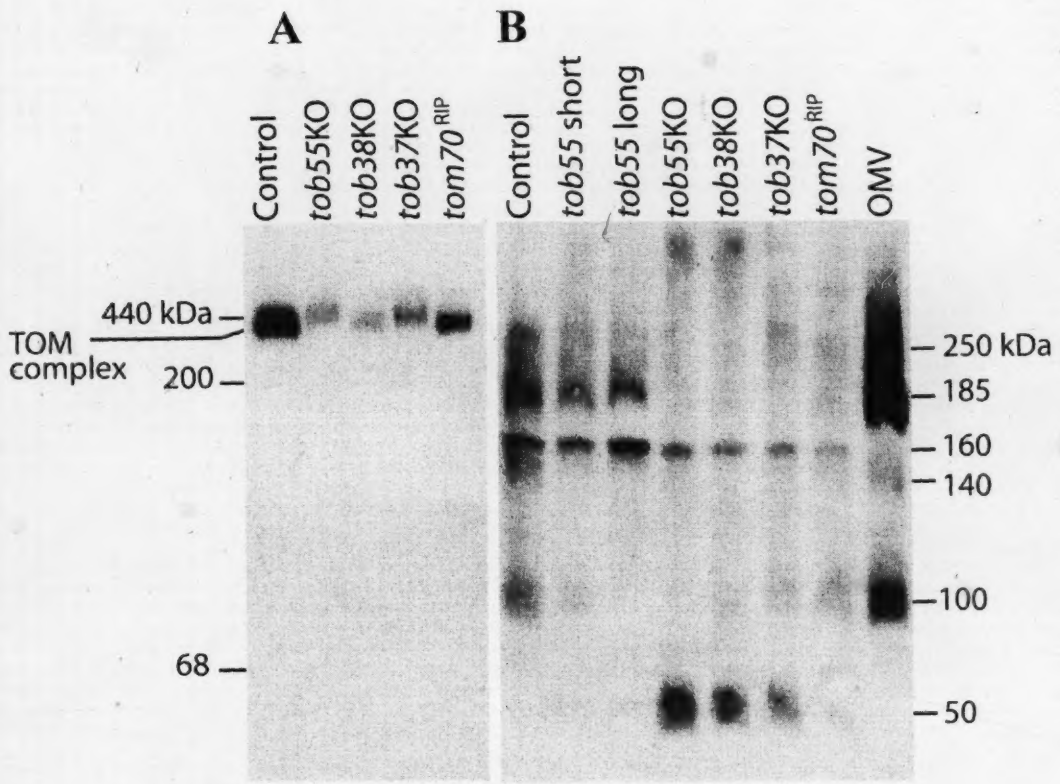

Figure 17: Analysis of TOM and TOB complexes by BNGE. **A.** Control (HP1), Tob38↓ (*tob38*KO fpa), Tob37↓ (*tob37*KO fpa), Tob55↓ (*tob55*KO fpa), and *tom70*^{RIP} mitochondria were examined. **B.** Strains used were as in A except strains expressing only the short (*tob55* short) or long (*tob55* long) alternatively spliced forms of Tob55 were analyzed. Strains were grown as described in Fig. 3, except for *tom70*^{RIP} which is a homokaryon containing a non-functional *tom70* gene inactivated by RIP (Grad *et al.*, 1999) and was grown in Vogel's medium plus pan. 50 μg of isolated mitochondria were lysed with 1% digitonin and electrophoresed on a 6 to 13% gradient blue native acrylamide gel. The gels were blotted to PVDF and probed with antibodies to either Tom40 (**A**) or Tob55 (**B**). The position of molecular weight standards is indicated on the left. The apparent molecular weights of the TOB complexes discussed in the text are indicated on the right. Control (HP1) OMVs were included on the Tob55 blot as a control.

due to high levels of background and low sensitivity[2].

In Neurospora, Tob55 is alternatively spliced into three isoforms called long, intermediate, and short (Hoppins, *et al.*, 2007). Strains expressing only the long version have growth defects and decreased levels and assembly of beta-barrel proteins at 37°C (Hoppins *et al.*, 2007) (Fig. 17). Interestingly, mitochondria containing only the long form appeared to lack the Tob55 100 kDa band.

3.8 *In vitro* Import

Numerous attempts to perform *in vitro* import of mitochondrial precursor protein into Tob38↓ and Tob37↓ mitochondria were made. However, examination of the mitochondria used in these experiments showed that the levels of IMS proteins (Tim13 and cytochrome *c* heme lyase (CCHL)) were decreased in Tob38↓ and Tob37↓ mitochondria especially following treatment with proteinase K (Fig. 18). Decreases in IMS proteins in isolated mitochondria are diagnostic for mitochondria with broken MOMs. To alleviate the problem, I tried to optimize the mitochondrial isolation procedure by decreasing the fpa concentration, minimizing grinding time, and increasing sucrose concentration in the isolation buffer. None of these conditions corrected the problem (data not shown). Since loss of IMS components can affect the import of various precursors, the value of import experiments into mitochondria isolated from these strains is questionable. However, the data in Fig. 18 show that severe loss of IMS proteins only occurred after proteinase K treatment and suggested that even though the MOM may be broken, there may be a high enough concentration of IMS proteins in isolated mitochondria to maintain import efficiency. Therefore, to gain possible insight into the import and assembly of certain proteins into mitochondria isolated from Tob37↓ and Tob38↓ strains, some experiments were done.

The wildtype version of Tom40, porin, short Tob55, Tob38 and Tob37 proteins were radiolabeled with ^{35}S-methionine during *in vitro* transcription/translation and imported into control (HP1), Tob38↓ and Tob37↓ mitochondria (Fig. 19A and B). When

[2] Antibodies to Tob37 and Tob38, which produce less background, obtained in house during the writing of the thesis showed bands of 185 and 250 kDa in control (HP1) mitochondria and OMVs when analyzed by BNGE. These bands were reduced in the *tom70*RIP mitochondria and absent in Tob37↓ and Tob38↓ mitochondria (data not shown).

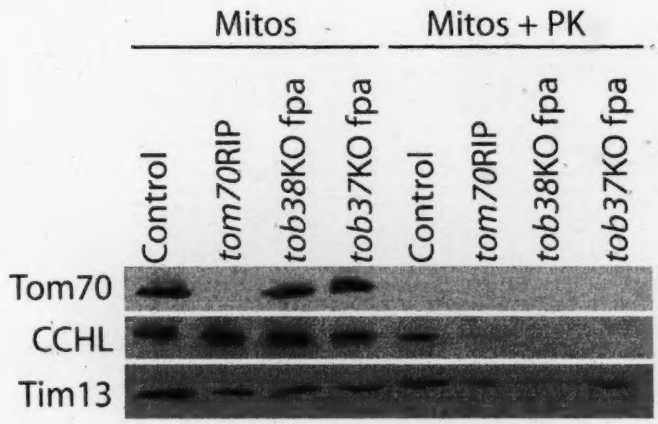

Figure 18: Broken mitochondria isolated from *tom70*^{RIP}, Tob38↓, and Tob37↓ strains following proteinase K treatment. 30 μg of control (HP1), *tom70*^{RIP}, Tob38↓ (*tob38*KO fpa), and Tob37↓ (*tob37*KO fpa) mitochondria were either untreated (Mitos) or treated with proteinase K (Mitos + PK). Strains were grown as described in Fig. 3. Mitochondrial proteins were electrophoresed on SDS-PAGE gels, blotted to nitrocellulose, and probed with specific antibodies.

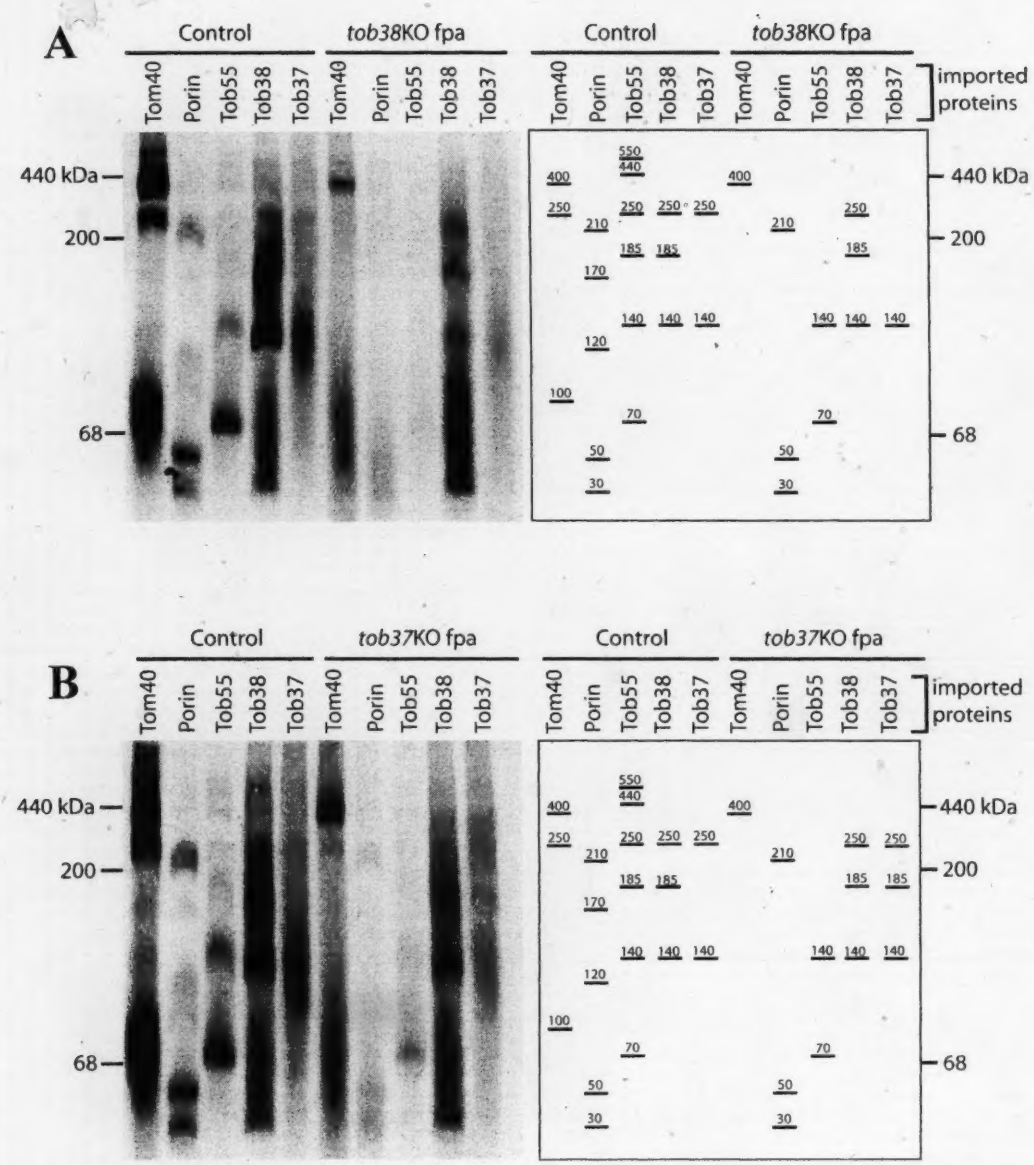

Figure 19: Import and assembly of mitochondrial precursor proteins into Tob deficient mitochondria. Radiolabeled Tom40, porin, short Tob55, Tob38 and Tob37 proteins were imported into 50 μg of mitochondria isolated from control (HP1) and Tob38↓ (*tob38*KO fpa) (**A**), and control (HP1) and Tob37↓ (*tob37*KO fpa) (**B**) cultures. Strains were grown as described in Fig. 3. Following 20 min of import at 25°C, mitochondria were washed in SEMK, lysed with 1% digitonin and analyzed by BNGE. The position of molecular weight standards is indicated on the left. Complexes discussed in the text are indicated in the right hand panel in cartoon form with their apparent molecular weight (kDa) indicated for each band.

imported into control (HP1) mitochondria, Tom40 was found in the expected 250 kDa intermediate I, the 100 kDa intermediate II, and the fully assembled 400 kDa TOM complex. In Tob38↓ or Tob37↓ mitochondria, levels of Tom40 imported were reduced compared to the control, with the Tom40 assembly intermediate I almost absent (Fig. 19). Porin imported into control mitochondria showed a 210 kDa intermediate representing an incoming porin molecule associated with the TOB complex (Hoppins *et al.*, 2007b) as well as other bands representing intermediates and assembled porin complexes. Levels of all porin complexes were severely reduced in both Tob38↓ and Tob37↓ mitochondria. Tob55 precursor imported into control mitochondria showed bands of 70, 140, 185, 250 kDa and faint bands of ca. 440 and 550 kDa. Most of Tob55 was present in the 70 and 140 kDa complexes. All of these bands were virtually absent following import of Tob55 precursor into Tob38↓ or Tob37↓ mitochondria. Tob38 imported into control mitochondria was present in 140, 185, 250 kDa complexes, also with the highest accumulation in the 140 kDa complex. Tob37 was detected as a smear from 250 to 140 kDa, most accumulating in the 140 kDa region. Import of Tob38 or Tob37 into Tob38↓ or Tob37↓ mitochondria was not obviously different from the controls. These experiments suggest changes in the import of the beta-barrel proteins Tom40, porin and Tob55 occur in Tob38↓ and Tob37↓ mitochondria. However, it is difficult to conclude this definitely because of the previously noted IMS leakage. The observation that import of Tob38 and Tob37 into Tob38↓ or Tob37↓ mitochondria does not drastically differ from the controls shows that these proteins do not depend on the TOB complex for their import. However, this finding is difficult to reconcile with the severely reduced steady state levels of these proteins in Tob38↓ and Tob37↓ mitochondria. Perhaps a fully formed TOB complex imparts long term stability to these proteins.

To determine if any of the 140, 185 or 250 kDa Tob38 bands were assembly intermediates, wildtype radiolabeled Tob38 protein was imported into control (HP1) mitochondria for 1 min at 25°C, excess radioactive protein was removed and mitochondria were re-incubated in fresh import buffer for 2, 5, 10, 30, 60 and 120 min (Fig. 20). The conversion of Tom40 from lower molecular weight intermediates to fully assembled TOM complex at approximately 400 kDa is shown as a control (Fig. 20A). None of the observed Tob38 bands decreased or increased in intensity over time (Fig.

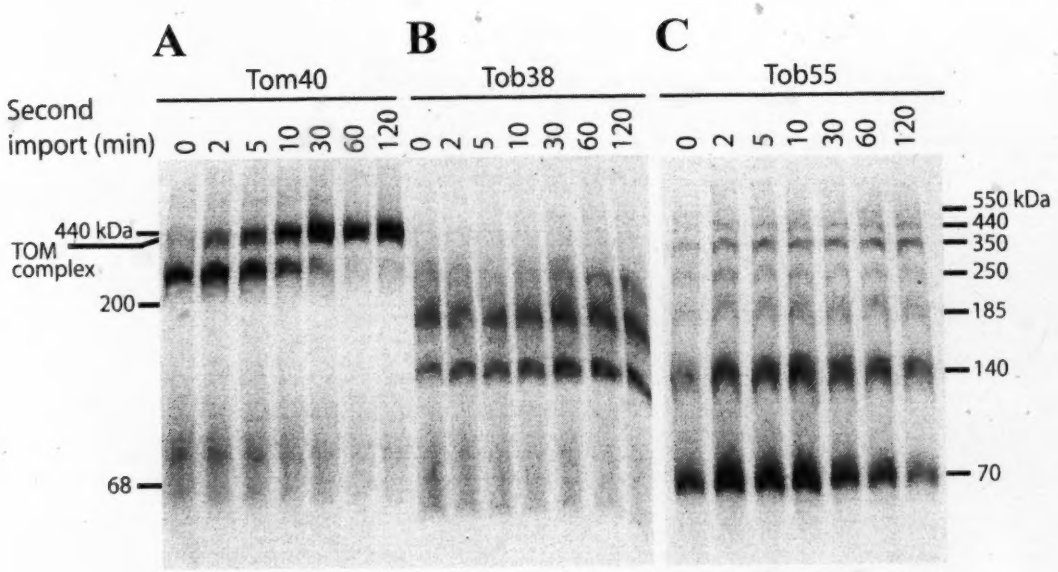

Figure 20: Pulse import and assembly of mitochondria precursor proteins into control (HP1) mitochondria. Radiolabeled Tom40 (**A**), Tob38 (**B**), and Tob55 (**C**) were imported into isolated mitochondria for 1 min at 25°C. The mitochondria were then washed in SEM to remove excess radiolabeled protein and resuspended in import buffer. Import was continued for the indicated times. The mitochondria were then washed in SEMK, lysed with 1% digitonin and analyzed by BNGE. The position of molecular weight standards is indicated on the left. Complexes discussed in the text are indicated on the right with their apparent molecular weight in kDa.

20B). This experiment was also done for 4 and 8 hrs after the initial import with similar results (data not shown). The short isoform of radiolabeled Tob55 was also imported into control (HP1) mitochondria as described for Tob38. As observed for Tob38, none of the Tob55 bands decreased or increased in intensity over time (Fig. 20C). This suggests that after the initial 1 min of import, no further conversion of Tob38 or Tob55 intermediates into fully assembled products occurs. Alternatively, the different forms could all be final forms. This might be tested using a shorter initial import time.

3.9 Conserved Regions of Tob38

Identity among different Tob38 proteins is not high. However, small regions of the protein relatively rich in similarity do exist. I wished to determine the effect of mutations in these regions on the function of Tob38. Tob38 has a relatively highly conserved region at amino acids 24 to 28 (*N. crassa* protein numbering) in fungal species and it was decided to create four mutations in this region: a five amino acid deletion of FDTFP (named version EKR30), a three amino acid deletion of FDT of residues 24 to 26 (EKR17), a single amino acid substitutions of F27A (EKR19), and a single substitution of D25A (EKR27) (Fig. 11 and Fig. 21). All of the above mutations were made in plasmid borne versions of *tob38*. Tob38 mutations EKR27 and EKR30 have been successfully transformed into the *tob38*KO strain. Both mutants rescue the lethal knockout phenotype and purified homokaryons expressing only the mutant forms have been isolated. The mutants are homokaryons of the his-requiring nucleus (Fig. 3A) that bears the knockout in the sheltered heterokaryon. Wildtype *tob38* also successfully rescued the knockout as did a C-terminal his-tagged (Tob38-his_6) version of the protein. To test if the Tob38 mutations affected the growth rate, mutant homokaryons were spotted on his supplemented medium. The mutants were found to grow at rates similar to the control (Fig. 22). Similar experiments done at 18°C or 37°C also showed no differences in growth rates (data not shown). The *tob38* alleles in the mutant strains Tob38-27-1 and Tob38-30-2 were sequenced and confirmed to be wildtype except for the intended mutation. These strains were chosen for further analysis. Mutant strains are named by adding the EKR mutation number (Table 2) as a suffix following "Tob38".

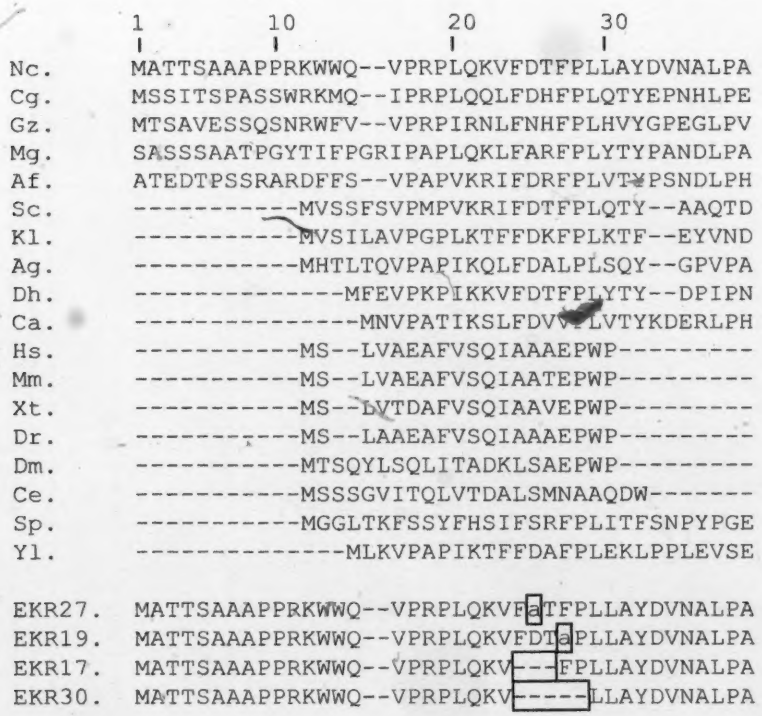

Figure 21: Region of Tob38 targeted for site-directed mutagenesis. Tob38 sequences from *Neurospora crassa* (Nc), *Chaetomium globosum* (Cg), *Magnaporthe grisea* (Mg), *Saccharomyces cerevisiae* (Sc), *Gibberella zeae* (Gz), *Aspergillus fumigatus* (Af), *Schizosaccharomyces pombe* (Sp), *Kluyveromyces lactis* (Kl), *Ashbya gossypii* (Ag), *Debaryomyces hansenii* (Dh), *Candida albicans* (Ca), *Yarrowia lipolytica* (Yl), *Xenopus tropicalis* (Xt), *Drosophila melanogaster* (Dm), *Caenorhabditis elegans* (Ce), *Homo sapiens* (Hs), *Danio rerio* (Dr), and *Mus musculus* (Mm) were aligned using ClustalW2 (Chenna *et al*., 2003). The mutants constructed in *N. crassa* Tob38 are shown in the four lines at the bottom of the alignment. Residues affected in the mutants are shown in boxes and are changes relative to the *N. crassa* sequence (top line). Dashes indicate deletion of residues and lower case "a" indicates changes to alanine. The mutation EKR17 is a deletion of FDT at amino acids 24 to 26, EKR19 is a single substitution of F27A, EKR27 is a single substitution of D25A, and EKR30 is a deletion of FDTFP at amino acids 24 to 28.

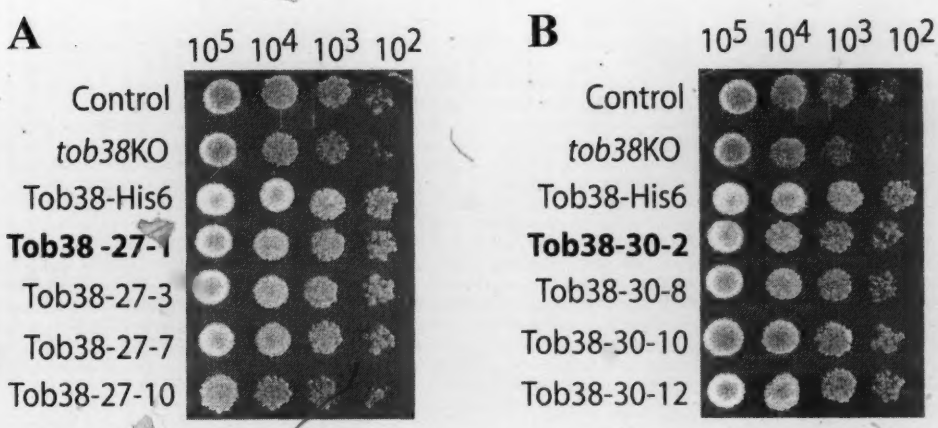

Figure 22: Growth rates of Tob38 mutant strains. Conidia were spotted in 10-fold dilutions on his supplemented medium and incubated at 30°C. Controls in all panels include HP1 (control), the *tob38*KO sheltered heterokaryon (*tob38*KO), and a strain carrying a C-terminal His_6 tagged version of Tob38 (Tob38-His_6). Note that the lack of fpa in the medium means that the *tob38*KO heterokaryon should grow at rates similar to the HP1 control (see Fig. 3A). **A.** Four isolates of the t*ob38*KO strain rescued with the Tob38-27 mutant allele containing a single amino acid substitution of D25A (Fig. 11). **B.** As in panel A but *tob38*KO rescued with the Tob38-30 mutant allele containing a deletion of FDTFP at amino acids 24 to 28. Strains indicated in bold are the strains used for further analysis. Mutant strains are named by adding the EKR mutation number (Table 2) as a suffix following "Tob38". This is followed by a second number which indicates the strain isolate number from a given transformation experiment.

This is followed by a second number which indicates the strain isolate number from a given transformation experiment.

Mitochondria were isolated from wild control (HP1), *tob38*KO and Tob38 mutant strains and examined by Western blot analysis (Fig. 23). Tob38-27-1 and Tob38-30-2 mutant mitochondria showed steady state levels of Tom70, Tom40, porin and Tob38 similar to the control. Size differences can be observed in Tob38 due to the addition of six histidine residues in the Tob38-His_6 protein or deletion of five amino acids in the Tob38-30-2 protein. Steady state levels of Tob55 and Hsp70 appear slightly reduced in the Tob38-27-1 and Tob38-30-2 mutants.

Control (HP1) and Tob38 mutant mitochondria were also analyzed by BNGE with respect to the TOM and TOB complexes (Fig. 24). The mutant strains Tob38-27-1 and Tob38-30-2 showed a slight decrease in the levels of the TOM complex as indicated on the Tom40 blot (Fig. 24A). Tob38-30-2 had slightly decreased levels of all potential TOB complex bands, especially the 250 and 185 kDa TOB complexes as seen on the Tob55 blot (Fig. 24B). The Tob38 and Tob37 antibodies available at the time of writing this thesis were not useful for probing native gels due to high levels of background and low sensitivity.

To determine if the mutations in Tob38 affected their membrane topology or membrane association, Tob38-27-1 and Tob38-30-2 mitochondria were analyzed by proteinase K treatment and carbonate extraction (Fig. 25). As with wildtype Tob38, both mutant proteins were degraded by proteinase K. The Tob38-27-1 protein also behaved identical to the wildtype protein following carbonate extraction. The Tob38-30-2 protein appeared to be less tightly bound to the membrane than wildtype Tob38 as about 50% is removed from the membrane by sodium carbonate at pH 10.8 and it is completely removed by sodium carbonate at pH 11.5. The wildtype protein is barely affected at pH 10.8 and is about 50% removed at pH 11.5. This may indicate that the residues affected in Tob38-30-2 (Fig. 11) are involved in interactions with other TOB complex components or other proteins of the MOM.

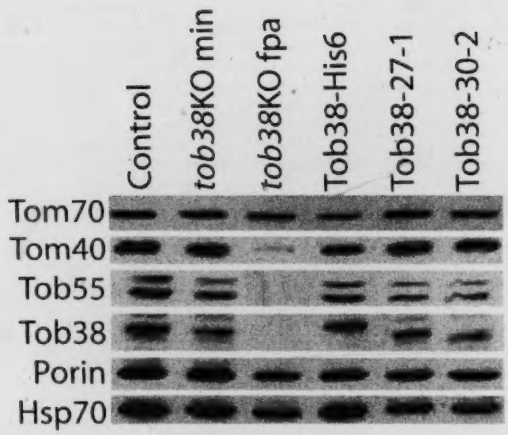

Figure 23: Mitochondrial proteins in the Tob38 mutants. Mitochondrial proteins were electrophoresed on SDS-PAGE gels, blotted to nitrocellulose, and probed with specific antibodies. The mitochondria analyzed were the control (HP1) strain, the *tob38*KO grown in minimal medium (*tob38*KO min), Tob38↓ (*tob38*KO fpa), the mutants Tob38-27-1 and Tob38-30-2. Tob38-27-1 contains a Tob38 mutant allele with a single amino acid substitution of D25A, and Tob38-30-2 contains a Tob38 mutant allele with a deletion of FDTFP at amino acids 24 to 28. Strains were grown as described in Fig. 3. All lanes contain 30 μg of mitochondrial protein.

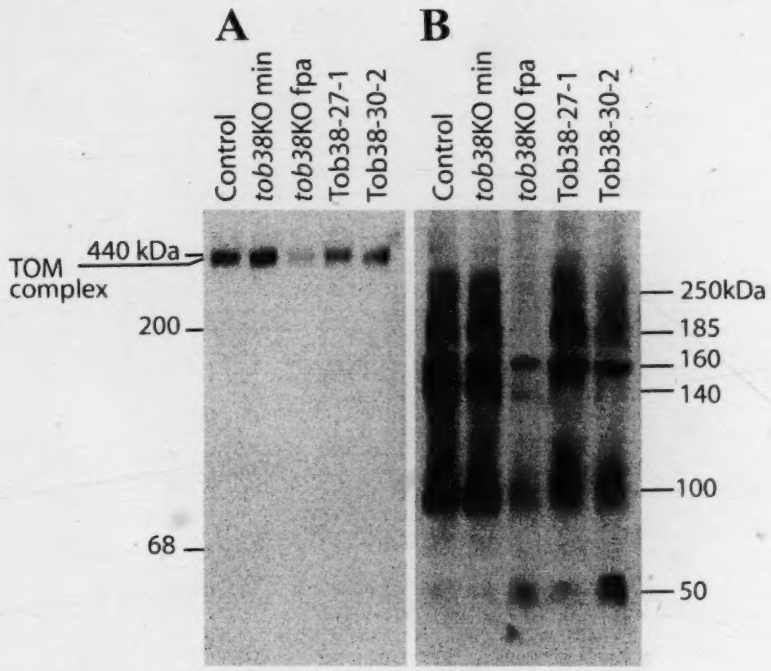

Figure 24: Analysis of the TOM and TOB complexes in the Tob38 mutants by BNGE. Control (HP1), Tob38↓ (*tob38*KO fpa), and Tob38-27-1 and Tob38-30-2 mutant mitochondria were analyzed. Tob38-27-1 contains a Tob38 mutant allele with a single amino acid substitution of D25A, and Tob38-30-2 contains a Tob38 mutant allele with a deletion of FDTFP at amino acids 24 to 28. Strains were grown as described in Fig. 3. 50 μg of mitochondria were lysed with 1% digitonin and electrophoresed on a 6 to 13% gradient blue native acrylamide gel. The gels were blotted to PVDF and probed with antibodies to either Tom40 (**A**) or Tob55 (**B**). The position of molecular weight standards is indicated on the left. Complexes discussed in the text are indicated on the right according to their apparent molecular weight in kDa.

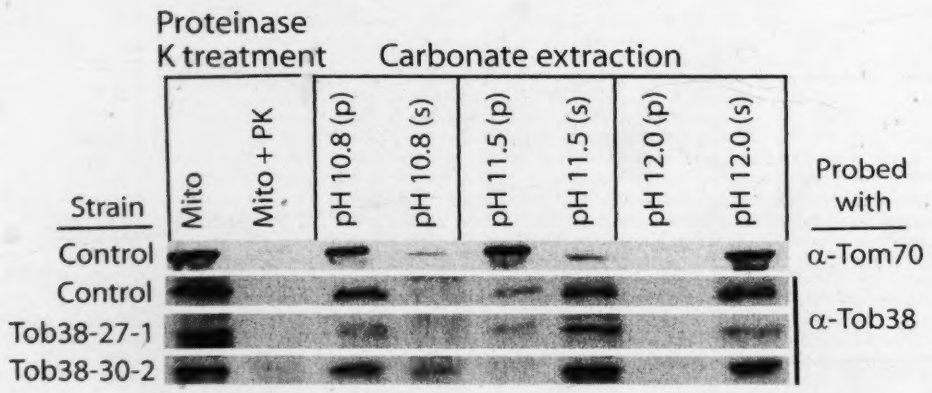

Figure 25: Membrane association of mutant Tob38 proteins. 30 μg of control (76-26), Tob38-27-1, or Tob38-30-2 mitochondria were either untreated (Mito) or treated with proteinase K (Mito + PK). Tob38-27-1 contains a Tob38 mutant allele with a single amino acid substitution of D25A, and Tob38-30-2 contains a Tob38 mutant allele with a deletion of FDTFP at amino acids 24 to 28. Mitochondrial proteins were electrophoresed on SDS-PAGE gels, blotted to nitrocellulose, and probed with specific antibodies. Mitochondria were also extracted with sodium carbonate at different pHs as indicated on the figure. The pellet (p) and supernatant (s) were obtained as described section 2.11 and examined on Western blots.

3.10 *In vitro* import of Tob38 mutant proteins into control (HP1) mitochondria

To determine if the mutant Tob38-27 and Tob38-30 proteins could be effectively imported into mitochondria, these mutations were also created in cDNA containing plasmids. Mutant Tob38 proteins were radiolabeled by *in vitro* transcription/translation in rabbit reticulocyte lysates, imported into control (HP1) mitochondria and analyzed by BNGE. Import of wildtype Tom40 was also done to control for the quality of mitochondria used. Radiolabeled Tob38 wildtype protein was found in complexes of 140, 185 and 250 kDa (Fig. 26). These complexes correspond to those identified previously (Fig. 17, 19, and 24). The Tob38-27 mutant showed a slight decrease in import, but Tob38-30 showed a drastic decrease in protein imported with complete absence of the 140 kDa complex. Since the Tob38-30 protein had shown increased sensitivity to carbonate extraction (Fig. 25), it was possible that Tob38-30 was imported but subsequently lost during the washing step of import analysis. The wash buffer includes 80 mM KCl which could conceivably dissociate the mutant protein from the mitochondria. This was tested by isolating mitochondria from the Tob38-30-2 strain and washing with increasing KCl concentrations. This treatment did not affect Tob38-30 attachment to the membrane (Fig. 26D). Thus, the *in vitro* import of this form of the protein is deficient. To investigate the region affected further, two additional mutant Tob38 proteins were made, Tob38-17 and Tob38-19 (Fig. 10B). These mutations have only been analyzed by synthesizing the proteins *in vitro* and analyzing *in vitro* import by BNGE. No genomic strains were created for analysis of an *in vivo* phenotype. Tob38-17 has amino acids 24 to 26 deleted and Tob38-19 is a single amino acid substitution of F27A. Tob38-17 and Tob38-19 showed decreased import, although not as drastically as Tob38-30 (Fig. 26). These results indicate that the region 24 to 28 may be required for proper import of Tob38 or TOB complex protein-protein interactions.

3.11 Conserved Regions of Tob37

As with Tob38, conservation of Tob37 sequence among species is not high. However, localized regions with good similarity do exist (Fig. 10). For example, in the N-terminal region of Tob37 residues LP are conserved in all species analyzed. These residues are located at positions 52 and 53 in the *N. crassa* protein. The only exception

Figure 26: Import and assembly of mutant Tob38 proteins. **A.** Loading controls for *in vitro* transcription/translation lysates containing each protein. Each lane shows 25% of the lysate used for that radiolabeled protein in the corresponding import experiment. Thus, the amount of each radiolabeled protein used was approximately equal. **B.** Summary of the mutant versions of Tob38 analyzed and their phenotypes *in vivo* (na, not applicable). **C.** Proteins were imported into wildtype mitochondria for 20 min at 0°C and 25°C, washed in SEMK buffer, lysed with 1% digitonin and analyzed by BGNE. **D.** The Tob38-30 mutation does not reduce association to mitochondria in high salt conditions. Mitochondria were isolated from a control (HP1) and the mutant strain Tob38-30-2 and then washed with versions of SEMK buffer containing increasing concentrations of KCl. All lanes contain 30 μg of mitochondrial protein. Mitochondrial proteins were electrophoresed on SDS-PAGE gels, blotted to nitrocellulose, and probed with specific antibodies.

A

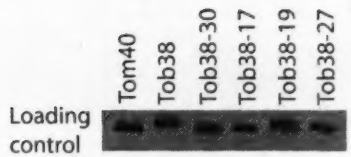

B

Name	Mutation	Phenotype
Tob38-30	Δ24-28	control growth rate, increased $NaCO_3$ extraction
Tob38-17	Δ24-26	na
Tob38-19	F27A	na
Tob38-27	D25A	control growth rate, control $NaCO_3$ extraction

C

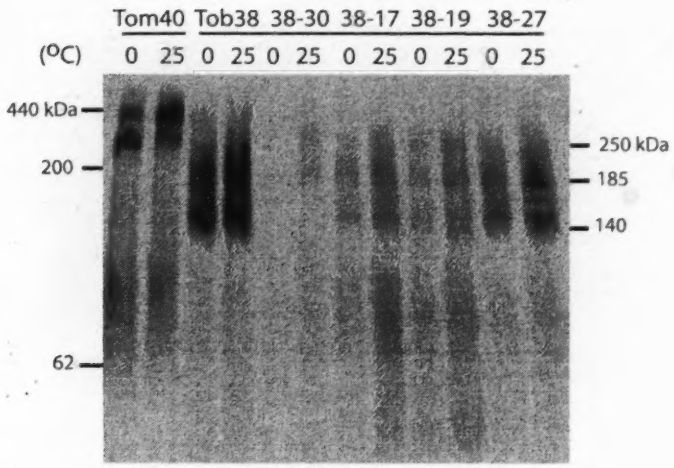

D

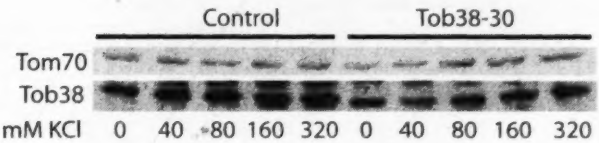

found to complete conservation of these two amino acids was in *Xenopus laevis*, where the leucine was replaced with the related amino acid valine (data not shown). Three mutants were created in this region: EKR20 was designed to give a deletion of both the L and P residues, but the strain examined is a mix of wildtype and an LP to AA substitution at residues 52 and 53 (a full discussion of the one peculiar strain arising from transformations with EKR20 is given in section 3.12), EKR21 is s single amino acid substitution of L52A, and EKR22 is a single amino acid substitution of P53A (Fig. 27A). Although not conserved in other species, *N. crassa* Tob37 contains a peculiar stretch of 17 amino acids at position 236 to 253, of which fourteen are glutamic acids (Fig. 27B). To determine if this unusual sequence is important for function, a mutant version of Tob37 (EKR23) was made with this region deleted.

As discussed in the introduction (section 1.4.10), some species appear to contain a TMD in the C-terminus of Tob37 while others do not. The C-terminal end of *N. crassa* Tob37 is predicted to contain one or two TMDs (residues 385 to 405 and 423 to 441) which are conserved in some fungal species but not others (Fig. 10). A single TMD near the C-terminus is predicted in the mammalian Tob37 homolog (Mtx1). As discussed in section 1.4.10, Mtx1 is not extracted by sodium carbonate and the predicted TMD was shown to be involved in targeting and maintenance of Mtx1 in the MOM (Armstrong *et al.*, 1999; Abdul *et al.*, 2000). To test the significance of the predicted TMDs in *N. crassa*, a premature stop codon (EKR15) at residue 337 was used to remove both putative TMDs resulting in the loss of last 108 amino acids (Fig. 27C). A less dramatic mutation (EKR35) was made to remove the first putative TMD by deleting eight internal amino acids (residues 396 to 404, Fig. 27D). A third mutation (EKR36) was designed to remove the second putative TMD by inserting a premature stop codon at residue 425 which resulted in the loss of the last 18 amino acids (Fig. 27E).

Each of the mutant alleles of *tob37* described above was transformed into the *tob37*KO sheltered heterokaryon strain and selection was imposed for rescue of the knockout nucleus by growth in the presence of his and fpa. Transformants were picked and purified as described in section 2.4. Mutant strains are named by adding the EKR mutation number (Table 2) as a suffix following "Tob37". This is followed by a second

Figure 27: Regions of Tob37 targeted for site-directed mutagenesis. Tob37 sequences from *Neurospora crassa* (Nc), *Chaetomium globosum* (Cg), *Magnaporthe grisea* (Mg), *Saccharomyces cerevisiae* (Sc), *Gibberella zeae* (Gz), *Aspergillus fumigatus* (Af), *Schizosaccharomyces pombe* (Sp), *Kluyveromyces lactis* (Kl), *Ashbya gossypii* (Ag), *Debaryomyces hansenii* (Dh), *Candida albicans* (Ca), *Yarrowia lipolytica* (Yl), *Xenopus tropicalis* (Xt), *Drosophila melanogaster* (Dm), *Caenorhabditis elegans* (Ce), *Homo sapiens* (Hs), *Danio rerio* (Dr), and *Mus musculus* (Mm) were aligned using ClustalW2 (Chenna *et al.*, 2003). **A.** EKR20 is a mix of wildtype and an LP to AA change at amino acids 52 to 53 (see section 3.12), EKR21 is a single substitution of L52A, and EKR22 is a single substitution of P53A. **B.** EKR23 is a deletion of 17 amino acids of the glutamic rich region encompasing amino acids 236 to 253. **C,D,E.** Tob37 contains two predicted TMDs in the C-terminus based on location in the protein (see Fig. 10). The first putative TMD likely corresponds to the domain predicted in the mammalian homologs of Tob37 (Mtx1). **C.** EKR15 is a premature stop codon at amino acid 337 removing both predicted TMDs. **D.** EKR35 is an eight amino acid deletion (LAINVAGL) in the first putative TMD at residues 396 to 404. **E.** EKR36 is a premature stop codon at amino acid 425, removing the second putative TMD. Mutants constructed in *N. crassa* Tob37 are shown in the bottom lines of the alignments. Residues affected in the mutants are shown in boxes and are changes relative to the *N. crassa* sequence (top line). Dashes indicate deletion of residues and lower case "a" indicates changes to alanine.

A

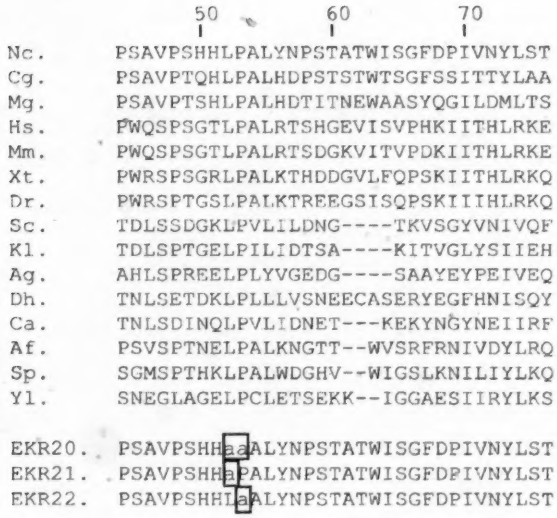
50
60
70
Nc. PSAVPSHHLPALYNPSTATWISGFDPIVNYLST
Cg. PSAVPTQHLPALHDPSTSTWTSGFSSITTYLAA
Mg. PSAVPTSHLPALHDTITNEWAASYQGILDMLTS
Hs. PWQSPSGTLPALRTSHGEVISVPHKIITHLRKE
Mm. PWQSPSGTLPALRTSDGKVITVPDKIITHLRKE
Xt. PWRSPSGRLPALKTHDDGVLFQPSKIITHLRKQ
Dr. PWRSPTGSLPALKTREEGSISQPSKIIIHLRKQ
Sc. TDLSSDGKLPVLILDNG----TKVSGYVNIVQF
Kl. TDLSPTGELPILIDTSA----KITVGLYSIIEH
Ag. AHLSPREELPLYVGEDG----SAAYEYPEIVEQ
Dh. TNLSETDKLPLLLVSNEECASERYEGFHNISQY
Ca. TNLSDINQLPVLIDNET---KEKYNGYNEIIRF
Af. PSVSPTNELPALKNGTT--WVSRFRNIVDYLRQ
Sp. SGMSPTHKLPALWDGHV--WIGSLKNILIYLKQ
Yl. SNEGLAGELPCLETSEKK--IGGAESIIRYLKS
EKR20. PSAVPSHHaaALYNPSTATWISGFDPIVNYLST
EKR21. PSAVPSHHLPALYNPSTATWISGFDPIVNYLST
EKR22. PSAVPSHHIaALYNPSTATWISGFDPIVNYLST

B

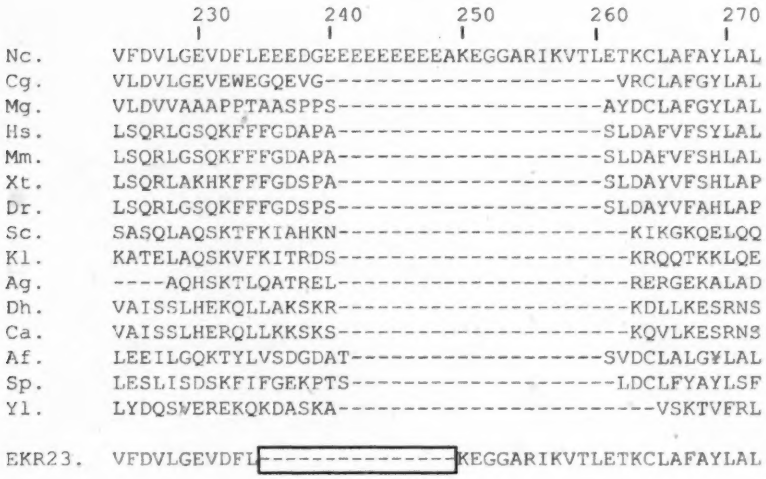
230
240
250
260
270
Nc. VFDVLGEVDFLEEEDGEEEEEEEEEAKEGGARIKVTLETKCLAFAYLAL
Cg. VLDVLGEVEWEGQEVG----------VRCLAFGYLAL
Mg. VLDVVAAAPPTAASPPS----------AYDCLAFGYLAL
Hs. LSQRLGSQKFFFGDAPA----------SLDAFVFSYLAL
Mm. LSQRLGSQKFFFGDAPA----------SLDAFVFSHLAL
Xt. LSQRLAKHKFFFGDSPA----------SLDAYVFSHLAP
Dr. LSQRLGSQKFFFGDSPS----------SLDAYVFAHLAP
Sc. SASQLAQSKTFKIAHKN----------KIKGKQELQQ
Kl. KATELAQSKVFKITRDS----------KRQQTKKLQE
Ag. ----AQHSKTLQATREL----------RERGEKALAD
Dh. VAISSLHEKQLLAKSKR----------KDLLKESRNS
Ca. VAISSLHERQLLKKSKS----------KQVLKESRNS
Af. LEEILGQKTYLVSDGDAT----------SVDCLALGYLAL
Sp. LESLISDSKFIFGEKPTS----------LDCLFYAYLSF
Yl. LYDQSVEREKQKDASKA----------VSKTVFRL
EKR23. VFDVLGEVDFL----------KEGGARIKVTLETKCLAFAYLAL

C

```
                330                                 340
                |                                   |
Nc.     SACDSALS--------------------------IVGRFVRAVIDDIP
Cg.     ---ASAVA--------------------------VGMRFVRGVLGEVP
Mg.     --ADSPLC--------------------------VASRLAAGCVAALP
Hs.     PETEEEPY-----------------------RRRNQILSVLAGLA
Mm.     PETEEEPY-----------------------RRRTQILSVLAGLA
Xt.     PDTEEEPH-----------------------KRRNQVLSVLVGLL
Dr.     SDFDNEPH-----------------------MRRNQILSVLFAVG
Sc.     LYVQLGLP-----------------------DGNRIRSKLEQTFG
Kl.     LKVQMALP-----------------------QGDLLRSHLRNQYP
Ag.     LYVQQQLP-----------------------DGARVTAHLRAHYP
Dh.     IHSLCLPE-----------------------LPDKFIVNYLTLKY
Ca.     IFCLTYEK-----------------------LPDRFIFNYLKLKQ
Af.     DATPLPWQ-----------------------PAQRANLTTVCSTL
Sp.     LTIARLAWNNVTAKANDTRKSITKFSVPPERKLLWARNGFFIFASAF
Yl.     LQLQMLPA-----------------------------LPDCAVAGLL

EKR15.  SACDSALS-----------------------IV*RFVRAVIDDIP
```

D

```
                380         390         400         410
                |           |           |           |
Nc.     GESERSLLLAGAGLTLLAINVAGLGIYWYRY
Cg.     GD---LLMFLGAGLGLTAM---GAGVFFYRG
Mg.     VVWTLGLGVLSASVVATAVMLLQDVVTTHR-
Hs.     EEE
Mm.     EED
Xt.     EEE
Dr.     DED
Sc.     NVVMSLYNLACKYI
Kl.     NVVTSTCYFLRTFV
Ag.     SVPRELYRYVTSYWTI
Dh.     NLWNELIYSTGYVKY
Ca.     SLTNEVKYWIGSIEY
Af.     ESRALSEYATGQKKDILVSIAAVAGGVAALV
Sp.     EKEIDETTESKATHDSSETSSSKELPKEEEK
Yl.     LWIYHLKQFLGWY

EKR35.  GESERSLLLAGAGLTI--------GIYWYRY
```

E

```
                420         430         440
                |           |           |
Nc.       TWHRP--LVGLGSFGAAGAMFAGLA
Cg.       VWRKP--MVSLSSFGAAGAMFSGALYGID
Mg.       VFERVRRVGGLWAVGSAGAVLGGAGRQLGAGQFAR
Hs.
Mm.
Xt.
Dr.
Sc.
Kl.
Ag.
Dh.
Ca.
Af.       EISFGGEEGHWEEEGHAGEEEGGSEFALPELPTSVSATI
Sp.       LSAQDLLFSGFAEDEIMDEEFGYDDDDDEEFDLDDLDDI
Yl.

EKR36.    TWHR[*]--LVGLGSFGAAGAMFAGLA
```

number which indicates the strain isolate number from a given transformation experiment.

All mutants gave rise to viable his-requiring homokaryons. The *tob37*KO was rescued previously with a wildtype Tob37 and a version with a hexa-histidine tag at the C-terminus (Tob37-His_6). Both restored the wildtype growth rate on his supplemented medium (Fig. 28A). To test if the Tob37 mutations affected the growth rate, mutant homokaryons were spotted and grown at 30°C on his supplemented medium. Several transformations with EKR20 produced only a single transformant, Tob37-20-1, which grew slowly (see section 3.12, Fig. 28B). Four randomly selected transformants of each mutant group Tob37-21 (Fig. 28C), Tob37-22 (Fig. 28D), Tob37-23 (Fig. 28E) and Tob37-36 (Fig. 28F) were tested for growth. In each case, three of the four strains grew at wildtype rates but one grew slowly. The poor growth of one strain in each group is likely due to secondary mutations caused by the insertion of the mutant allele or poor expression of the transforming DNA due to position effects. The Tob37-15 strains all had reduced growth rates (Fig. 28G). Two of the Tob37-35 strains that were examined had reduced growth rates while two were similar to the control (Fig. 28H). Eight more Tob37-35 transformants were examined and one had a reduced growth rate while seven were similar to the control (Fig. 28I and 28J). Thus, the Tob37-35 strains with slower growth rates are likely due to indirect effects. The mutant strains were also spotted and grown at 18°C and 37°C and showed no temperature-sensitive phenotype (data not shown). The *tob37* genes introduced into the mutant strains Tob37-15-3, Tob37-20-1, Tob37-21-1, Tob37-22-7, Tob37-23-12, Tob37-35-12 and Tob37-36-6 were sequenced from genomic DNA and confirmed to be wildtype except for the intended mutation. These strains were chosen for further analysis. The Tob37-20-1 mutant is discussed in section 3.12

Mitochondria isolated from the Tob37 mutant strains were examined by Western blot analysis (Fig. 29A). As a control for protein loading, an identical gel was stained with coomassie blue (Fig. 29B). All mutants contained wildtype steady state levels of Tom70, except Tob37-20-1 which had a slightly increased level of the protein. The steady state level of Tom40 was decreased in all mutant strains except Tob37-20-1, which showed wildtype levels of the protein. Porin levels were similar to the control in

Figure 28: Growth rates of Tob37 mutants. Conidia were spotted in 10-fold dilutions on his supplemented medium. Controls in all panels include HP1 (control), the *tob37*KO sheltered heterokaryon (*tob37*KO), and a strain carrying a C-terminal His_6 tagged version of Tob37 (Tob37-His_6). Note that the lack of fpa in the medium means that the *tob37*KO heterokaryon should grow at rates similar to the HP1 control. **A.** Four isolates of the t*ob37*KO strain rescued with wildtype *tob37* compared to the control (HP1) and Tob37-His_6 strains. **B.** As in panel A but t*ob37*KO rescued with the Tob37-20 mutant allele which is a mix of wildtype and LP to AA at amino acids 52 to 53 (see section 3.12 for a further description of this mutant). **C.** As in panel A but t*ob37*KO rescued with the Tob37-21 mutant allele which has single substitution of L52A. **D.** As in panel A but t*ob37*KO rescued with the Tob37-22 mutant allele which has a single substitution of P53A. **E.** As in panel A but t*ob37*KO rescued with the Tob37-23 mutant allele which has a deletion of a 17 amino acid glutamic rich region 236 to 253. **F.** As in panel A but t*ob37*KO rescued with Tob37-36 which contains a premature stop codon at amino acid 425, removing the second putative TMD. **G.** As in panel A but t*ob37*KO rescued with the Tob37-15 mutant allele which contains a premature stop codon at amino acid 337 removing both predicted TMDs. **H.** As in panel A but t*ob37*KO rescued with Tob37-35 which contains an eight amino acid deletion (LAINVAGL) in the first putative TMD at residues 396 to 404. **I.** As in panel G, but showing more isolates from the transformation. **J.** As in as panel I. Strains indicated in bold are the strains used for further analysis. Mutant strains are named by adding the EKR mutation number (Table 2) as a suffix following "Tob37". This is followed by a second number which indicates the strain isolate number from a given transformation experiment.

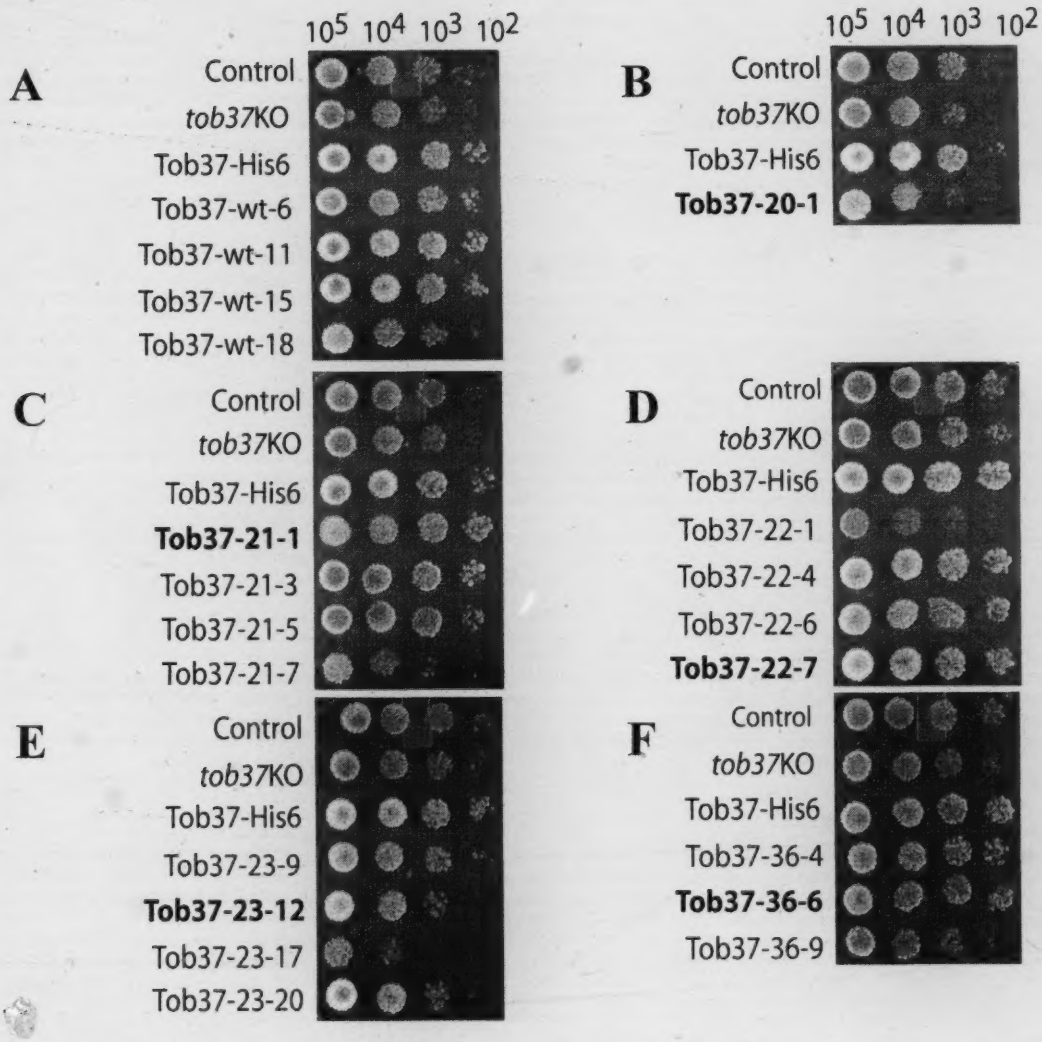
A
10^5 10^4 10^3 10^2
Control
*tob37*KO
Tob37-His6
Tob37-wt-6
Tob37-wt-11
Tob37-wt-15
Tob37-wt-18
B
10^5 10^4 10^3 10^2
Control
*tob37*KO
Tob37-His6
Tob37-20-1
C
Control
*tob37*KO
Tob37-His6
Tob37-21-1
Tob37-21-3
Tob37-21-5
Tob37-21-7
D
Control
*tob37*KO
Tob37-His6
Tob37-22-1
Tob37-22-4
Tob37-22-6
Tob37-22-7
E
Control
*tob37*KO
Tob37-His6
Tob37-23-9
Tob37-23-12
Tob37-23-17
Tob37-23-20
F
Control
*tob37*KO
Tob37-His6
Tob37-36-4
Tob37-36-6
Tob37-36-9

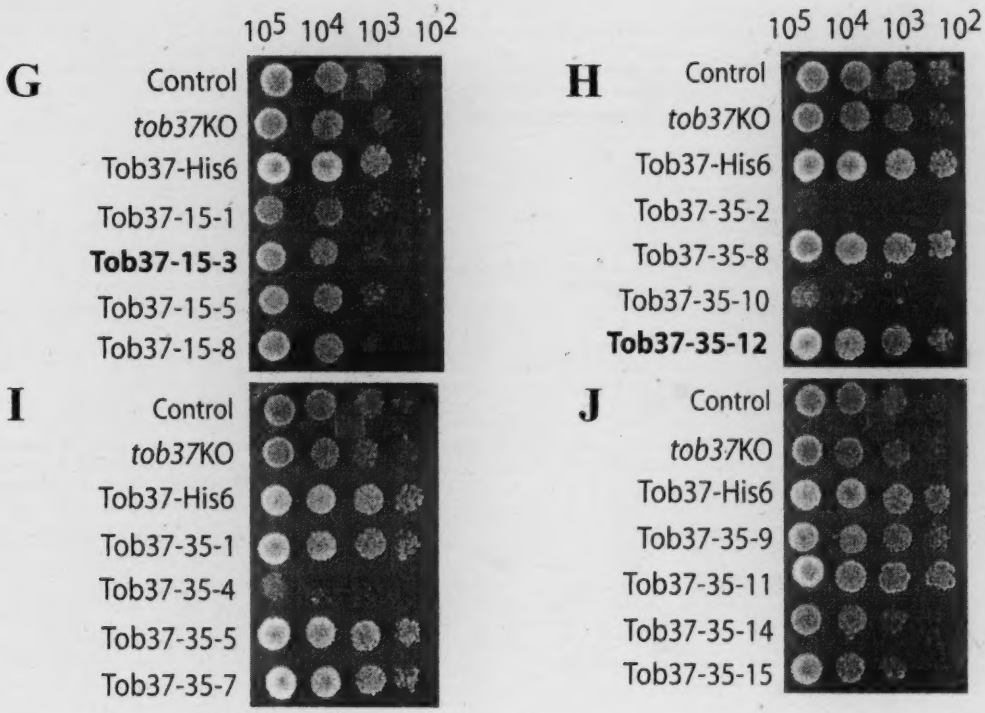
G
10^5 10^4 10^3 10^2
Control
*tob37*KO
Tob37-His6
Tob37-15-1
Tob37-15-3
Tob37-15-5
Tob37-15-8
H
10^5 10^4 10^3 10^2
Control
*tob37*KO
Tob37-His6
Tob37-35-2
Tob37-35-8
Tob37-35-10
Tob37-35-12
I
Control
*tob37*KO
Tob37-His6
Tob37-35-1
Tob37-35-4
Tob37-35-5
Tob37-35-7
J
Control
*tob37*KO
Tob37-His6
Tob37-35-9
Tob37-35-11
Tob37-35-14
Tob37-35-15

Figure 29: Mitochondrial proteins in the Tob37 mutants. **A.** Mitochondrial proteins were electrophoresed on SDS-PAGE gels, blotted to nitrocellulose, and probed with specific antibodies. Mitochondria analyzed were the control (HP1) strain, *tob37*KO grown in minimal medium (*tob37*KO min), Tob37↓ (*tob37*KO fpa), the his-tagged version of Tob37 (Tob37-His_6), and the mutants Tob37-15-3, Tob37-20-1, Tob37-21-1, Tob37-22-7, Tob37-23-12, Tob37-35-12, and Tob37-36-6. Tob37-15-3 has a mutant Tob37 allele with a premature stop codon at amino acid 337 removing both predicted TMDs. Tob37-20-1 has a mutant Tob37 allele with LP mutated to AA at residues 52 to 53. Tob37-21-1 has a mutant Tob37 alleles with a single substitution of L52A and Tob37-22-7 is a single substitution of P53A. Tob37-23-12 has a mutant Tob37 allele lacking 17 amino acids of the glutamic rich region encompasing amino acids 236 to 253. Tob37-35-12 has a mutant Tob37 allele with an eight amino acid deletion (LAINVAGL) in the first putative TMD at residues 396 to 404 and Tob37-36-6 which has a mutant Tob37 allele with a premature stop codon at amino acid 425, removing the second putative TMD. Strains were grown as described in Fig. 3. All lanes contain 30 μg of mitochondrial protein and 5 μg control (HP1) OMVs were used to indicate the appropriate Tob37 band. Arrows indicate faint bands thought to represent Tob37 in Tob37-15-3 and Tob37-20-1. Porin* is an overexposure of the porin blot directly above. **B.** Commassie blue stained gel showing equal loading of mitochondrial protein without the control OMVs.

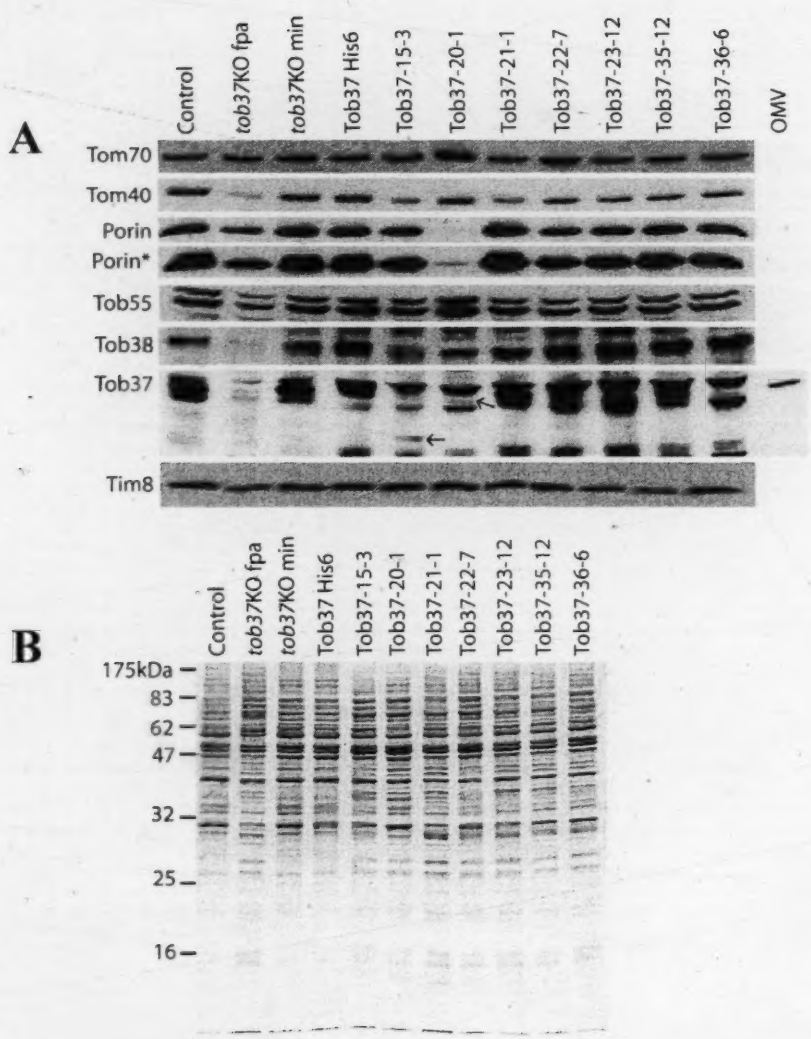
A
Control
tob37KO fpa
tob37KO min
Tob37 His6
Tob37-15-3
Tob37-20-1
Tob37-21-1
Tob37-22-7
Tob37-23-12
Tob37-35-12
Tob37-36-6
OMV
Tom70
Tom40
Porin
Porin*
Tob55
Tob38
Tob37
Tim8
B
Control
tob37KO fpa
tob37KO min
Tob37 His6
Tob37-15-3
Tob37-20-1
Tob37-21-1
Tob37-22-7
Tob37-23-12
Tob37-35-12
Tob37-36-6
175kDa
83
62
47
32
25
16

all mutant strains except Tob37-20-1, which showed extremely low amounts of porin, only visible on over-exposures of the blot (asterix, Fig. 29A). For Tob37 protein levels, the α-Tob37 peptide 1 GenScript antibody used gave background in the Tob37 region but a control (HP1) OMV lane showed the band that is likely Tob37 (Fig. 29A). Tob37 is decreased in size by 108 amino acids in Tob37-15-3 and a faint band can be seen near the bottom of the Tob37 blot (arrow, Fig. 29A) at a molecular weight of 37 kDa as predicted for the mutant. The remaining mutant versions of Tob37 are within 20 amino acids of the wildtype length and appropriate size differences can be seen. Intensity of the Tob37 band varies in the different mutants. For Tob37-20-1, a faint Tob37 band is visible (arrow, Fig. 29A), indicating the presence of a low amount of mutant Tob37 in this strain. The steady state levels of Tob55 and Tim8 were wildtype for most mutants, though Tob37-20-1 showed a slight increase in these protein levels. Tob38 steady state levels were similar to the control in all of the mutants except Tob37-15-3 which had decreased levels of the protein.

Mitochondria were isolated from control (HP1), Tob37↓ and seven of the Tob37-35 mutant strains to determine if the growth defects observed in certain isolates corresponded with changes in mitochondrial protein levels. Mitochondrial proteins were examined by Western blot analysis and the steady state levels of Tom70 and porin were similar to the control. The level of Tom40 appeared to vary in the individual isolates, but there was no relationship between the Tom40 amounts and the growth rates of the isolates (Fig. 30). Since there were no apparent differences in the steady state levels of the two beta-barrel proteins examined, and because several Tob37-35 strains grew at the same rate as the control strain, it seems unlikely that the growth defects observed in the slow growing isolates (Tob37-35-2, Tob37-35-4 and Tob37-35-10) were caused by defects in Tob37 function (Fig. 30).

3.12 Tob37-20-1 Mutant

The mutagenic primer EKR20 was designed to introduce a deletion of residues 52 and 53 (LP) from Tob37. However, genomic sequencing of Tob37-20-1 revealed that it was a mixture of wildtype and LP to AA substitution at residues 52 and 53 in *tob37*. The mechanism by which an AA substitution was generated in place of the intended LP

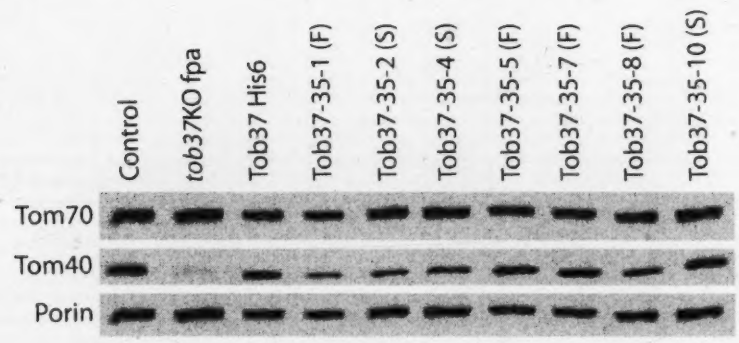

Figure 30: Mitochondrial proteins in different isolates of the Tob37-35 mutant. The Tob37-35 strains have mutant Tob37 alleles with an eight amino acid deletion (LAINVAGL) in the first putative TMD at residues 396 to 404. Mitochondrial proteins were electrophoresed on SDS-PAGE gels, blotted to nitrocellulose, and probed with specific antibodies. Mitochondria analyzed were the control (HP1), the *tob37*KO grown in minimal medium (*tob37*KO min), Tob37↓ (*tob37*KO fpa), the his-tagged version of Tob37 (Tob37-His6), and seven isolates of the Tob37-35 mutant. Strains were grown as described in Fig. 3. All lanes contain 30 μg of mitochondrial protein. Strains with slow growth rates are indicated as "S" and strains with the wildtype growth rate are indicated "F" (see Fig. 28H to J).

deletion is unknown. This was the only strain isolated from transformations with the mutant EKR20 plasmid despite many attempts. Due to its interesting phenotype of lacking porin and being deficient in Tob37 (Fig. 29A), further experiments were performed prior to determining that it contained two different (and unexpected) alleles of Tob37. BNGE showed that in Tob37-20-1 the wildtype size of the TOM complex was restored from the slightly larger size seen in Tob37↓ mitochondria. However, a destabilization of the TOM complex seems to have occurred as well since lower molecular weight forms are observed upon longer exposures of the blots (Fig. 31A). Levels of the TOB complex were also decreased and the intensity of the band in the 100 kDa region was increased (Fig. 31B).

Import and assembly of Tom40 in Tob37-20-1 mitochondria occurred quite slowly, but assembly intermediate I (250 kDa), II (100 kDa), and the fully assembled TOM complex (400 kDa) were eventually observed (Fig. 32). Some Tom40 precursor also appeared to accumulate in a complex of 185 kDa which is occasionally observed as a faint band when Tom40 is imported into control mitochondria (Fig. 32). Porin import and assembly in the mutant was also reduced and the precursor accumulated in the 170 kDa porin complex, versus the bulk of porin assembling into the 210 kDa porin complex in control mitochondria. Only a slight reduction of smaller porin bands (< 68 kDa) was observed in the mutant mitochondria. It is unclear if the smaller porin complexes represent intermediates, fully assembled complexes, or unimported and unassembled porin molecules. Of particular interest in these experiments is the observation that Tom40 intermediate I (250 kDa) in the Tom40 assembly pathway, which represents Tom40 associated with the TOB complex, exists and Tom40 continues assembly into the TOM complex. This is in contrast to porin which appears not to reach the analogous putative intermediate complex at 210 kDa in the Tob37-20-1 mutant. Rather, incoming porin molecules accumulate at 170 kDa.

3.13 Tom70

Problems with import into Tob38↓ and Tob37↓ mitochondria due to poor MOM stability have been discussed (section 3.7). It was thought that a Tom70 mutant (*tom70*^{RIP}) might provide a control for import experiments into Tob38↓ and Tob37↓

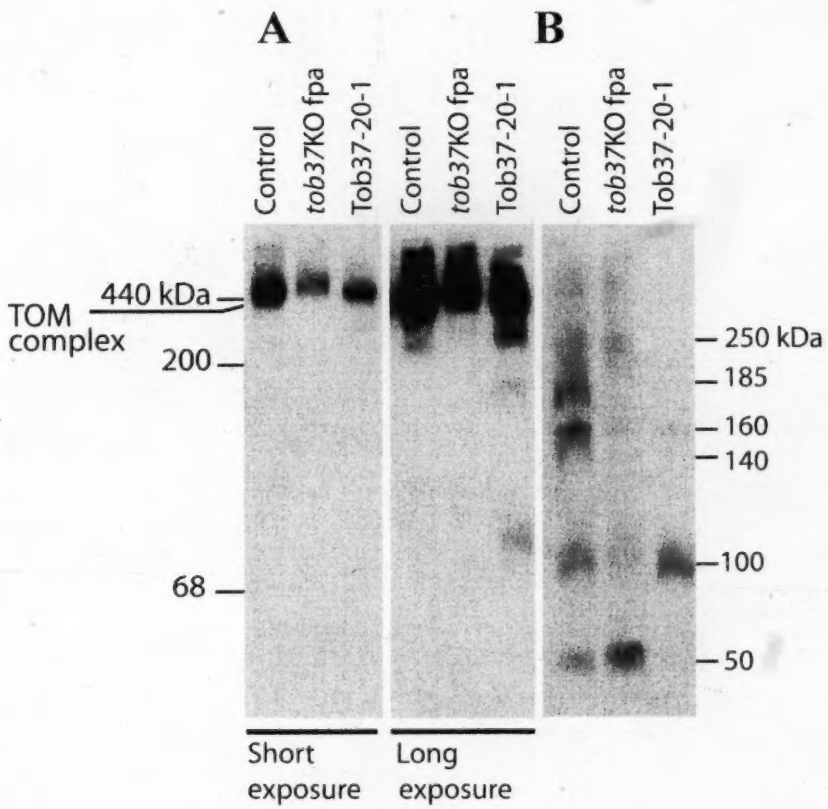

Figure 31: Analysis of the TOM and TOB complexes in Tob37-20-1 by BNGE. Control (HP1), Tob37↓ (*tob37*KO fpa), and Tob37-20-1 mitochondria were analyzed. The Tob37-20-1 strain has a mutant Tob37 allele with LP mutated to AA at residues 52 to 53. Strains were grown as described in Fig. 3. 50 μg of mitochondria isolated from each strain were lysed with 1% digitonin and electrophoresed on a 6 to 13% gradient blue native acrylamide gel. The gels were blotted to PVDF and probed with antibodies to either Tom40 (**A**) or Tob55 (**B**). The position of molecular weight standards is indicated on the left. Complexes discussed in the text are indicated on the right according to their apparent molecular weight in kDa. Short and long exposures of the Tom40 blot are shown.

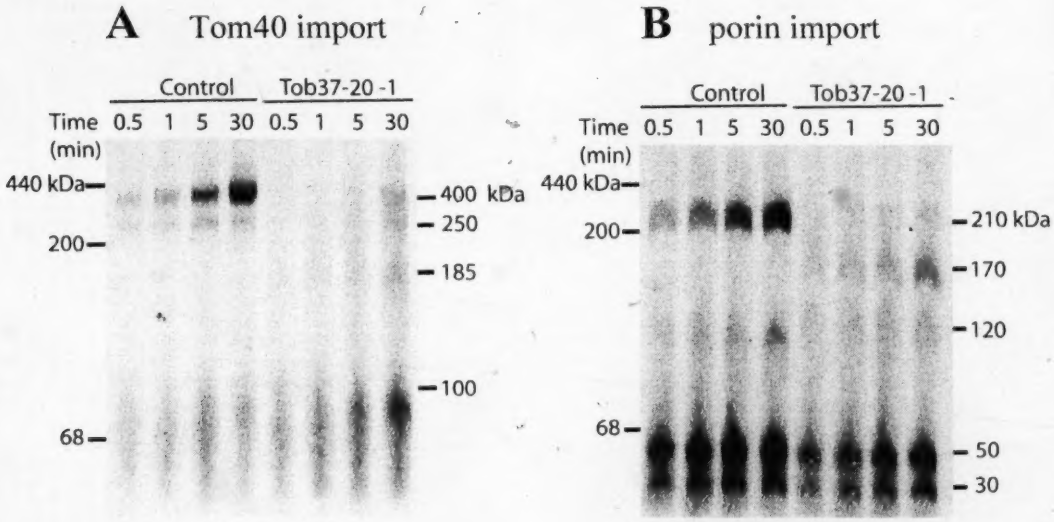

Figure 32: Import and assembly of mitochondrial precursor proteins into Tob37-20-1 mitochondria. The Tob37-20-1 strain has a mutant Tob37 allele with LP mutated to AA at residues 52 to 53.Radiolabeled Tom40 (**A**) and porin (**B**) were imported into 50 μg of mitochondria isolated from the control (76-26) and Tob37-20-1 strains. Import time ranged from 0.5 to 30 min at 25°C. Following import, mitochondria were washed in SEMK, lysed with 1% digitonin and analyzed by BNGE. The position of molecular weight standards is indicated on the left. Complexes discussed in the text are indicated on the right according to their apparent molecular weight in kDa.

mitochondria because mitochondria lacking Tom70 have similar problems (Grad *et al.*, 1999). The *tom70*^{RIP} mutant is a homokaryon containing a non-functional *tom70* gene inactivated by RIP (Grad *et al.*, 1999). As the use of this strain proceeded, interesting defects in the Tom70 mutant strain were revealed. Decreased steady state levels of porin were observed (Fig. 33). In addition, Tob37 appeared to be decreased but non-specific bands in the same region make this difficult to say definitively. Tob37 antibodies detect a prominent band slightly above Tob37 in the Tom70 and Tob38 mutants. The significance of this band is not known. Unexpectedly, Tob38 appears to be reduced in size in the Tom70 mutant strain. This result was similar using either the α-Tob38 N3-2 or the α-Tob38 GenScript antibody (Fig. 33). Genomic sequencing of *tob38* in the Tom70 mutant revealed a premature stop codon 11 amino acids from the C-terminus in the *tob38* sequence. The loss of 11 amino acids from the C-terminus could account for the decreased size of Tob38 in the Tom70 mutant.

BNGE blots showed a slight decrease in the TOM, TOB and porin complexes in the Tom70 mutant (Fig. 34A, B, C), although not to the extent observed in the Tob37↓ and Tob38↓ mitochondria (Fig. 17). As expected, mitochondria from the Tom70 mutant do not have complexes containing Tom70 (Fig. 34D).

Quantitative defects of import and assembly into the Tom70 mutant were observed for all precursors examined: Tom40, porin, Tob55, Tob38 and Tob37, with the beta-barrel proteins being the most severely affected (Fig. 35). However, it should be remembered that Tom70 deficient mitochondria have been shown to have a fragile MOM (Grad *et al.*, 1999) and import defects of beta-barrel precursors may be due to lack of IMS components.

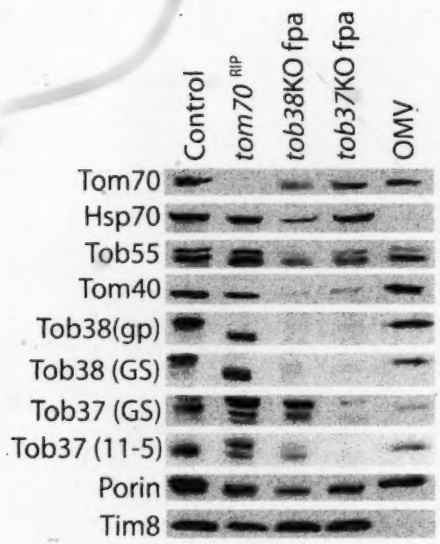

Figure 33: Mitochondrial protein levels in the *tom70*^{RIP} strain. Mitochondrial proteins were electrophoresed on SDS-PAGE gels, blotted to nitrocellulose, and probed with specific antibodies for control (HP1), *tom70*^{RIP}, Tob38↓ (*tob38*KO fpa), and Tob37↓ (*tob37*KO fpa). Tob38 (gp) is the antibody created in a guinea pig to the N-terminal half of Tob38 (in house). Tob38 (GS) and Tob37 (GS) are the GenScript antibodies created using peptides. Tob37 (11-5) is an α-Tob37 antibody, created in guinea pig (in-house) to peptide 1 (Fig. 10) (This antibody became available only at the end stages of writing this thesis). Strains were grown as described in Fig. 3, except for *tom70*^{RIP} which is a homokaryon containing a non-functional *tom70* gene inactivated by RIP (Grad *et al.*, 1999) and was grown in Vogel's medium plus pan. All lanes contain 30 μg of mitochondrial protein or 5 μg of control (HP1) OMVs.

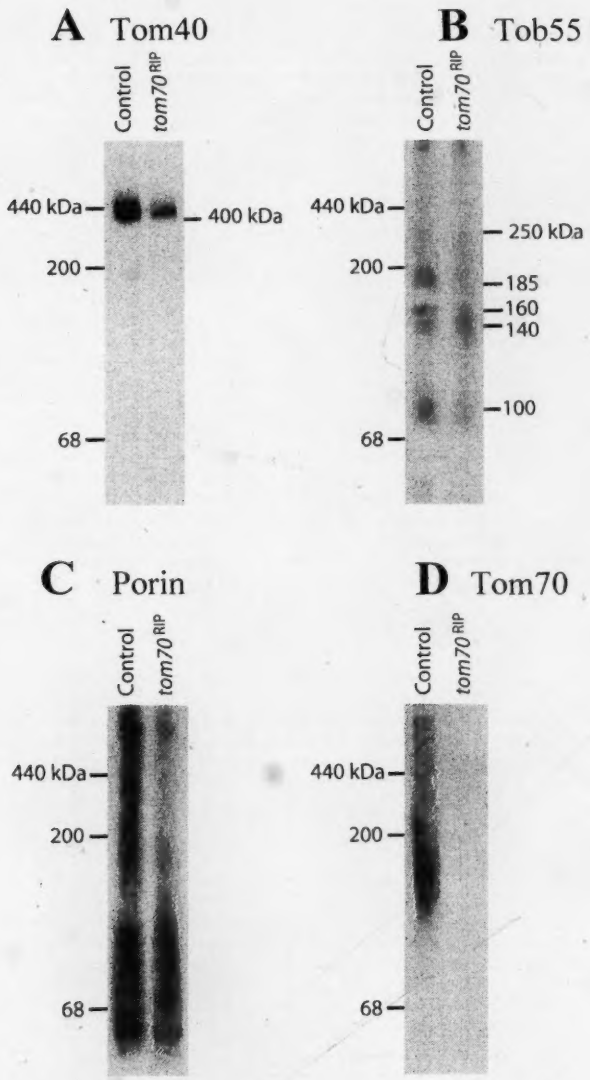

Figure 34: Analysis of the TOM, TOB, and porin complexes in mitochondria lacking Tom70. 50 μg of mitochondrial protein from control (HP1) and the *tom70*^{RIP} mutant mitochondria were lysed with 1% digitonin and electrophoresed on a 6 to 13% gradient blue native acrylamide gels. The gels were blotted to PVDF and probed with antibodies to Tom40 (**A**), Tob55 (**B**), porin (**C**), or Tom70 (**D**). The control (HP1) was grown in Vogel's medium and *tom70*^{RIP}, which is a homokaryon containing a non-functional *tom70* gene inactivated by RIP (Grad *et al.*, 1999), was grown in Vogel's medium plus pan. The position of molecular weight standards is indicated on the left. Complexes discussed in the text are indicated on the right of panel B by their apparent molecular weight in kDa.

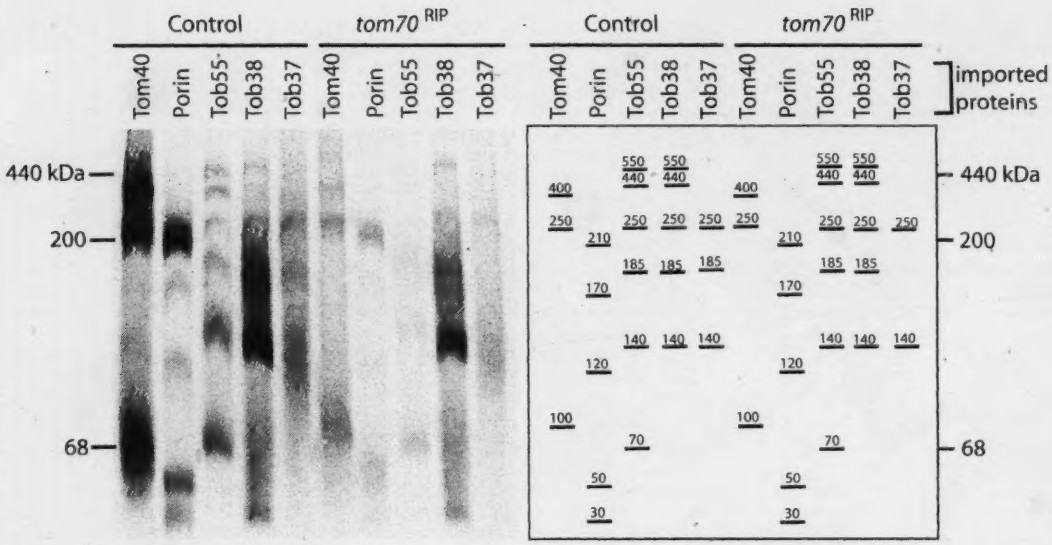

Figure 35: Import and assembly of mitochondrial precursor proteins into mitochondria lacking Tom70. Radiolabeled Tom40, Porin, short Tob55, Tob38 and Tob37 were imported into 50 μg of mitochondria isolated from control (HP1) and *tom70*^{RIP}. Following 20 min of import at 25°C, mitochondria were washed in SEMK, lysed with 1% digitonin and analyzed by BNGE. The position of molecular weight standards is indicated on the left. Complexes discussed in the text are indicated in the right hand panel in cartoon form with their apparent molecular weight (kDa) indicated for each band.

4. Discussion

4.1 The *tob38* and *tob37* Sheltered Heterokaryon Knockout Strains

Tob38 (Milenkovic *et al.*, 2004; Paschen *et al.*, 2003), but not Tob37 (Gratzer *et al.*, 1995; Wiedemann *et al.*, 2003), was shown to be essential in yeast. In this analysis I have shown that both the *tob38* and *tob37* genes are essential in *N. crassa*. Interestingly, the Tob37 of mammals, which also contains a putative transmembrane domain (TMD) like the *N. crassa* protein, is also essential for viability (Bornstein *et al.*, 1995; Wang *et al.*, 2001). Both the Tob38↓ and Tob37↓ strains grew slowly likely due to an inability of mitochondria to function properly without either of these two essential proteins.

Tob38↓ and Tob37↓ mitochondria have reduced steady state levels of Tom6, Tom5, Tob38, Tob37, Tob55, Tom40, porin and Tim13. Levels of the other mitochondrial proteins analyzed were also slightly reduced. The reductions of the beta-barrel proteins Tom40, Tob55, and porin are likely due to decreased function of the TOB complex required for the insertion of these proteins into the MOM. This is consistent with observations of beta-barrel protein levels in yeast (Wiedemann *et al.*, 2003; Ishikawa, *et al.*, 2004; Waizenegger *et al.*, 2004; Stojanovski *et al.*, 2007). In mammals, Tob38↓ mitochondria had wildtype levels of Tom40 and only a moderate reduction of porin, although Tob55↓ mitochondria did have reduced steady state levels of Tom40 and porin (Kozjak-Pavlovic *et al.*, 2007). Tom5 was not reduced in yeast tob37Δ or Tob38↓ mitochondria, although both Tom5 and T[illegible] were reduced in *N. crassa* mutants (Stojanovski *et al.*, 2007). The steady state level of Tob55 in *tob37*Δ mitochondria and levels of Tom6 and Tim13 in Tob38↓ or *tob37*Δ mitochondria have not been analyzed in yeast.

Recent research in yeast has implicated Tob37, but not Tob38, in the assembly of the small Tom proteins into the TOM complex (Stojanovski *et al.*, 2007). My analysis showed that depletion of Tob38 and Tob37 resulted in a similar depletion of Tom5 and Tom6. If Tob37 performs the same function in *N. crassa*, then the loss of Tob37 in Tob38↓ mitochondria may account for the reduction of the small Toms in both strains. It is also possible that both Tob37 and Tob38 are involved in the import of the small Toms in *N. crassa*.

My findings show that the level of Tom22 does not greatly decrease in the Tob38↓ or Tob37↓ mutants. This is in contrast to recent work in yeast which showed that the Tob38 and Tob37 were required for efficient import and assembly of Tom22 (Stojanovski *et al.*, 2007). Yeast mitochondria depleted of Tob38 or lacking Tob37 had decreased steady state levels and assembly of Tom22 into the TOM complex. Overall, the differences in mitochondrial protein levels and essential genes observed in this analysis highlight the differences in mitochondrial protein import between *N. crassa* and yeast.

The differences in the reduction of proteins observed in the whole cell protein analysis in comparison to the isolated mitochondria suggests that in the Tob37↓ or Tob38↓ cultures specific proteins were lost during mitochondrial isolation, mitochondria isolated were contaminated with other cellular proteins, or that the mitochondria isolated are somehow different than usual. These results may be due to increased fragility of the MOM in the Tob38↓ and Tob37↓ mitochondria. If this is the case, the slight reduction of some mitochondrial proteins may have been due to the isolation procedure and not a direct result of decreased levels of Tob37 or Tob38.

In yeast, depletion or mutation of Tob37, Tob38, Tob55, Tom7, Tom40, Mdm10, or Mim1 has been shown to result in aberrant mitochondrial morphology including enlarged mitochondria (Stojanovski *et al.*, 2006; Altmann and Westermann, 2005; Meisinger *et al.*, 2004). Enlarged mitochondria are indicative of a problem in the tubulation pathway, and connections between tubulation pathway members Mmm1, Mdm12 and Mdm10 and the TOB complex have been shown in yeast (Meisinger *et al.*, 2006; Meisinger *et al.*, 2007). Transmission electron microscopy of *N. crassa* showed that Tob38↓ and Tob37↓ mitochondria may have an increased proportion of enlarged mitochondria but this phenotype was not exclusive to the knockdowns. A detailed statistical analysis of a large number of random electron micrographs would be necessary to determine if there is an increased occurrence of larger mitochondria in these strains.

Tob38 and Tob37 have a co-dependent relationship in *N. crassa*, such that in Tob38↓ mitochondria the steady state levels of Tob37 are greatly reduced, and vice versa. This is further supported by very similar phenotypes observed in Tob38↓ and Tob37↓ cultures. This co-dependent relationship has been observed in yeast and is likely

indicative of the requirement of both Tob38 and Tob37 in the formation of a functional TOB complex (Waizenegger *et al.*, 2004; Kozjak-Pavlovic *et al.*, 2007; Chan and Lithgow, 2007). Tob55 was also depleted in Tob38↓ and Tob37↓ mitochondria. Thus, when one TOB component is lacking, the TOB complex cannot form and the unassembled components may be degraded. Phenotypes in yeast due to the depletion of Tob38 or Tob37 have been overcome to various degrees by overexpression of the other protein, indicating a level of partial functional overlap between these two proteins (Chan and Lithgow, 2007). Overexpression studies have not been done in *N. crassa* so it is unknown if Tob38 and Tob37 have functional overlap in this organism.

4.2 The TOB complexes

In yeast, the TOB core complex (200 to 250 kDa) is predicted to contain Tob55, Tob38 and Tob37 (Abdul *et al.*, 2000; Habib *et al.*, 2005; Paschen *et al.*, 2005). A 160 kDa complex without Tob37 has also been reported, as has a larger (350 kDa) complex involving associations of the complex with either Mim1 or Mdm10 (Meisinger *et al.*, 2004; Habib *et al.*, 2005; Meisinger *et al.*, 2006; Becker *et al.*, 2007). My data from pulldown experiments have shown that Tob55, Tob38 and Tob37 all interact, although Tob37 interactions may be weaker than interactions between Tob55 and Tob38. Similar observations have been made in yeast (Paschen *et al.*, 2003; Waizenegger *et al.*, 2004). BNGE analysis using either the α-Tob55 antibody or import of radiolabeled Tob38 and Tob55 proteins indicated the TOB complex in *N. crassa* consisted of 140, 185, and 250 kDa complexes. After longer exposures of blue native gel electrophoresis (BNGE) blots, radiolabeled Tob55 and Tob38 also appear in 440 and 550 kDa complexes, suggesting smaller amounts of larger complexes may also occur. Tob37 was present in a smear between 150 and 250 kDa following BNGE. A similar result was observed in mammals, supporting the idea of a loose association of Tob37 with the TOB complex (Kozjak-Pavlovic *et al.*, 2007).

4.3 Tob38 Location, Topology, and Conserved Regions

In yeast, Tob38 is a hydrophilic, peripheral MOM protein with no TMD that is exposed to the cytosol (Milenkovic *et al.*, 2004; Ishikawa *et al.*, 2004; Waizenegger *et*

al., 2004). My analysis confirmed this finding in *N. crassa*. One difference between yeast and *N. crassa* Tob38 is the extent to which it is bound to the MOM. My data showed that *N. crassa* Tob38 remained bound to the MOM following carbonate extraction at pH 10.8, but *S. cerevisiae* Tob38 was completely extracted at this pH (Milenkovic *et al.*, 2004). This may indicate a different association of Tob38 with TOB complex members or the MOM in *N. crassa*.

A conserved region in Tob38 (amino acids 24 to 28) was shown to be important for this association with the MOM since deletion of these five amino acids in the Tob38-30 mutant resulted in an increased sensitivity to carbonate extraction. Steady state levels of Tom40 and porin were not reduced in the Tob38-30-2 mutant, indicating a functional TOB complex. Steady state levels of Tob55 and Tob38 were slightly reduced, possibly because of slight changes in expression level of the mutant Tob38 due to ectopic integration in the transformant or decreased stability of the mutant protein. BNGE analysis of Tob38-30-2 mitochondria showed that the level of the TOB complex was slightly reduced and more Tob55 accumulated in the lower molecular weight complexes. These changes in the TOB complex did not appear to greatly affect the levels of the TOM complex which was only slightly reduced, again indicating function of the TOB complex in this strain. The phenotype of increased steady state levels of Tob55 in smaller TOB complexes but near wildtype steady state levels of the TOM complex is consistent with the yeast Tob38 mutant sam35-424 (Chan and Lithgow, 2007). Interestingly, where the sam35-424 yeast mutant had a temperature-sensitive growth phenotype, this was not observed in Tob38-30-2 (Chan and Lithgow, 2007). The site of the mutation in Sam35-424 was not published.

The *in vitro* import of Tob38 precursor protein carrying the Tob38-30 mutation was also reduced. This may indicate that the region is important for protein-protein interactions required for interactions with other TOB complex components or that the mutant protein suffers from folding problems that make it less competent for import.

4.4 Tob37 Location, Topology, and Conserved Regions

In yeast, Tob37 is a peripheral membrane protein facing the cytosol and in mammals is anchored to the membrane by a C-terminal transmembrane domain

(Armstrong *et al.*, 1997; Paschen *et al.*, 2005). My experiments confirmed the location of *N. crassa* Tob37 in the MOM facing the cytosol. Carbonate extraction experiments suggested that Tob37 was anchored more strongly to the MOM than Tom70, a protein anchored by a known TMD (Komiya *et al.*, 1997; Wiedemann *et al.*, 2003; Pfanner *et al.*, 2004; Paschen *et al.*, 2005). These data strongly suggest that *N. crassa* Tob37 also contains at least one C-terminal TMD and is more structurally similar to the mammalian Tob37 (Mtx1) than yeast. The *N. crassa* Tob37 contains two predicted TMDs near the C-terminus, similar to where the mammalian Tob37 TMD is located (Armstrong *et al.*, 1997). I have begun a study to determine the roles of the two *N. crassa* Tob37 TMDs by creating mutants lacking either or both domains. Unfortunately, the lab supply of useful Tob37 antibody was gone when these constructs were ready so that carbonate extraction experiments could not be analyzed satisfactorily. A new antibody recently generated in the lab will make this possible. Interestingly, the Tob37-15 mutant strain lacking both potential TMDs is viable. This suggests that a membrane anchor is not required for Tob37 function. Tob37-15-3 had decreased steady state levels of Tom40 but wildtype levels of porin and Tob55, suggesting a possible separation of beta-barrel protein import pathways.

The Tob37-20-1 mutant, containing a mix of wildtype and LP to AA substitution at residues 52 and 53 alleles, also had a slow growth phenotype. This mutant had extremely low steady state levels of porin but wildtype levels of Tom40 and Tob55. Porin assembly was also altered in the Tob37-20-1 mutant mitochondria with the precursor accumulating at 170 kDa versus 210 kDa as observed in control mitochondria. Interestingly, the steady state level of the TOB complexes were reduced similar to that of the Tob37↓, but the level of the TOM complex was only slightly reduced. Smaller complexes containing Tom40 were also present in the Tob37-20-1 mutant, indicating altered assembly or decreased association of the TOM complex. Mutations in other conserved regions of Tob37 had little to no effect on steady state proteins levels and growth rate.

4.5 The TOM complex and assembly intermediates

Incoming molecules of Tom40 precursor protein interact with the TOB complex at assembly intermediate I in the pathway to formation of the TOM complex. I have shown that steady state levels of the TOM complex were depleted in Tob38↓, Tob37↓, and Tob55↓ mitochondria. Unexpectedly, the size of the TOM complex was increased in the Tob37↓ and Tob55↓ mitochondria. The normal size of the complex was restored in the Tob37-20-1 mutant, suggesting the difference was somehow caused by a lack of Tob37. Tob38↓ mitochondria did not show this size difference, the only phenotype examined in this study that was not shared by both Tob38↓ and Tob37↓ mitochondria. The importance of this size change is currently unknown, but could indicate aberrant assembly of the TOM complex. Assembly of Tom40 into Tob38↓ and Tob37↓ mitochondria showed reduced levels of assembly intermediates and the TOM complex. This supports previous research for the placement of a Tob38- and Tob37-containing TOB complex at the initial stage of Tom40 assembly (Abdul *et al.*, 2000; Habib *et al.*, 2005; Paschen *et al.*, 2005).

The level of the TOM complex in the Tob37-20-1 mutant was reduced, although not the extent observed in the Tob37↓ mitochondria. Assembly of Tom40 in Tob37-20-1 showed a decreased amount of assembly intermediate I and TOM complex, but increased levels of lower molecular weight complexes 50 – 100 kDa in size. In *N. crassa*, Tom40 intermediate II is a 100 – 50 kDa smear, and although this increase in lower molecular weight bands in the mutant could represent an increase of intermediate II it could also represent an increase in TOM complex destabilization or incorrectly assembled products. In addition, some Tom40 precursor also appeared to accumulate in a complex of 185 kDa which is occasionally observed as a faint band when Tom40 is imported into control mitochondria, but may be due to degradation, incorrect assembly, or an altered TOB complex.

4.6 The Involvement of Tom70

Previous research in yeast has linked the Tom70 receptor to Tob37. The two proteins were thought to function as a heterodimeric receptor for a certain class of MIM precursors engaging the TOM complex (Gratzer *et al.*, 1999). It was later shown that

these proteins did not function together as a receptor and that Tom70 could perform the receptor function alone (Gratzer *et al.*, 1999; Ryan *et al.*, 1999; Habib *et al.*, 2005). Tom70 has now been shown to have an additional role in the recruitment of the soluble Mfb1 protein to the mitochondrial surface, (Kondo-Okamoto *et al.*, 2007). Mfb1 is involved in yeast mitochondrial morphology (Durr *et al.*, 2006; Kondo-Okamoto *et al.*, 2006). In addition, Tom70 appears to insert some integral MOM proteins into the membrane without the need for the TOM complex (Otera *et al.*, 2007). Thus, it is possible that Tob38, another soluble MOM protein might be targeted to the mitochondria via Tom70 in *N. crassa*. Tob37 is likely not localized in this manner in *N. crassa*, as yeast mitochondria lacking Tom70 still imported Tob37 efficiently (Habib *et al.*, 2005).

Tom70^{RIP} mitochondria also showed reduced import and assembly of Tom40, porin and Tob55, although all intermediates and complexes were present. Tob38 was present in greater amounts in the 140 kDa TOB complex and an increase in low molecular weight products was observed. Tob37 import did not appear to be affected in the Tom70 mutant. Thus, it seems there may be a connection between Tom70 and the TOB complex in *N. crassa*.

4.7 Future Work

Overall, this work showed that Tob38 and Tob37 are involved in the TOB complex in *N. crassa*. Possibilities for these roles include interaction with beta-barrel protein assembly intermediates within the Tob55 pore for folding and/or release of substrates, or interaction with additional proteins (such as Mdm10 or Mim1) required for import of specific beta-barrel proteins. Further work is required to determine the precise roles of Tob38 and Tob37 in *N. crassa*.

The interaction of mitochondrial import and morphology has been of recent interest in yeast (Meisinger *et al.*, 2006; Stojanovski *et al.*, 2006; Meisinger *et al.*, 2007). Although depletion of Tob38 or Tob37 did not result in extreme alterations in mitochondrial morphology in *N. crassa*, the number of enlarged mitochondria should be determined. Further analysis of this would require quantification of the enlarged mitochondria in the Tob38↓ and Tob37↓ cells, and analysis of Tob55↓ cells by TEM.

The presence of three TOB complexes in *N. crassa* is interesting, and it would be beneficial to know how many interact with Tom40 or porin during assembly of the relative complexes. This could be analyzed using antibody shift experiments and may further determine pathway specificities.

The Tob37-20-1 mutant seemed to separate the Tom40 and porin assembly pathways at the TOB complex, a result not previously observed in any system. Further analysis of this mutant could include import of beta-barrel proteins to determine the rates of import and analysis of mutants with single amino acid

References

Abdul, K.M., Terada, K., Yano, M., Ryan, M.T., Streimann, I., Hoogenraad, N.J., Mori, M. 2000. Functional Analysis of Human Metaxin in Mitochondrial Protein Import in Cultured Cells and Its Relationship with the TOM Complex. Biochemical and Biophysical Research Communications. 276: 1028 – 1034.

Abe, Y., Shodai, T., Muto, T., Mihara, K., Torii, H., Nishikawa, S., Endo, T., Kohda, D. 2000. Structural basis of presequence recognition by the mitochondrial protein import receptor Tom20. Cell. 100 (5): 551 – 560.

Adolph, K.W. 2005. Characterization of the cDNA and amino acid sequences of *Xenopus* Metaxin 3, and relationship to *Xenopus* Metaxins 1 and 2. DNA Seq. 16 (4): 252 – 259.

Ahmed, U.A., Beech, P.L., Lay, S.T., Gilson, P.R., Fisher, P.R. 2006. Import-Associated Translation Inhibition: Novel In Vivo Evidence for Cotranslational Protein Import into *Dictyostelium discoideum* Mitochondria. Euk. Cell. 5 (8): 1314 – 1327.

Ahting, U. Thun, C., Hegerl, R., Typke, D., Nargang, F.E., Neupert, W., Nussberger, S. 1999. The TOM Core Complex: The General Protein Import Pore of the Outer Membrane of Mitochondria. J. Cell Biol. 147 (5): 959 – 968.

Ahting, U., Thieffry, M., Engelhardt, H., Hegerl, R., Neupert, W., Nussberger, S. 2001. Tom40, the Pore-forming Component of the Protein-conducting TOM Channel in the Outer Membrane of the Mitochondria. J. Cell Biol. 153 (6): 1151 – 1160.

Altmann, K. and Westermann, B. 2005. Role of essential genes in mitochondrial morphogenesis in Saccharomyces cerevisiae. Mol. Biol. Cell. 16: 5410 – 5417.

Andersson, S.G., and Kurland, C.G. 1999. The origins of mitochondria and hydrogenosomes. Curr. Opin. Microbiol. 2: 535 – 541.

Andersson, S.G., Zomorodipour, A., Andersson, J.O., Sicheritz-Ponten, T., Alsmark, U.C.M., Podowski, R.M., Naslund, A.K., Eriksson, A. Winkler, H.H., Kurland, C.G. 1998. The genome sequence of *Rickettsia prowazekii* and the origin of mitochondria. Nature. 396 (6707): 133 – 140.

Armstrong, L.C., Komiya, T., Bergman, B.E., Mihara, K., Bornstein, P. 1997. Metaxin Is a Component of a Preprotein Import Complex in the Outer Membrane of the Mammalian Mitochondrion. J. Biol. Chem. 272 (10): 6510 – 6518.

Armstrong, L.C., Saenz, A.J., Bornstein, P. 1999. Metaxin1 interacts with metaxin2, a novel related protein associated with the mammalian mitochondrial outer membrane. J. Cell. Biochem. 74: 11 – 22.

Attardi, G. and Schatz, G. 1988. Biogenesis of Mitochondria. Annu. Rev. Cell. Biol. 4: 289 – 333.

Ausubel, R.A., Brent, R., Kingston, R.E., Moore, D.D., Seidman, J.G., Smith, J.A., Struhl, K. 1992. Current Protocols in Molecular Biology. Greene and Wiley Interscience, New York.

Baker, K.P. Schaniel, A. Vestweber, D., Schatz, G. 1990. A yeast mitochondrial outer membrane protein is essential for protein import and cell viability. Nature. 348: 605 – 609.

Bartlett, K., and Eaton, S. 2004. Mitochondrial beta-oxidation. Eur. J. Biochem. 271: 462 – 469.

Bauer, M.F., Sirrenberg, C., Neupert, W., Brunner, M., 1996. Role of Tim23 as voltage sensor and presequence receptor in protein import into mitochondria. Cell. 87: 33 – 41.

Bauer, M.F., Hofmann, S., Neupert, W., Brunner, M. 2000. Protein translocation into mitochondria: the role of TIM complexes. Trends Cell Biol. 10: 25 – 32.

Becker, L., Bannwarth, M., Meisinger, C., Hill, K., Model, K., Krimmer, T., Cadadio, R., Truscott, K., Schulz, G.E., Pfanner, N., Wagner, R. 2005. Preprotein translocase of the outer mitochondrial membrane: Reconstituted Tom40 forms a characteristic TOM pore. J. Mol. Biol. 353: 1011 – 1020.

Becker, T., Pfannschmidt, S., Guiard, B., Stojanovski, D., Milenkovic, D., Kutik, S., Pfanner, N., Meisinger, C., Wiedemann, N. 2008. Biogenesis of the mitochondrial TOM complex: Mim1 promotes insertion and assembly of signal-anchored receptors. J. Biol. Chem. 283 (1): 120 – 127.

Beddoe, T., and Lithgow, T. 2002. Delivery of nascent polypeptides to the mitochondrial surface. Biochim. Biophys. Acta. 1592 (1): 35 – 39.

Berger, K.H., Sogo, F., Yaffe, M.P.1997. Mdm12p, a Component Required for Mitochondrial Inheritance That Is Conserved between Budding and Fission Yeast. J. Cell Biol. 136 (3): 545 – 553.

Berthold, J., Bauer, M.F., Schneider, H.C., Klaus, C., Dietmeier, K., Neupert, W., Brunner, M. 1995. The MIM complex mediates preproteins translocation across the mitochondrial inner membrane and couples it to the mt-Hsp70 / ATP driving system. Cell. 81: 1085 – 1093.

Bjellqvist, B., Hughes, B., Pasquali, C., Paquet, N., Ravier, F., Sanchez, J., Frutiger, W., Hochstrasser, D.F. 1993. The focusing positions of polypeptides in immobilized pH gradients can be predicted from their amino acid sequence. Electrophoresis. 14: 1023 – 1031.

Blatch, G.L., and Lassle, M. 1999. The tetratricopeptide repeat: a structural motif mediating protein-protein interactions. Bioessays. 21(11): 932 – 939.

Boldogh, I.R., Nowakowski, D.W., Yang, H., Chung, H., Karmon, S., Royes, P., Pon, L.A. 2003. A protein complex containing Mdm10p, Mdm12p, and Mmm1p links mitochondrial membranes and DNA to the cytoskeleton-based segregation machinery. Mol. Biol. Cell. 14: 4618 – 4627.

Boldogh, I., Vojtov, N., Karmon, S., Pon, L.A. 1998. Interaction between mitochondria and the actin cytoskeleton in budding yeast requires two integral mitochondrial outer membrane proteins, Mmm1p and Mdm10p. J. Cell Biol. 141: 1371 – 1381.

Bornstein, P., McKinney, C.E., Lamarca, M.E., Winfield, S., Shingu, T., Devarayalus, S., Vos, H.L., Ginns, E.I. 1995. Metaxin, A gene contiguous to both Thrombospondin-3 and Glucocerebrosidase, is required for embryonic-development in the mouse – implications for Gaucher-Disease. PNAS. 92 (10): 4547 – 4551.

Boxma, B., Graff, R.M., van der Staay, G.W.M., van Alen, T.A., Ricard, G., Gabaldon, T., van Hoek, A.H.A.M., Moon-van der Staay, S.Y., Koopman, W.J.H., van Hellemond, J.J., Tielens, A.G.M., Friedrich, T., Veenhuis, M., Huymen, M.A., Hackstein, J.H.P. 2005. An anaerobic mitochondrion that produces hydrogen. Nature. 434: 74 – 79.

Burgess, S.M., Delannoy, M., Jensen, R.E. 1994. MMM1 encodes a mitochondrial outer membrane protein essential for establishing and maintaining the structure of yeast mitochondria. J. Cell Biol. 126: 1375 – 1391.

Chacinska, A., Lind, M., Frazier, A.E., Dudek, J., Meisinger, C., Geissler, A., Sickmann, A., Meyer, H.E., Truscott, K.N., Guiard, B., Pfanner, N., Rehling, P. 2005. Mitochondrial presequence translocase: Switching between TOM tethering and motor recruitment involves Tim21 and Tim17. Cell. 120 (6): 817 – 829.

Chacinska, A., Pfannschmidt, S., Wiedemann, N., Kozjak, V., Szklarz, L.K.S., Schulze-Specking, A., Truscott, K.N., Guiard, B., Meisinger, C., Pfanner, N. 2004. Essential role of Mia40 in import and assembly of mitochondrial intermembrane space proteins. EMBO J. 23: 3735 – 3746.

Chae, M.S., Lin, C.C., Kessler, K.E., Nargang, C.E., Tanton, L.L., Hahn, L.B., Nargang, F.E. 2007. Identification of an alternative oxidase induction motif in the promoter region of the aod-1 gene in *Neurospora crassa*. Genetics. 175 (4): 1597 – 1606.

Chan, N.C., and Lithgow, T. 2008. The peripheral membrane subunits of the SAM complex function co-dependently in mitochondrial outer membrane biogenesis. Article In Press.

Chaudhuri, M., Ott, R.D., Hill, G.C. 2006. Trypanosome alternative oxidase: from molecule to function. Trends Parasitol. 22: 484-491.

Chenna, R., Sugawara, H., Koike, T., Lopez, R., Gibson, T.J., Higgins, D.G., Thompson, J.D. 2003. Multiple sequence alignment with the Clustal series of programs. Nucleic Acid Res. 31 (13): 3487 – 3500.

Claros, M.G., and von Heijne, G. 1994. TopPred II: An Improved Software For Membrane Protein Structure Predictions. CABIOS. 10: 685 - 686.

Court, D.A, Lill, R., Neupert, W. 1995 . The protein import apparatus of the mitochondrial outer membrane. Can. J. Bot. 73(Suppl. 1): S193 – S197.

Curran, S.P., Leuenberger, D., Oppliger, W., Koehler, C. 2002. The Tim9p-Tim10p transmembrane domains of the ADP/ATP carrier. EMBO J. 21 (5): 942 – 953.

Davis, A.J., and F.J. De Serres. 1970. Genetic and Microbiological Research Techniques for Neurospora crassa. Methods Enzymology. 17: 79 – 143.

Davis, A.J., Sepuri, N.B., Holder, J., Johnson, A.E., Jensen, R.E. 2000. Two Intermembrane Space TIM Complexes Interact with Different Domains of Tim23p during Its Import into Mitochondria. J. Cell Biol. 150 (6): 1271 – 1282.

Davis, R.H., 2000. Neurospora: Contributions of a model organism. Oxford University Press. Inc. New York.

Dekker, P.J.T., Ryan, M.T., Brix, J., Muller, H., Honlinger, A., Pfanner, N. 1998. Preprotein Translocase of the Outer Mitochondrial Membrane: Molecular Dissection and Assembly of the General Import Pore Complex. Mol. Cell. Biol. 18 (11): 6515 – 6524.

Dembowski, M., Künkele, K., Nargang, F.E., Neupert, W., Rapaport, D. 2001. Assembly of Tom6 and Tom7 into the TOM Core Complex of *Neurospora crassa*. J. Biol. Chem. 276 (21): 17679 – 17685.

Detmer, S.A., and Chan, D.C. 2007. Functions and dysfunctions of mitochondrial dynamics. Nature Rev. Mol. Cell Biol. 8 (11): 870 – 879.

Dietmeier, K., Honlinger, A., Bomer, U., Dekker, P.J.T., Eckerskorn, C., Lottspeich, F., Kubrich, M., Pfanner, N. 1997. Tom5 functionally links mitochondrial preproteins receptors to the general import pore. Nature. 388: 195 – 200.

Durr, M., Escobar-Henriques, M., Merz, S., Geimer, S., Langer, T., Westermann, B. 2006. Nonredundant roles of mitochondria-associated F-box proteins Mfb1 and Mdm30 in maintenance of mitochondrial morphology in yeast. Mol. Biol. Cell. 17: 3952 – 3963.

Dyall, S.D., Koehler, C.M., Delgadillo-Correa, M.G., Bradley, P.J., Plumper, E., Leuenberger, D., Turck, C.H., Johnson, P.J. 2000. Presence of a Member of the Mitochondrial Carrier Family in Hydrogenosomes: Conservation of Membrane targeting Pathways between Hydrogenosomes and Mitochondria. Mol. Cell. Biol. 20 (7): 2488 – 2497.

Dyall, S.D., Lester, D.C., Schneider, R.E., Delgadillo-Correa, M.G., Plumper, E., Martinez, A., Koehler, C.M., Johnson, P.J. 2006. *Trichomonas vaginalis* Hmp35, a Putative Pore-forming Hydrogenosomal Membrane Protein, Can Form a Complex in Yeast Mitochondria. J. Biol. Chem. 278 (3): 30548 – 30561.

Eck, R.V. and M.O. Dayhoff. 1966. Atlas of Protein Sequence and Structure, National Biomedical Research Foundation, Silver Springs, MD.

Embley, T.M. van der Giezen, M., Horner, D.S., Dyal, P.L., Bell, S., Foster, P.G. 2003. Hydrogenosomes, Mitochondria and Early Eukaryotic Evolution. IUBMB Life. 55 (7): 387 – 395.

Endo, T., and Kohda, D. 2002. Functions of outer membrane receptors in mitochondrial protein import. Biochim. Biophys. Acta. 1592: 3 – 14.

Esaki, M., Shimizu, H., Ono, T., Yamamoto, H., Kanamori, T., Nishikawa, S., Endo, T. 2004. Mitochondrial protein import. Requirement of presequence elements and Tom components for precursor binding of the TOM complex. J. Biol. Chem. 279: 45701 – 45707.

Fitch, W.M. 1971. Toward defining the course of evolution: minimum change for a specific tree topology. Syst. Zool. 20: 406 – 416.

Fitch, W.M., and E. Margoliash. 1967. Construction of phylogenetic trees. Science. 155: 279 - 284.

Fiumera, H.L., Broadley, S.A., Fox, T.D. 2007. Translocation of mitochondrially synthesized Cox2 domains from the matrix to the intermembrane space. Mol. Cell Biol. 27: 4664 – 4673.

Fuchs, F., Prokisch, H., Neupert, W., Westermann, B. 2002. Interaction of mitochondria with microtubules in the filamentous fungus *Neurospora crassa*. J. Cell Sci. 115 (10):1931 – 1937.

Fujiki, M., and Verner, K. 1993. Coupling of cytosolic protein synthesis and mitochondrial protein import in yeast. Evidence for cotranslational import in vivo. J. Biol. Chem. 268 (3): 1914 – 1920.

Gakh, O., Cavadini, P., Isaya, G. 2002. Mitochondrial processing peptidases. Biochim. Biophys. Acta. 1592: 63 – 77.

Galagan, G.E., Calvo, S.E., Borkovich, K.A., Selker, E.U., Read, N.D., Fitzhugh, D.J., Ma, L., Smirnov, S., Purcell, S., Rehman, B., Elkins, T., Engels, R., Wang, S., Nielsen, C.B., Butler, J., Endrizzi, M., Qui, D., Ianakiev, P., Bell-Pedersen, D., Nelson, M.A., Werner-Washburne, M., Selitrennikoff, C.P., Kinsey, J.A., Braun, E.L., Zelter, A., Schulte, U., Kothe, G.O., Jedd, G., Mewes, W., Staben, C., Marcotte, E., Greenberg, D., Roy, A., Foley, K., Naylor, J., Stange-Thomann, N., Barrett, R., Gnerre, S., Kamal, M., Kamvysselis, M., Mauceli, E., Bielke, C., Rudd, S., Frishman, D., Krystofova, S., Rasmussen, C., Metzenberg, R.L., Perkins, D.D., Kroken, S., Cogoni, C., Macino, G., Catcheside, D., Li, W., Pratt, R.J., Osmani, S.A., Desouza, C.P.C., Glass, L., Orbach, M.J., Berglund, J.A., Voelker, R., Yarden, O., Plamann, M., Seiler, S., Dunlap, J., Radford, A., Aramayo, R., Natvig, D.O., Alex, L.A., Mannhaupt, G., Ebbole, D.J., Freitag, M., Paulsen, I., Sachs, M.S., Lander, E.S., Nusbaum, C., Birren, B. 2003. The genome sequence of the filamentous fungus *Neurospora crassa*. Nature. 422: 859 – 868.

Gentle, I., Gabriel, K., Beech, P., Waller, R., Lithgow, T. 2004. The Omp85 family of proteins is essential for outer membrane biogenesis in mitochondria and bacteria. J. Cell Biol. 164 (1): 19 – 24.

Good, A.G., and Crosby, W.L. 1989. Anaerobic induction of alanine amino transferase in barley root tissue. Plant Physiol. 90: 1305 – 1309.

Grad, L.I., Descheneau, A.T., Neupert, W., Lill, R., Nargang, F.E. 1999. Inactivation of the *Neurospora crassa* mitochondrial outer membrane protein TOM70 by repeat-induced point mutation (RIP) causes defects in mitochondrial protein import and morphology. Curr. Genet. 36: 137 – 146.

Graier, W.F., Frieden, M., Malli, R. 2007. Mitochondria and Ca^{2+} signaling: old guests, new functions. Eur. J. Physiol. 455: 375 – 396.

Gratzer, S., Lithgow, T., Bauer, R.E., Lamping, E., Paltauf, F., Kohlwein, S.D., Haucke, V., Junne, T., Schatz, G., Horst, M. 1995. Mas37p, a novel receptor subunit for protein import into mitochondria. J. Cell Biol. 129 (1): 25 – 34.

Gray, M.W., Burger, G., Lang, B.F. 1999. Mitochondrial Evolution. Science. 283: 1476 – 1481.

Gray, M.W., Lang, B.F., Burger, G. 2004. The mitochondria of protists. Ann. Rev. Genetics. 38: 477 – 524.

Griparic, L, van der Bliek, A.M. 2001. The many shapes of mitochondrial membranes. Traffic. 2: 235 – 244.

Grumbt, B., Stroobant, V., Terziyska, N., Israle, L., Hell, K. 2007. Functional Characterization of Mia40p, the Central Component of the Disulfide Relay System of the Mitochondrial Intermembrane Space. J. Biol. Chem. 282 (52): 37461 – 37470.

Gunter, T.E., Yule, D.I., Gunter, K.K., Eliśeev, R.A., Salter, J.D. 2004. Calcium and mitochondria. FEBS Letters. 567: 96 – 102.

Habib, S.J., Waizenegger, T., Lech, M., Neupert, W., Rapaport, D. 2005. Assembly of the TOB complex of Mitochondria. J. Biol. Chem. 280 (8): 6434 – 6440.

Habib, S.J., Waizenegger, T., Niewienda, A., Paschen, S.A., Neupert, W., Rapaport, D. 2007. The N-terminal domain of Tob55 has a receptor like function in the biogenesis of mitochondrial b-barrel proteins. J. Cell Biol. 176 (1): 77 – 88.

Hachiya, N., Mihara, K., Suda, K., Horst, M., Schatz, G., Lithgow, T. 1995. Reconstitution of the initial steps of mitochondrial protein import. Nature. 376: 705 – 709.

Harkness, T.A.A., Metzenberg, R.L., Schneider, H., Lill, R., Neupert, W., Nargang, F.E. 1994a. Inactivation of the *Neurospora crassa* Gene Encoding the Mitochondrial Import Receptor MOM19 by the Technique of "Sheltered RIP". Genetics. 136 (1): 107 – 118.

Harkness, T.A., Nargang, F.E., van der Klei, I., Neupert, W., Lill, R. 1994b. A crucial role of the mitochondrial protein import receptor MOM19 for the biogenesis of mitochondria. J Cell Biol. 124: 637 – 648.

Hackstein, J.H.P., Tjaden, J., Huynen, M. 2006. Mitochondria, hydrogenosomes and mitosomes: products of evolutionary tinkering. Curr. Genet. 50: 225 – 245.

Heggeness, M. H., Simon, M. and Singer, S. J. 1978. Association of mitochondria with microtubules in cultured cells. Proc. Natl. Acad. Sci. 75: 3863 – 3866.

Hell, K. 2007. The Erv1-Mia20 disulfide relay system in the intermembrane space of mitochondria. Biochim. Biophys. Acta. Mol. Cell Biol. Article In Press.

Herrmann, J.M., and Bonnefoy, N. 2004. Protein export across the inner membrane of mitochondria: the nature of translocated domains determines the dependence on the Oxa1 translocase. J. Biol. Chem. 279: 2507 – 2512.

Hill, K., Model, K., Ryan, M.T., Dietmeier, K., Martin, F., Wagner, R., Pfanner, N. 1998. Tom40 forms the hydrophilic channels of the mitochondrial import pore for preproteins. Nature. 395: 516 – 521.

Hines, V., Brandt, A., Griffiths, G., Horstmann, H., Brutsch, H., Schatz, G., 1990. Protein import into yeast mitochondria is accelerated by the outer membrane proteins MAS70. EMBO J. 9: 3191 – 3200.

Honlinger, A., Bomer, U., Alconada, A., Eckerskorn, C., Lottspeich, F., Dietmeier, K., Pfanner, N. 1996. Tom7 modulates the dynamics of the mitochondrial outer membrane Translocase and plays a pathway-related role in protein import. EMBO J. 15: 2125 – 2137.

Hoppins, S., Lackner, L., Nunnari, J. 2007a. The Machines that Divide and Fuse Mitochondria. Annu. Rev. Biochem. 76: 751 – 780.

Hoppins, S.C., Go, N.E., Klein, A., Schmitt, S., Neupert, W., Rapaport, D., Nargang. F.E. 2007b. Alternative splicing gives rise to different isoforms of the *Neurospora crassa* Tob55 protein that vary in their ability to insert beta-barrel proteins into the outer mitochondrial membrane. Genetics. 177 (1): 137 – 149.

Hoppins, S.C., Nargang, F.E. 2004. The Tim8-Tim13 Complex of *Neurospora crassa* Functions in the Assembly of Proteins into Both Mitochondrial Membranes. J. Biol. Chem. 279 (13): 12396 – 12405.

Horie, C., Suzuki, H., Sakaguchi, M., Mihara, K. 2003. Targeting and assembly of mitochondrial tail-anchored protein Tom5 and the TOM complex depend on a signal distinct from that of tail-anchored proteins dispersed in the membrane. J. Biol. Chem. 278: 41462 – 41471.

Hulett, J.M., Lueder, F., Chan, N.C., Perry, A.J., Wolynec, P., Likic, V.A., Gooley, P.R., Lithgow, T. 2008. The Transmembrane Segment of Tom20 Is Recognized by Mim1 for Docking to the Mitochondrial TOM Complex. J. Mol. Biol. Article In Press.

Humphries, A.D., Streimann, I.C., Stojanovski, D., Johnston, A.J., Yano, M., Hoogenraad, J., Ryan, M.T. 2005. Dissection of the mitochondrial import and assembly pathway for human Tom40. J. Biol. Chem. 280 (12): 11535 – 11543.

Ishikawa, D., Yamamoto, H., Tamura, Y., Moritoh, K., Endo, T. 2004. Two novel proteins in the mitochondrial outer membrane mediated β-barrel protein assembly. J. Cell Biol. 166 (5): 621 – 627.

Jones, D.T., Taylor, W.R., Thornton, J.M. 1992. The rapid generation of mutation data matrices from protein sequences. Comput. Appl. Biosci. 8: 275 – 282.

Joseph-Horne, T., Hollomon, D.W., Wood, P.M. 2001. Fungal respiration: a fusion of standard and alternative components. Biochim. Biophys. Acta. 1504: 179 – 195.

Kennell, J.C., Collins, R.A., Griffiths, A.J.F., Nargang, F.E. 2004. Mitochondrial Genetics of Neurospora. The Mycota, Vol. 2: Genetics and Biotechnology. 2nd Edition. 95 – 112.

Kerscher, O., Holder, J., Srinivasan, M., Leung, R.S., Jensen, R.E. 1997. The Tim54p – Tim22p complex mediates insertion of proteins into the mitochondrial inner membrane. J. Cell Biol. 139: 1663 – 1675.

Kerscher, O., Sepuri, N.B., Jensen, R.E. 2000. Tim18p is a new component of the Tim54p – Tim22p translocon in the mitochondrial inner membrane. Mol. Biol. Cell. 11: 103 – 116.

Kiebler, M., Keil, P., Schneider, H., van der Klei, I.J., Pfanner, N., Neupert, W. 1993. The mitochondrial receptor complex: A central role of MOM22 in mediating transfer of preproteins from receptors to the general insertion pore. Cell. 74: 483 – 492.

Koehler, C.M., Leuenberger, D., Merchant, S., Renold, A., Junne, T., Schatz, G. 1999. Human deafness dystonia syndrome is a mitochondrial disease. PNAS. 96 (5): 2141 – 2146.

Koehler, C.M., Merchant, S., Oppliger, W., Schmid, K., Jarosch, E., Dolfini, L., Junne, T., Schatz, G., Tokathdis, L. 1998. Tim9p, an essential partner subunit of Tim10p for the import of mitochondrial carrier proteins. EMBO J. 17 (22): 6477 – 6486.

Koehler, C.M. 2004. New Developments in Mitochondrial Assembly. Annu. Rev. Cell Dev. Biol. 20: 309 – 335.

Komiya, T., Rospert, S., Schatz, G., Mihara, K. 1997. Binding of mitochondrial precursor proteins to the cytoplasmic domains of the import receptors Tom70 and Tom20 is determined by cytoplasmic chaperones. EMBO. 16 (14): 4267 – 4275.

Kondo-Okamoto, N., Ohkuni, K., Kitagawa, K., NcCaffery, J.M., Shaw, J.M., Okamoto, K. 2006. The novel F-box protein Mfb1p regulates mitochondrial connectivity and exhibits asymmetric localization in yeast. Mol. Biol. Cell. 17: 3756 – 3767.

Kondo-Okamoto, N., Shaw, J.M., Okamoto, K. 2003. Mmm1p spans both the outer and inner mitochondrial membranes and contains distinct domains for targeting and foci formation. J. Biol. Chem. 278: 48997–9005.

Kondo-Okamoto, N., Shaw, J.M., Okamoto, K. 2007. Tetratricopeptide repeat proteins Tom70 and Tom71 mediate yeast mitochondrial morphogenesis. EMBO Reports. 9 (1):63 – 69.

Kovermann, P., Truscott, K.N., Guiard, B., Rehling, P., Sepuri, N.B., Muller, H., Jensen, R.E., Wagner, R., Pfanner, N. 2002. Tim22, the Essential Core of the Mitochondrial Protein Insertion Complex, Forms a Voltage-Activated and Signal-Gated Channel. Mol. Cell. 9: 363 – 373.

Kozany, C., Mokranjac, D., Sichting, M., Neupert, W., Hell, K. 2004. The J domain-related cochaperone Tim16 is a constituent of the mitochondrial TIM23 preprotein translocase. Nature Struct. Mol. Biol. 11 (3): 234 – 241.

Kozjak, V., Wiedemann, N., Milenkovic, D., Lohaus, C., Meyer, H., Guiard, B., Meisinger, C., Pfanner, N. 2003. An Essential Role of Sam50 in the Protein Sorting and Assembly Machinery of the Mitochondrial Outer Membrane. J. Biol. Chem. 278 (49): 48520 – 48523.

Kozjak-Pavlovic, V., Ross, K., Benlasfer, N., Kimmig, S., Karlas, A., Rudel, T. 2007. Conserved roles of Sam50 and metaxins in VDAC biogenesis. EMBO Reports. 8 (6): 576 – 582.

Kunkele, K.P., Juin, P., Pompa, C., Nargang, F.E., Henry, J.P., Neupert, W., Lill, R., Thieffry, M. 1998. The isolated complex of the Translocase of the outer membrane of mitochondria. J. Biol. Chem. 273 (47): 31032 – 31039.

Kurz, M., Martin, H., Rassow, J., Pfanner, N., Ryan, M.T. 1999. Biogenesis of Tim proteins of the mitochondrial carrier import pathway: differential targeting mechanisms and crossing over with the main import pathway. Mol. Biol. Cell. 10: 2461 – 2474.

Kutik, S., Guiard, B., Meyer, H., Wiedemann, N., Pfanner, N. 2007. Cooperation of translocase complexes in mitochondrial protein import. J. Cell Biol. 179 (4): 585 – 591.

Lambowitz, A.M., Smith, E.W, Slayman, C.W. 1972. Electron transport in Neurospora mitochondria; studies on wild type and poky. J. Biol. Chem. 247: 4850-4858.

Lang, B.F., Burger, G., O'Kelly, C.J., Cedergren, R., Golding, G.B. *et al.* 1997. An ancestral mitochondrial DNA resembling a eubacterial genome in miniature. Nature. 387 (6632): 493 -497.

Lang, B.F., Gray, M.W., Burger, G. 1999a. Mitochondrial Genome Evolution and the Origin of Eukaryotes. Annu. Rev. Genet. 33: 351 – 397.

Lang, B.F., Seif, E., Gray, M.W., O'Kelly, C., Burger, G. 1999b. A Comparative Genomics Approach to the Evolution of Eukaryotes and their Mitochondria. J. Eukaryot. Microbiol. 46 (4): 320 – 326.

Lill, R. and Kispal, G. 2000. Maturation of cellular Fe/S proteins: the essential function of the mitochondria. Trends Biochem. Sci. 25: 352 – 356.

Lill, R. and Muhlenhoff, U. 2005. Iron-sulfur-protein biogenesis in eukaryotes. Trends Biochem. Sci. 30: 133 – 141.

Lithgow, T., Junne, T., Suda, K., Gratzer, S., Schatz, G. 1994. The mitochondrial outer membrane protein Mas22p is essential for protein import and viability of yeast. PNAS. 91: 11973 – 11977.

Lowry, R.T., Durkee, T.J., Sussman, A. 1967. Ultrastructural studies of microconidium formation in *Neurospora crassa*. J. Bacteriol. 94: 1757 – 1763.

Lu, H., Allen, S., Wardleworth, L, Savory, P., Tokatlidis, K. 2004. Functional TIM10 Chaperone Assembly is Redox-regulated *in Vivo*. J. Biol. Chem. 279 (18): 18952 – 18958.

MacKenzie, J.A., and Payne, R.M. 2007. Mitochondrial protein import and human health and disease. Biochim. Biophys. Acta. 1772 (5): 509 – 523.

Mannella, C.A. 2006. The relevance of mitochondrial membrane topology to mitochondrial function. Biochim. Biophys. Acta. 1662: 140 – 147.

Margolin, B.S., Freitag, M., Selker, E.U. 1997. Improved plasmids for gene targeting at the his-3 locus of Neurospora crassa by electrophoration. Fungal Genetic. Newsl. 44: 34 – 36.

Margloin, B.S., Freitag, M., Selker, E.U. 2000. Improved plasmids for gene targeting at the his-3 locus of Neurospora crassa by electrophoration: correction. Fungal Genetic. Newsl. 47: 112.

Margolin, B.S., Garrett-Engele, P.W., Stevens, J.N., Fritz, D.Y., Garrett-Engele, C., Metzenbert, R.L., Selker, E.U. 1998. A methylated Neurospora 5S rRNA pseudogene contains a transposable element inactivated by repeat-induced point mutation. Genetics. 149: 1787 – 1797.

Margulis, L. 1975. Symbiotic theory on the origin of eukaryotic organelles; criteria for proof. Symposia for the Society of Experimental Biology. 21 – 38.

Martin, W., and Muller, M. 1998. The hydrogen hypothesis for the first eukaryote. Nature. 392: 37 – 41.

Martinez-Caballero, S., Grigoriev, S.M., Herrmann, J.M., Campo, M.L., Kinnally, K.W. 2007. Tim17p Regulates the Twin Pore Structure and Voltage Gating of the Mitochondrial Protein Import Complex TIM23. J. Biol. Chem. 282 (6): 3584 – 3593.

Mayer, A., Nargang, F.E., Neupert, W., Lill, R. 1995. MOM22 is a receptor for mitochondrial targeting sequences and cooperates with MOM19. EMBO J. 14: 4204 – 4211.

McDonald, A.E., and Vanlerberghe, G.C. 2004. Branched mitochondrial electron transport in the animalia: Presence of alternative oxidase in several animal phyla. IUBMB Life 56: 333-341

Meisinger, C., Pfannschmidt, S., Rissler, M., Milenkovic, D., Becker, T., Stojanovski, D., Youngman, M.J., Jensen, R.E., Chacinska, A., Guiard, B., Pfanner, N., Wiedemann, N. 2007. The morphology proteins Mdm12/Mmm1 function in the major b-barrel assembly pathway of mitochondria. EMBO. 26 (9): 2229 – 2239.

Meisinger, C., Rissler, M., Chacinska, A., Milenkovic, D., Kozjac, V., Schonfisch, B., Lohaus, C., Meyer, H.E., Yaffe, M.P., Guiard, N., Wiedemann, N., Pfanner, N. 2004. The mitochondrial morphology protein Mdm10 functions in assembly of the preproteins translocase of the outer membrane. Dev. Cell. 7: 61 – 71.

Meisinger, C., Wiedmann, N., Rissler, M., Strub, A., Milenkovic, D., Schonfisch, B., Muller, H., Kozjak, V., Pfanner, N. 2006. Mitochondrial Protein Sorting, Differentiation of beta-barrel assembly by Tom7-mediated segregation of Mdm10. J. Biol. Chem. 281 (32): 22819 – 22826.

Mesecke, N., Terziyska, N., Kozany, C., Baumann, F., Neupert, W., Hell, K., Herrmann, J.M. 2005. A Disulfide Relay System in the Intermembrane Space of Mitochondria that mediates Protein Import. Cell. 121 (7): 1059 – 1069.

Milenkovic, D., Kozjak, V., Wiedemann, N., Lohaus, C., Meyer, H.E., Guiard, B., Pfanner, N., Meisinger, C. 2004. Sam35 of the Mitochondrial Protein Sorting Assembly Machinery Is a Peripheral Outer Membrane Protein Essential for Cell Viability. J. Biol. Chem. 279 (21): 22781 – 22785.

Model, K., Meisinger, C., Prinz, T., Wiedemann, N., Truscott, K.N., Pfanner, N., Ryan, M.T. 2001. Multistep assembly of the protein import channel of the mitochondrial outer membrane. Nature Struct. Biol. 8 (4): 361 – 370.

Mokranjac, D., Paschen, S.A., Kozany, C., Prokisch, H., Hoppins, S.C., Nargang, F.E., Neupert, W., Hell, K. 2003a. Tim50, a novel component of the TIM23 preprotein translocase of mitochondria. EMBO J. 22 (4): 816 – 825.

Mokranjac, D., Popov-Celeketic, D., Hell, K., Neupert, W. 2005. Role of Tim21 in mitochondrial translocation contact sites. J. Biol. Chem. 280 (25): 23437 – 23440.

Mokranjac, D., Sichting, M., Neupert, W., Hell, K. 2003b. Tim14, a novel key component of the import motor of the TIM23 protein translocase of mitochondria. EMBO J. 22 (19): 4945 – 4956.

Muller, M. 1993. The hydrogenosome. J. Gen. Microbiol. 139: 2879 – 2889.

Nargang, F.E., Kunkele, K, Mayer, A., Ritzel, R.G., Neupert, W., Lill, R. 1995. 'Sheltered disruption' of *Neurospora crassa* MOM22, an essential component of the mitochondrial protein import complex. EMBO J. 14 (6): 1099 – 1108.

Nargang, F.E., Preuss, M., Neupert, W., Herrmann, J.M. 2002. The Oxa1 Protein Forms a Homooligomeric Complex and Is an Essential Part of the Mitochondrial Export Translocase in *Neurospora crassa*. J. Biol. Chem. 277 (15): 12846 – 12853.

Neupert, W., and Brunner, M. 2002. The Protein Import Motor of Mitochondria. Nature Reviews. 3: 555 – 565.

Neupert, W., and Herrmann, J.M. 2007. Translocation of Proteins into Mitochondria. Annu. Rev. Biochem. 76: 723 – 749.

Nicastro, D., Frangakis, A.S., Typke, D., Baumeister, W. 2000. Cryo-electron tomography of *Neurospora* mitochondria. Journal of Structural Biology. 129: 48 – 56.

Okamoto, K., and Shaw, J.M. 2005. Mitochondrial Morphology and Dynamics in Yeast and Multicellular Eukaryotes. Annu. Rev. Genet. 39: 503 – 536.

Otera, H., Taira, Y., Horie, C., Suzuki, Y., Suzuki, H., Setoguchi, K., Kato, H., Oka, T., Mihara, K. 2007. A novel insertion pathway of mitochondrial outer membrane proteins with multiple transmembrane segments. J. Cell Biol. 179 (7): 1355 – 1363.

Paschen, S.A., Neupert, W., Rapaport, D. 2005. Biogenesis of b-barrel membrane proteins of mitochondria. Trends in Biochem. Sci. 30 (10): 575 – 582.

Paschen, S.A., Rothbauer, U., Kaldi, K., Bauer, M.F., Neupert, W., Brunner, M. 2000. The role of the TIM8-13 complex in the import of Tim23 into mitochondria. EMBO J. 19 (23): 6392 – 6400.

Paschen, S.A., Waizenegger, T., Stan, T., Preuss, M., Cyrklaff, M., Hell, K., Rapaport, D., Neupert, W. 2003. Evolutionary conservation of biogenesis of beta-barrel membrane proteins. Nature. 426: 862 – 866.

Petrozzi, L., Ricci, G., Noemi, J.G., Siciliano, G., Mancuso, M. 2007. Mitochondria and neurodegeneration. Bioscience Reports. 27: 87 – 104.

Pfanner, N., and Neupert, W. 1985. Transport of proteins into mitochondria: a potassium diffusion potential is able to drive the import of ADP/ATP carrier. EMBO J. 4: 2819 – 2825.

Pfanner, N., Wiedemann, N., Meisinger, C., Lithgow, T. 2004. Assembling the mitochondrial outer membrane. Nature Struct. Mol. Biol. 11 (11): 1044 – 1048.

Plumper, E., Bradley, P.J., Johnson, P.J. 2000. Competition and protease sensitivity assays provide evidence for the existence of a hydrogenosomal protein import machinery in *Trichomonas vaginalis*. Mol. Bioc. Parasit. 106: 11 – 20.

Poole, A.M., and Penny, D. 2007. Evaluating hypotheses for the origin of eukaryotes. Bioessays. 29: 74 – 84.

Popov-Celeketicm J., Waizenegger, T., Rapaport, D. 2007. Mim1 Functions in an Oligomeric Form to Facilitate the Integration of Tom20 into the Mitochondrial Outer Membrane. JMB. Article In Press.

Prokisch, H., Neupert, W., Westermann, B. 2000. Role of MMM1 in Maintaining Mitochondrial Morphology in *Neurospora crassa*. Mol. Biol. Cell. 11: 2961 – 2971.

Prokisch, H., Nussberter, S., Westermann, B. 2002. Protein import into mitochondria of *Neurospora crassa*. Fungal Genet. Biol. 36 (2): 85 – 90.

Ramage, L., Junne, T., Hahne, K., Lithgow, T., Schatz, G. 1993. Functional cooperation of mitochondrial protein import receptors in yeast. EMBO J. 12 (11): 4115 – 4123.

Rapaport, D. 2002. Biogenesis of the mitochondrial TOM complex. Trends in Biochem. Sci. 27 (4): 191 – 197.

Rapaport, D. 2005. How does the TOM complex mediate insertion of precursor proteins into the mitochondrial outer membrane? J. Cell Biol. 171 (3): 419 – 423.

Rapaport, D., Kunkele, K., Dembowski, M., Ahting, U., Nargang, F.E., Neupert, W., Lill, R. 1998a. Dynamics of the TOM Complex of Mitochondria during Binding and Translocation of Preproteins. Mol. Cell. Biol. 18 (9): 5256 – 5262.

Rapaport, D., Mayer, A., Neupert, W., Lill, R. 1998b. *cis* and *trans* sites of the TOM complex of mitochondria in unfolding and initial translocation of preproteins. J. Biol. Chem. 273: 8806 – 8813.

Rapaport, D., and Neupert, W. 1999. Biogenesis of Tom40, core component of the TOM complex of mitochondria. J. Cell Biol. 146: 321 – 331.

Rapaport, D., Taylor, R.D., Kaser, R.D., Langer, M., Neupert, T., Nargang, F.E. 2001. Structural requirements of Tom40 for assembly into preexisting TOM complexes of mitochondria. Mol. Biol. Cell. 12: 1189 – 1198.

Rehling, P., Model, K., Brandner, K., Kovermann, P., Sickmann, A., Meyer, H.E., Kuhlbrandt, W., Wagner, R., Truscott, K.N., Pfanner, N. 2003. Protein insertion into the mitochondrial inner membrane by a twin-pore Translocase. Science. 299: 1747 – 1751.

Ryan, M.T., Muller, H., Pfanner, N. 1999. Functional staging of ADP/ATP carrier translocation across the outer mitochondrial membrane. J. Biol. Chem. 274 (29): 20619 – 20627.

Saitoh, T., Igura, M., Obita, T., Ose, T., Kojima, R., Maenaka, K., Endo, T., Kohda, D. 2007. Tom20 recognizes mitochondrial presequences through dynamic equilibrium among multiple bound states. EMBO J. 26 (22): 4777 – 4748.

Sambrook, J., and Russell, D.W. 2001. Molecular cloning. A laboratory manual. Cold Spring Harbor, New York, Cold Spring Harbor Laboratory Press.

Sankoff, D. 1975. Minimal mutation trees of sequences. SIAM J. Appl. Math. 28: 35 – 42.

Saraste, M. 1999. Oxidative phosphorylation at the fin de siecle. Science. 283: 1488 – 1493.

Schagger, H., Cramer, W.A., von Jagow, G. 1994. Analysis of molecular masses and oligomeric states of protein complexes by blue native electrophoresis and isolation of membrane protein complexes by two-dimensional native electrophoresis. Anal. Biochem. 217: 220 – 230.

Schagger, H., and von Jagow, G. 1991. Blue native electrophoresis for isolation of membrane protein complexes in enzymatically active form. Anal. Biochem. 199: 223 – 231.

Schapira, A.H. 1999. Mitochondrial disorders. Biochim. Biophys. Acta. 1410: 99 – 102.

Schlossmann, J., Lill, R., Neupert, W., Court, D.A. 1996. Tom71 a novel homologue of the mitochondrial preprotein receptor Tom70. J. Biol. Chem. 271: 17890 – 17896.

Schlossmann, J. and Neupert, W. 1995. Assembly of the preproteins receptor MOM72 / MOM70 into the protein import complex of the outer membrane of mitochondria. J. Biol. Chem. 270: 27116 – 27121.

Schmitt, S., Ahting, U., Eichacker, L., Granvogl, B., Go, N.E., Nargang, F.E., Neupert, W., Nussberger, S. 2005. Role of Tom5 in Maintaining the Structural Stability of the TOM Complex of Mitochondria. J. Biol. Chem. 280 (15): 14499 – 12506.

Schmitt, S., Prokisch, H., Schlunck, T., Camp, D.G., Ahting, U., Waizenegger, T., Scharfe, C., Meitinger, T., Imhof, A., Neupert, W., Oefner, P.J., Rapaport, D. 2006. Proteome analysis of mitochondrial outer membrane from *Neurospora crassa*. Proteomics. 6: 72 – 80.

Schneider, H.C., Berthold, J., Bauer, M.F., Dietmeier, K., Guiard, B., Brunner, M., Neupert, W. 1994. Mitochondrial Hsp70 / MIM44 complex facilitates protein import. Nature. 371: 768 – 774.

Schneider, H., Sollner, T., Dietmeier, K., Eckerskorn, C., Lottspeich, F., Trulzsch, B., Neupert, W., Pfanner, N. 1991. Targeting the master receptor MOM19 to mitochondria. Science. 254: 1659 – 16632.

Selker, E.U. 1990. Premeiotic instability of repeated sequence in Neurospora crassa. Annu. Rev. Genet. 24: 579 – 613.

Sherman, E.L., Go, N.E., Nargang, F.E. 2005. Functions of the Small Proteins in the TOM Complex of *Neurospora crassa*. Mol. Biol. Cell. 16: 4172 – 4182.

Sherman, E.L., Taylor, R.D., Go, N.E., Nargang, F.E. 2006. Effects of Mutations in Tom40 on Stability of the Translocase of the Outer Mitochondrial Membrane (TOM) Complex, Assembly of Tom40, and Import of Mitochondrial Preproteins. J. Biol. Chem. 281 (32): 22554 – 22565.

Singh, K.K. 2004. Mitochondrial dysfunction is a common phenotype in aging and cancer. Ann. NY Acad. Sci. 1019: 260 – 264.

Sirrenberg, C., Endres, M., Folsch, H., Stuart, R.A., Neupert, W., Brunner, M. 1998. Carrier protein import into mitochondria mediated by the intermembrane space proteins Tim10/Mrs11p and Tim12/Mrs10p. Nature. 391: 912 – 915.

Sogo, L.F. and Yaffe, M.P. 1994. Regulation of Mitochondrial Morphology and Inheritance by Mdm10p, A Protein of the Mitochondrial Outer Membrane. J. Cell Biol. 126 (6): 1361 – 1373.

Steger, H.F., Sollner, T., Kiebler, M., Dietmeier, K.A., Trulzsch, K.S., Tropschug, M., Neupert, W., Pfanner, N. 1990. Import of ADP / ATP carrier into mitochondria: two receptors act in parallel. J. Cell Biol. 111: 2353 – 2363.

Steinberg, G. and Schliwa, M. 1993. Organelle movements in the wild type and wall-less fz;sg;os-1 mutants of Neurospora crassa are mediated by cytoplasmic microtubules. J. Cell Sci. 106: 555 – 1641

Stojanovski, D., Guiard, B., Kozjak-Pavlovic, V., Pfanner, N., Meisinger, C. 2007. Alternative function for the mitochondrial SAM complex in biogenesis of a-helical TOM proteins. J. Cell Biol. 179 (5): 881 – 893.

Stojanovski, D., Rissler, M., Pfanner, N., Meisinger, C. 2006. Mitochondrial morphology and protein import – A tight connection? Biochim. Biophys. Acta. 1763: 414 – 421.

Stuart, R. 2002. Insertion of proteins into the inner membrane of mitochondria: the role of the Oxa1 complex. Biochim. Biophys. Acta. 1592: 79 – 87.

Sutak, R., Dolezal, P., Fiumera, H.L., Hrdy, I., Dancis, A., Delgadillo-Correa, M., Johnson, P.J., Muller, M., Tachezy, J. 2004. Mitochondrial-type assembly of FeS centers in the hydrogenosomes of the amitochondriate eukaryote *Trichomonas vaginalis*. PNAS. 101 (28): 10368 – 10373.

Sylvestre, J., Margoet, A., Jacq, C., Dujardin, G., Corral-Debrinski, M. 2003. The Role of the 3′ Untranslated Region in mRNA Sorting to the Vicinity of Mitochondria Is Conserved from Yeast to Human Cells. Mol. Biol. Cell. 14 (9): 3848 – 3856.

Taylor, R.D., McHale, B.J. Nargang, F.E. 2003. Characterization of the *Neurospora crassa* Tom40-deficient mutants and effect of specific mutations on Tom40 assembly. J. Bio. Chem. 278 (2): 765 – 775.

Tovar, J., Fischer, A., Clark, C.G. 1999. The mitosome, a novel organelle related to mitochondria in the amitochondrial parasite *Entamoeba histolytica.* Mol. Microbiol. 32: 1013 – 1021.

Truscott, K.N., Voos, W., Frazier, A.E., Lind, M., Li, Y.F., Geissler, A., Dudek, J., Muller, H., Sickmann, A., Meyer, H.E., Meisinger, C., Guiard, B., Rehling, P., Pfanner, N. 2003. A J-protein is an essential subunit of the presequence translocase-associated protein import motor of mitochondria. J. Cell Biol. 163 (4): 707 – 713.

Waizenegger, T., Habib, S.J., Lech, M., Mokranjac, D., Paschen, S.A., Hell, K., Neupert, W., Rapaport, D. 2004. Tob38, a novel essential component in the biogenesis of β-barrel proteins of mitochondria. EMBO Reports. 5 (7): 704 – 709.

Waizenegger, T., Schmitt, S., Zivkovic, J., Neupert, W., Rapaport, D. 2005. Mim1, a protein required for the assembly of the TOM complex of mitochondria. EMBO Reports. 6 (1): 57 – 62.

Wiedemann, N., Kozjak, V., Chacinska, A., Schonfisch, B., Rospert, S., Ryan, M.T., Pfanner, N., Meisinger, C. 2003. Machinery for protein sorting and assembly in the mitochondrial outer membrane. Nature. 242: 565 – 571.

Wiedemann, N., Truscott, K.N., Pfannschmidt, S., Guiard, B., Meisinger, C., Pfanner, N. 2004. Biogenesis of the Protein Import Channel Tom40 of the Mitochondrial Outer Membrane. J. Biol. Chem. 279 (18): 18188 – 18194.

Vanlerberghe, G.C., and McIntosh, L. 1997. Alternative oxidase: from gene to function. Annu. Rev. Plant Physiol. Plant Mol. Biol. 48: 703 – 734.

van Wilpe, S., Ryan, M.T., Hill, K., Maarse, A.C., Meisinger, C., Brix, J., Dekker, P.J.T., Moczko, M., Wagner, R., Meijer, M., Guiard, B., Honlinger, A., Pfanner, N. 1999. Tom22 is a multifunctional organizer of the mitochondrial preproteins Translocase. Nature. 401: 485 – 489.

Voulhoux, R. and Tommassen, J. 2004. Omp85, an evolutionary conserved bacterial proteins involved in outer-membrane-protein assembly. Rec. Microbiol. 155: 129 – 135.

Yaffe, M. P., Harata, D., Verde, F., Eddison, M., Toda, T. and Nurse, P. 1996. Microtubules mediate mitochondrial distribution in fission yeast. Proc. Natl. Acad. Sci. 93: 11664 – 11668.

Youngman, M.J., Hobbs, A.E.A., Burgess, S.M., Srinivasan, M., Jensen, R.E. 2004. Mmm2p, a mitochondrial outer membrane protein required for yeast mitochondrial shape and maintenance of mtDNA nucleoids. J. Biol. Chem. 164 (5): 677 – 688.